DRAI-AHP VULNERABILITY ASSESSMENT OF THE QUATERNARY AQUIFER IN THE KETA STRIP

BY

JOSEPH VALCORY KIPPO

THIS DESSERTATION IS SUBMITTED TO THE UNIVERSITY OF GHANA, LEGON IN PARTIAL FULFILMENT OF THE REQUIREMENTS FOR THE AWARD OF PhD GEOLOGY

DEGREE

JUNE, 2012

DECLARATION

This is to certify that the content of the PhD dissertation has not been previously submitted to any University or Institue for the award of PhD degree. This dissertation is strictly my work and all published materials in this dissertation have been accordingly referenced to the best of my ability.

The research was carried out under the supervision of Professor Bruce Banoeng-Yakubo, Professor Daniel Asiedu and Dr. Mark Sandow Yidana all of the University of Ghana.

I have acknowledged contributions to this research.

…….	…….
Joseph Valcory Kippo (Candidate)	Date
……...	……...
Prof. Bruce Banoeng-Yakubo (Principal Supervisor)	Date
……	……
Prof. Daniel K. Asiedu (Supervisor)	Date
……	……..
Dr. Mark S. Yidana (Supervisor)	Date

DEDICATION

This work is dedicated to God and my family.

ACKNOWLEDGMENT

I wish to express my sincere appreciation to Professor Bruce Banoeng-Yakubo of the University of Ghana, my principal supervisor for the support, advice and guidance during this research.

I sincerely appreciate the role played by Professor Daniel Asiedu from the start to the end of this research work. I value every single sentence of advice you gave me.

I will also want to express my gratitude to Dr. Mark Sandow Yidana for his immerse support and guidance during this research. His words of encouragement when I looked tired were stimulating and helped keep me working to the end of my research work.

I thank all the lecturers in the Department for their supporting roles, especially Prof. David Atta Peters, Dr. Prosper Nude and Dr. Johnson Manu who urged me on till the end of this work.

I will like to thank Mr. Ahiabor and his family for the support they gave to me during my stay at Keta to gather data for my research work. I appreciate the useful information he provided on the Keta strip.

Finally I will like to express my gratitude to my family and friends for their support during this work.

ABSTRACT

The Quaternary aquifer in the Keta basin is a source of fresh water to the over 130,000 inhabitants living along the Keta Strip. Groundwater quality is deteriorating due to pollution from mainly agriculture, sewage, septic tanks and solid waste

disposal in the area. This research was undertaken to assess the intrinsic vulnerability to pollution of the aquifer. The DRASTIC methodology was applied to delineate zones vulnerable to pollution. Data was gathered on the seven DRASTIC parameters which include static water levels, soil sampling to determine soil media and aquifer media types, hydraulic conductivity, elevations and water quality. Using GIS methods the data was prepared, processed and analysed. Interpolation techniques were used to generate raster layers of the parameters. The seven raster maps were combined in a GIS environment to produce a composite vulnerability map. The map was reclassified into five classes namely, very low, low, moderate, high and very high pollution potential. The resulting map shows the relative intrinsic vulnerability of the unconfined aquifer to pollution. The map was tested by plotting on it April, 2004 nitrate concentration data. Statistical correlation between nitrate values and vulnerability class values extracted from the nitrate points yielded a low Spearman rho correlation coefficient of 36.3%. The model was calibrated using statistical correlations between each of the seven parameters and nitrate values. Soil media, topography and hydraulic conductivity parameters were found not significantly correlated to nitrate pollution and were eliminated from the model parameters leaving depth to water (D), recharge (R), aquifer media (A) and influence of the vadose media (I) to form the acronym DRAI. The weights of the parameters were revised based on the seven correlation coefficients. The rating values were also revised based on the mean nitrate values for each rating class of the original DRASTIC. The model accuracy was tested by applying correlation to the vulnerability classes and nitrate concentration data. A correlation coefficient of 62 % was obtained. The Analytic Hierarchy Process (AHP) was used to calibrate the model by determining a different set of parameter weights. The model accuracy

improved to 66% after correlation between nitrate values and intrinsic vulnerability classes. Based on the correlation coefficient the AHP model was selected for the study area. The AHP optimized intrinsic vulnerability map shows that 10.6%, 26.8%, 30.1%,22.6% and 9.9% of the study area have very low, low, moderate, high and very high vulnerability to groundwater pollution respectively. Nitrate concentration values sampled in July, 2003 was used to evaluate validation of the AHP model. The nitrate values were plotted on the AHP vulnerability map and statistical correlation tests between nitrate values and vulnerability values yielded a correlation coefficient of 75%, confirming a close agreement between model values and actual nitrate pollution on the ground. Anloga and Woe area where agriculture is predominant have the lowest intrinsic vulnerability. Dzelukope and Keta which are heavily populated residential areas have very high groundwater pollution potential. The validation evaluation shows that the research results are realistic and representative of the actual groundwater pollution on the ground. Therefore, the DRAI model is applicable in the study area.

TABLE OF CONTENTS

Page

CHAPTER FOUR

LIST OF FIGURES

LIST OF TABLES

CHAPTER ONE

INTRODUCTION

1.1 BACKGROUND AND JUSTIFICATION

The Keta strip is located at the south eastern part of the Volta Region. The strip is surrounded by the Atlantic Ocean, the Keta Lagoon, Avu lagoon and the Volta river estuary. There is the perception of unlimited water resources in the area. However with increase in the population growth there is an increasing demand for water for industrial, domestic and agricultural purposes. This has led to over exploitation of groundwater resources in the area, especially from the unconfined Quaternary aquifer. Poor agricultural practices and other forms of land use have resulted in the contamination of groundwater. Probably as a result of climate changes, rainfall has been declining and temperatures rising, putting this vital natural resource at risk. Pollution of groundwater threatens the existence of ecosystems. Once an aquifer is contaminated it is costly to remediate. As a developing country Ghana may not have the resources to carry out aquifer remediation. The loss of one aquifer system through pollution will put stress on the remaining aquifers. It is important to identify

which aquifer systems are more susceptible to degradation so that the necessary steps can be taken to protect them from pollution.

Serious health hazards can result from contaminants of groundwater. For example, high nitrate levels from the use of fertilizers and human waste can reduce oxygen levels in the blood, especially in babies, resulting in the "blue baby syndrome" and can increase the risk of cancer in humans (Focazio et. al., 2002; Yang and Wang, 2010).

Shallot cultivation as a cash crop is the predominant farming activity in the area. Pepper, okro and tomatoes are also cultivated but to a lesser extent. Shallot cultivation depends highly on manure and irrigation water. Cow dung and poultry droppings are the main sources of manure (Awardzi et al., 2008). Fertilizers are also used for a variety of other crops including maize and tomatoes.

Many of the communities in the area depend largely on the shallow sandy unconfined aquifers as the main source of water supply for domestic and irrigation purposes (Banoeng-Yakubo et al., 2005). These shallow aquifers lie below sea level at most parts of the strip and are sandwiched between the saline Keta Lagoon and the Atlantic Ocean. Buckets and watering cans, as well as motorised systems are used to extract large quantities of groundwater from thousands of privately owned hand-dug wells located in households and on agricultural lands for irrigation purposes throughout the year.

Nerquaye-Tetteh (1993); Bannerman (1994); Jorgensen and Banoeng-Yakubo (2001) carried out various researches in the study area. Their findings revealed that

nitrate levels and electrical conductivity of the shallow groundwater were increasing and recommended efforts to protect the groundwater resource from pollution due to human activities.

Kortatsi and Agyekum (1999) conducted studies to estimate the aquifer water balance in the Anloga area. They concluded among others that the fresh water lens was under the threat of pollution from saline water intrusion due to an increase in mechanised pumping for sprinkler irrigation purposes. Saline water is unsuitable for irrigating most crops and has adverse effects when used at the domestic level for washing.

Hotor (2003) conducted research to assess the water quality and to trace the high salinity in the study area in relation to land use. One of the findings of the study was that groundwater quality in the study area was deteriorating as a result of human activities. It recommended that efforts be made to protect the quality of groundwater from degradation.

Banoeng-Yakubo et al. (2005) have shown that groundwater in the area is under significant and increasing threat to contamination. The study revealed that most of the communities in the area are unaware of how vulnerable these shallow aquifers are and continue to discharge human and other wastes directly into the aquifer system. Large quantities of organic and inorganic fertilizers are used for agricultural purposes. Rain and irrigation water leach these fertilisers directly into the groundwater system. This has led to high nitrate levels in many parts. There is a continuous trend in water pollution as a result of all year round agricultural activities

and an increasing population density, with the associated increase in the production of human wastes.

Awardzi et. al. (2008) conducted research into the development and sustainability of a horticultural system at the Keta basin. They concluded among others that environmental problems relating to the depletion of the fresh water aquifer and pollution of the aquifer by nutrients and pesticides were eminent.

The above studies emphasise the need for further research to develop sustainable groundwater management practices to protect groundwater quality degradation in the area due to improper land use, poor agricultural practices and excessive groundwater abstraction. The studies have, however, fallen short of developing or even suggesting any groundwater management plan for the study area. This research seeks to address the issue of a groundwater management plan.

In Ghana most land use decisions are made at the national, regional and local government levels. Foster and Skinner (1995); Zaporozec et al., (2002); Nolan et al., (2002) note that land use planners and environmental decision makers are not sufficiently aware of the need for, or the methods of, protecting groundwater. In order to inform these management decisions, detail knowledge of the qualitative and quantitative characterization of the aquifer is needed (Soupios et al., 2008). It is important that any public policy on protecting groundwater quality be guided by scientific research that will lead to identifying hot spots with regard to the risk of contamination. This is what this research seeks to achieve.

The concept of Vulnerability is one of the methodologies developed for assessing the environmental impact of groundwater pollution. Vulnerability assessment models are important management tools for the implementation of environmental projects and protecting groundwater resources (National Research Council, 1993; Carbonell, et. al., 1993; Atiqur, 2008; Yang and Wang, 2010). These models can be used to delineate vulnerability and predict system response based on different stress scenarios. The absence of any long term water quality monitoring data and a groundwater model as a management tool in the study area makes it difficult to predict the future of groundwater with regard to pollution. In order to adequately address this problem a hydrogeological vulnerability assessment model will be developed for use and protection of the groundwater resource of the study area. Groundwater protection begins with the assessment of the sensitivity of its environment (Kouli et al., 2008).

This research adopts the DRASTIC vulnerability assessment model as a groundwater management tool. In this respect spatial data on water quality and hydrogeological parameters will be generated from field work to be used with the aid of Geographic Information System (GIS) concepts to evaluate and delineate vulnerability.

1.2 MOTIVATION

A study by Banoeng-Yakubo et a.l,(2005) to assess the water quality status in the area showed high nitrate and bacteria in many of the dug wells sampled.

The impetus for this research work is largely driven by the lack of any groundwater management model for the area. It is important that the aquifer is protected and remains as a source of water supply to the inhabitants of the Keta strip. To ensure

this, it is necessary to determine if certain locations within the aquifer are more susceptible to receive and transmit pollution. This study therefore seeks to evaluate the aquifer vulnerability to nitrate pollution using the DRASTIC method. An optimization of the DRASTIC method will be done based on revision of the factor weights using statistical methods and analytical hierarchy process (AHP). Groundwater vulnerability maps will be produced. These maps will serve as tools for identifying and prioritising regions of potential concern with respect to groundwater pollution.

1.3 RESEARCH AIMS AND OBJECTIVES

The aim of this research is to assess the vulnerability of the unconfined aquifer along the Keta strip using the DRASTIC model.

In order to achieve the aim the following broad objectives are identified.

(a) To evaluate the vulnerability of the unconfined aquifer in the study area using DRASTIC (Depth to water, net Recharge, Aquifer media, Soil media, Topography, Impact of vadose zone, and hydraulic Conductivity)

(b) To provide a spatial analysis of the parameters and conditions under which groundwater may become contaminated by applying DRASTIC.

(c) To evaluate the relative importance of the DRASTIC model parameters (using statistics and Analytical hierarchy process.) in the study area for assessing aquifer vulnerability.

(d) To determine groundwater vulnerable zones to contamination and produce groundwater vulnerability maps of the study area within GIS environment capable of predicting the specific vulnerability or pollution risk of the quaternary aquifer under environmental stress.

1.4 CONTRIBUTIONS OF THE RESEARCH

The following are envisaged to be the contribution to knowledge of this research:

(a) The development of a comprehensive DRASTIC groundwater vulnerability assessment model for the unconfined aquifer along the Keta strip, and

(b) The development of quantitative methods for assessing the relative values of DRASTIC parameters of groundwater vulnerability in the study area.

1.5 DESCRIPTION OF RESEARCH AREA

1.5.1. Location and Extent

The Keta Basin forms one of the five coastal sedimentary basins in southern part of the country and lies at the extreme southeast corner of Ghana. The Basin covers an area of about 3577 km^2 of which 2201.50 km^2 are on-shore and the remainder extends below the Gulf of Guinea. A sizeable portion of this basin lies in a region dominated by the Volta River Delta Complexes (Kesse, 1985). The Keta basin lies in the Volta Region and shares its western boundary with the Dagme-east district of the Greater Accra Region. It is bounded on the east by the Republic of Togo and to the south by the Gulf of Guinea. On the north the area is bounded by the South Tongu and Ketu Districts. The Keta Strip is the study area and forms part of the larger Keta basin. The study area lies between the Keta lagoon to the north and the Gulf of Guinea to the south (i.e. the area within latitudes 5° 47^1 and 5° 55^1 N and longitudes 0° 53^1 and 1° 0^1 E). The research area is a narrow sand spit about 27km long and barely 2km at its widest portion. It separates the lagoon from the sea and occupies approximately 45 km^2 (540ha) of land surface (Awadzi et al., 2008).

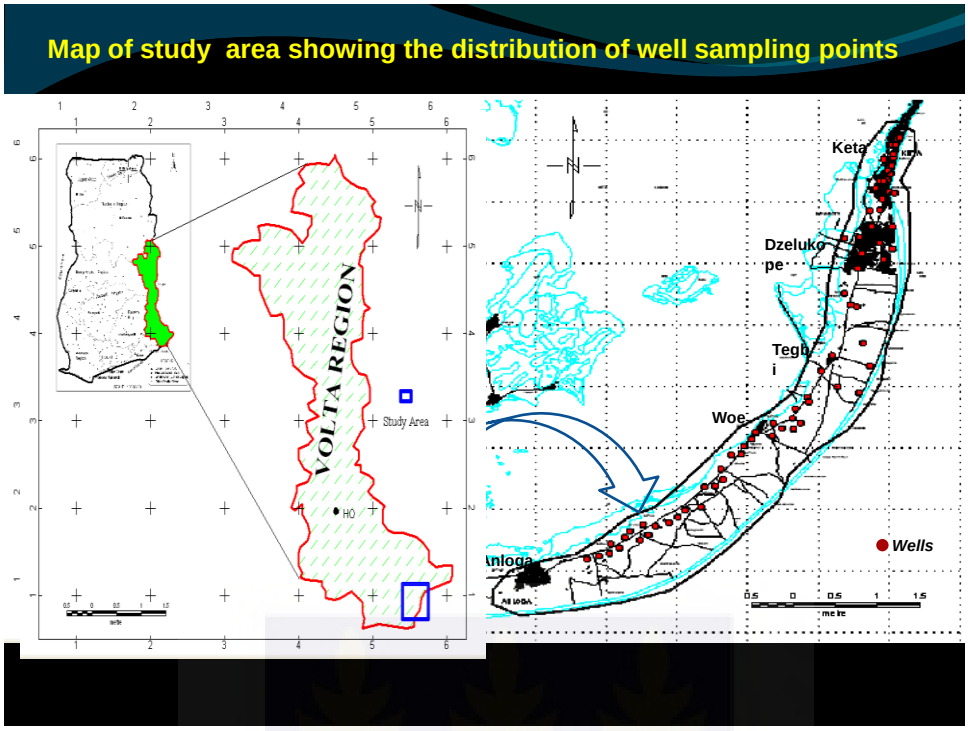

Figure 1.1 Map of Volta Region showing the study area with the location of sampled wells.

1.5.2. Climate

There is no meteorological station in the study area. The nearest stations are at Ada and Akatsi. Data from these stations may be used to represent the study area. According to (Dickson and Benneh, 1995), the study area lies within the Equatorial climatic zone. Temperatures are quite high with a mean monthly temperature of about 30 ^{o}C in the warmest month, March and about 26 ^{o}C in the coldest month, August. This is the driest climatic region in Ghana. The relative humidity is between 60% and 75 % and a mean annual temperature of about 27.5 ^{o}C is recorded (Benneh and Dickson, 1995). From November to February the harmattan dominates with

winds from northeast and gives rise to a long dry season. From March, the winds blow from southwest and the monthly precipitation increases and reaches a peak between April, May and June, which is the main rainy season. In July, August precipitation is very low representing the minor dry season. September to November is the minor rainy season which is not often reliable. The annual rainfall varies from 400 mm in some years to 1200 mm in others.

There are two annual rainfall maxima following the bi-annual passage of the Inter-tropical Convergence Zone over Ghana. Despite this the annual total rainfall is lower than areas with similar latitude. The average annual rainfall is below 900mm with an uneven distribution throughout the year. According to Dickson and Benneh (1995) the climate of the area is controlled by the movement and position of the Inter Tropical Continental Zone (ITCZ) within the sub region. The ITCZ is a common imaginary front between two dominant air masses namely the Northeast Trade winds and the Southwest Monsoon winds in the sub-region. The coastline is very smooth and thereby having no significant effect on rainfall events in the study area. The prevailing moisture-laden winds from the Atlantic Gulf of Guinea travel virtually uninterrupted for considerable distances inland. The bulk of the rain is due mainly to cyclonic and or convectional causes (Hortor, 2005).

The annual evapotranspiration is estimated based on Christensen and Awadzi, (2000) to be about 1500mm evenly distributed over the year and monthly evapotranspiration varies between 100mm and 150mm. It is only in June that the precipitation exceeds the potential evaporation. Figures 1.2 to 1.9 show the variations in rainfall, evapotranspiration, temperature and relative humidity at Akatsi and Ada.

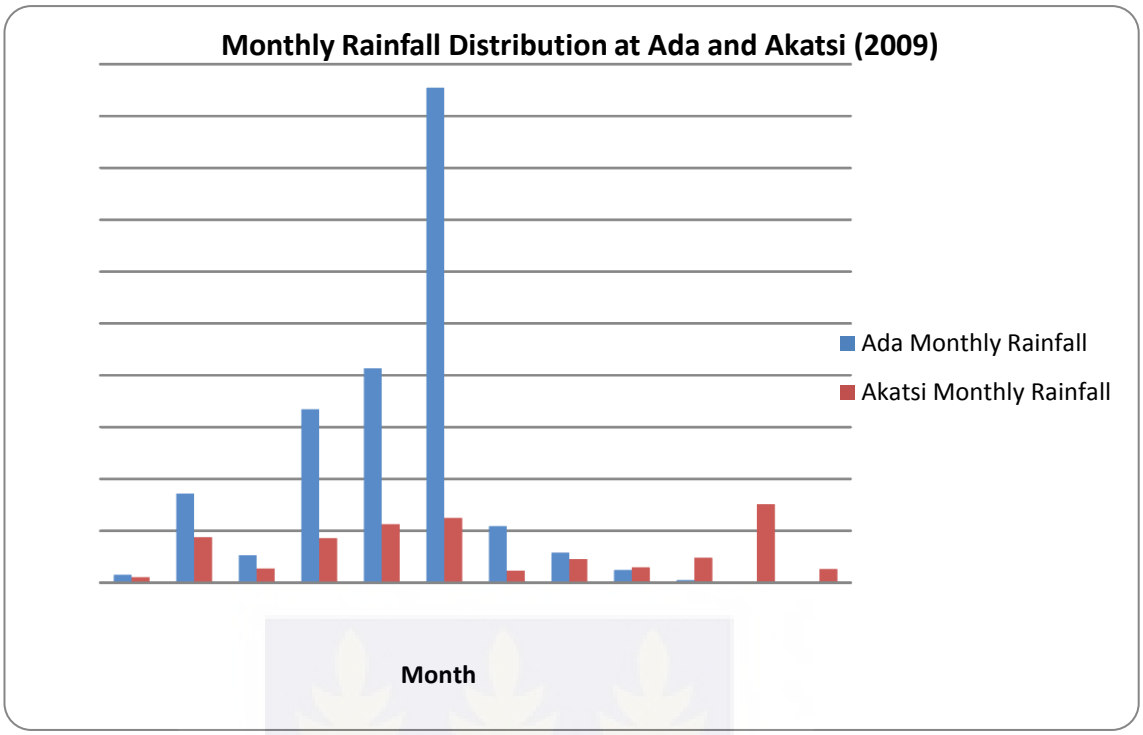

Fig. 1.2 Monthly rainfall distribution at Ada and Akatsi. Data Source:Ghana Meteorological Agency, Accra.

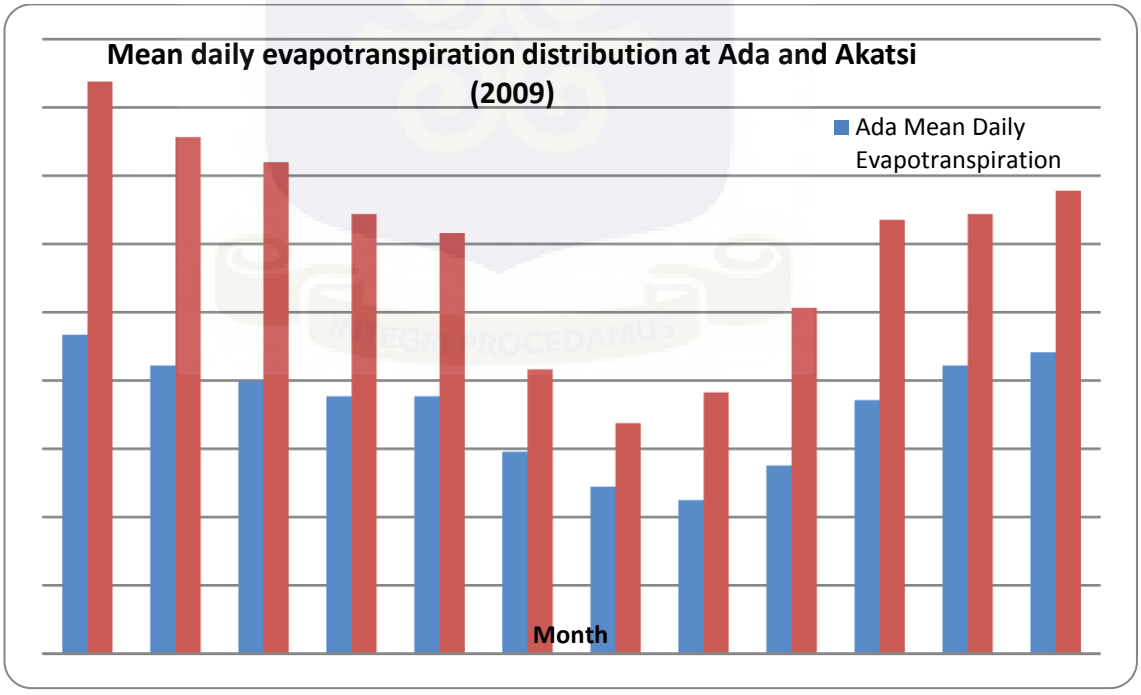

Fig. 1.3.Mean daily Evapotranspiration distribution at Akatsi and Ada

Source: Ghana Meteorological Agency. East Legon Accra

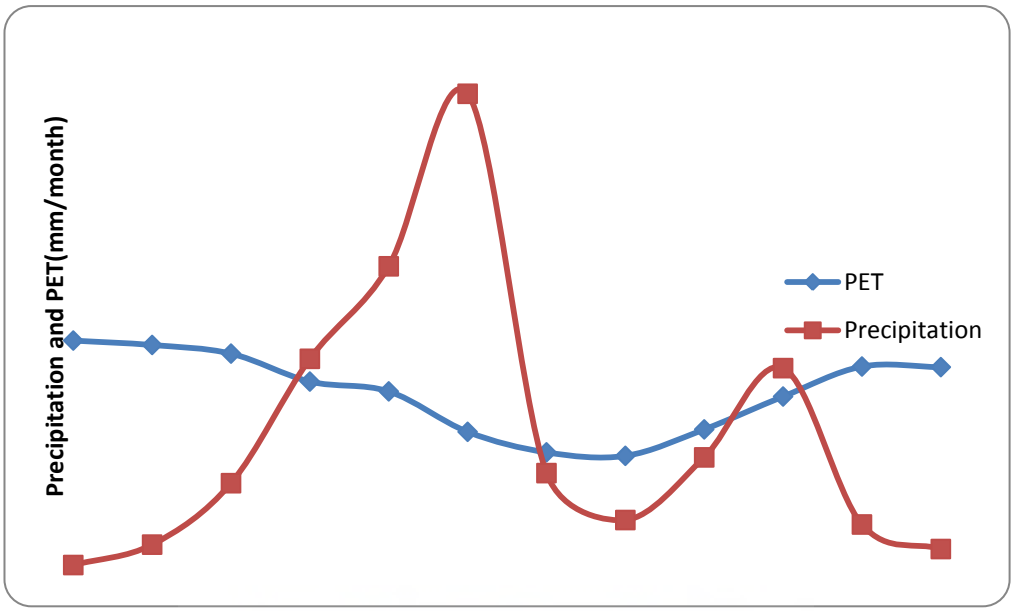

Fig. 1.4 Average Monthly means of Precipitation(P) and potential Evapotranspiration (PET) at Ada from (2000-2009). Source Ghana Meteorological Agency , East Legon Accra

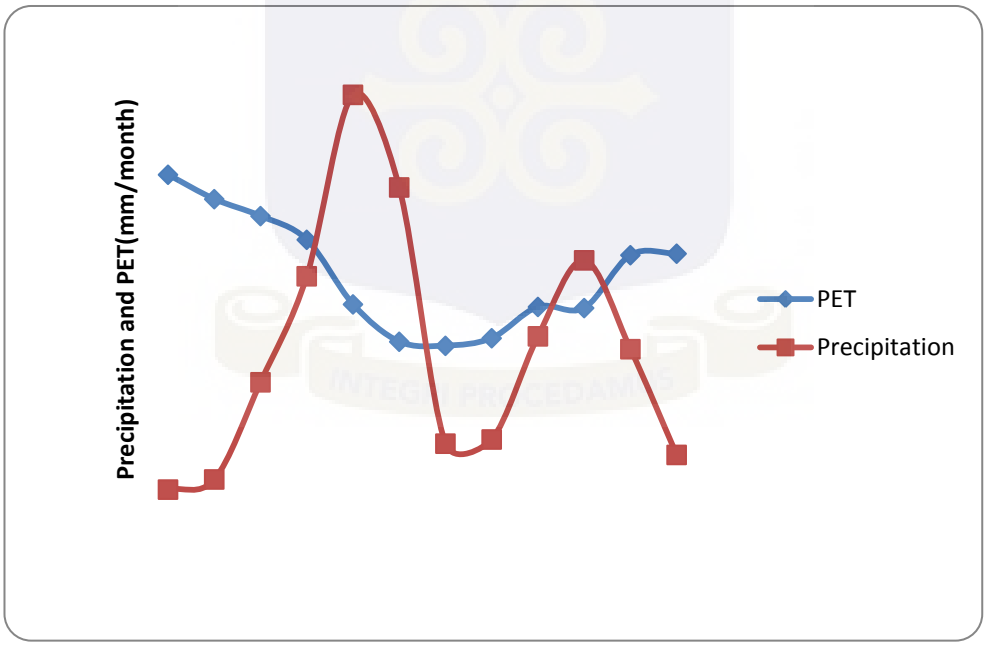

Fig. 1.5 Average monthly means of precipitation (P) and Potential Evapotranspiration (PET) at Akatsi from (2000-2009) Source: Ghana Meteorological Agency

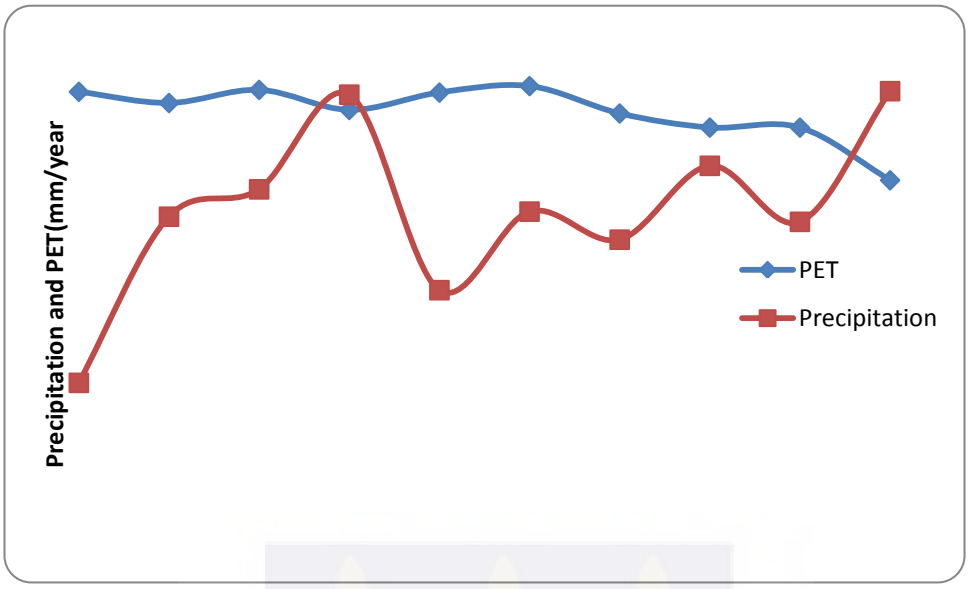

Fig. 1.6 Average annual Precipitation (P) and Potential Evapotranspiration (PET) at Ada from (2000-2009).Data source: Meteorological Services Agency East Legon Accra (2009)

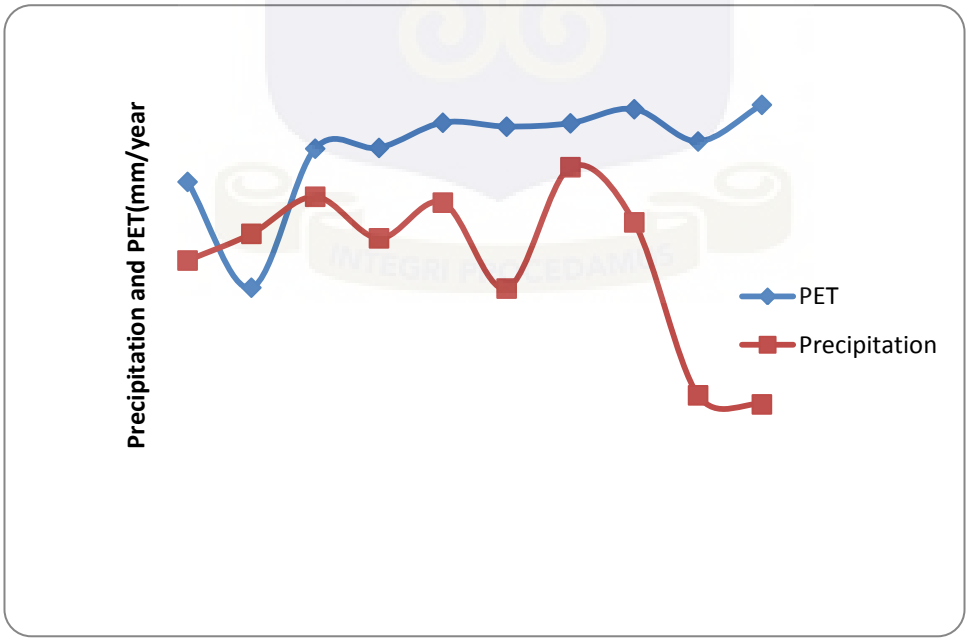

Fig. 1.7 Average annual Precipitation (P) and Potential Evapotranspiration (PET) at Akatsi from (2000-2009). Source: Ghana Meteorological Agency East Legon Accra

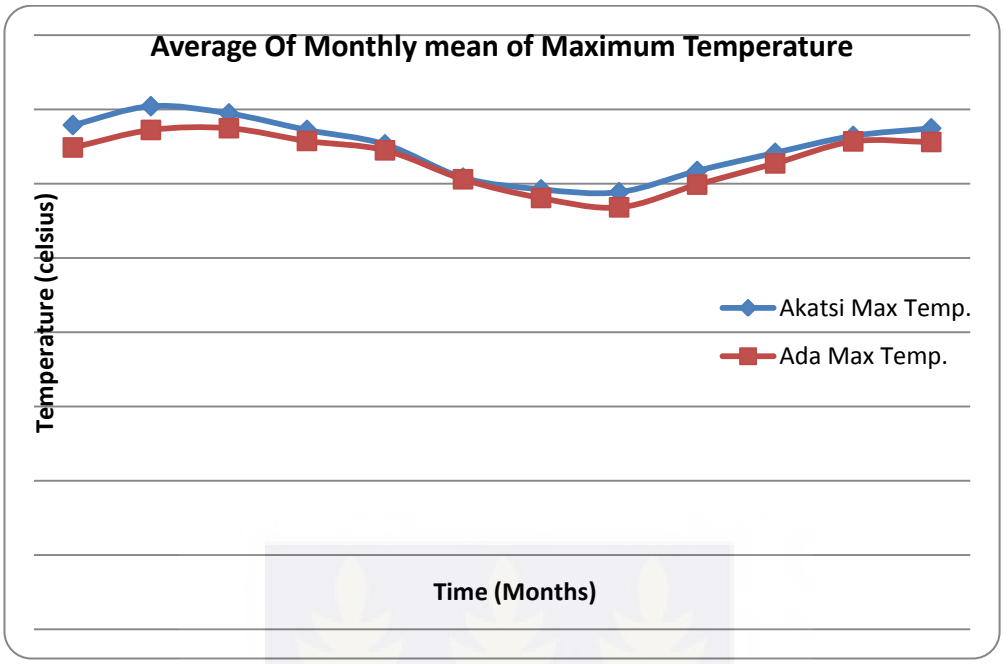

Fig. 1.8 Average Monthly means of maximum temperature at Ada and Akatsi from (2000-2009).Source: Ghana Meteorological Agency. East Legon Accra

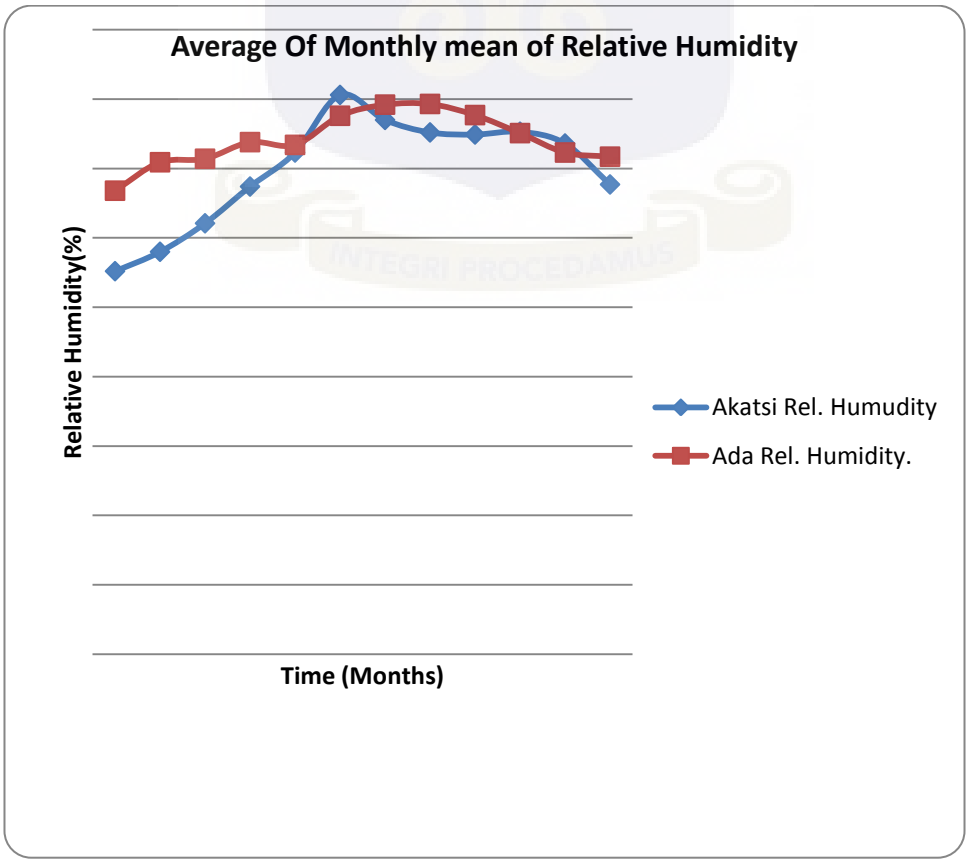

Fig. 1.9 Average Monthly relative humidity at Ada and Akatsi from (2000-2009). Data source: Ghana Meteorological Agency. East Legon Accra.

1.5.3 Population Growth, Industry and Land Use

According to Statistical Services, (2000), the Keta District population has been growing at a rate of 0.5 per cent since 1970. The 2000 population census puts the total population of the district at 133,661 which forms 8.2% of the regional total population. The district is relatively more urbanized based on the criterion that any settlement with a population of 5000 or more represents an urban centre. The average density for the district is 164 persons/km^2 (water bodies excluded), which is significantly higher compared with the national and regional figures of 65.7 persons/km^2, and 69.1 persons/km^2 ,respectively. This can be attributed to the presence of large water bodies, which occupy a third of the total land area. The main population density zone is the coastal area comprising a narrow strip of sand bar between Anloga and Keta where the density rises to about 500 persons/km^2 and compares favourably with densities in Greater Accra Region (609.7 persons/km^2) which is the highest in the country (www.ghanadistricts.com, 2009).

Agriculture, wetlands, urban land and water, are the major land-use categories in the area. Agriculture is the predominant land-use category. Agricultural lands are scattered throughout the area but are found more around Whuti through Woe to Tegbi. Agriculture is the predominant economic activity. The most important type of agriculture is shallot production. Fishing , trading and weaving also play a role in the local economy but to a lesser extent. Urban land composes about 40 percent of the

study area, and is mostly concentrated in communities around Keta and Dzelukope. Water covers about 10percent of the area (www.ghanadistricts.com, 2009).

1.5.4 Topography

The Keta municipal is a low-lying coastal plain with the highest point of only 53 metres above sea level around Abor in the north. The lowest point is approximately between 1-3.5 m below sea level along the coast around Vodza, Kedzi and Keta township. Three main geographic belts may be identified namely the Narrow Coastal Strip, the Lagoon Basin of the middle belt and the Plains of the North. The Coastal Strip is marked by sand bars with a few sea cliffs bordering the coast. This belt is affected by severe sea erosion. The worst hit areas are Keta, Kedzikope, Vodza, Kedzi and Horvi. The general elevation of the lagoon basin is also below sea level. It is made up of lagoons and islands such as Atiavi, Alakple, Seva, Anyako and Dudu. The basin is generally marshy due to the underlying sandy-clay geological formation.

The Northern plains are generally gently undulating with a relatively higher elevation of about 50 metres above sea level. The generally low-lying nature of the terrain has exposed particularly the eastern parts of the coastal strip to intense sea erosion and occasional flooding.

1.5.5 Climate and Vegetation

The entire Keta municipality falls within the coastal savannah zone. However, five vegetation zones can be reclassified. The northern part of the municipality marked by tall grasses and interspersed with medium sized trees with relatively higher density. The mid-section of the municipality with short grasses and short trees

including baobab trees. The South-western part, is characterized by mangrove plants along the Volta estuary and tall grasses used for fuel, and mat/hat weaving, respectively.

The south-eastern part along the coast from Whuti marked by short grasses and many neem trees. Most of the coconut trees along the coast have been affected by the Cape St. Paul Wilt disease. This has had a major influence on the pattern of rainfall in the municipality. There exist pockets of land mostly along the Dabala-Srogboe-Whuti highway that supports little or no vegetation. The municipality falls within the Dry Coastal Equatorial Climate with an annual average rainfall of less than 1,000mm. The amount of rainfall reduces as one travels from the north to the coastal parts where only about 800mm annual may be recorded. The municipality is thus one of the driest along the coast of Ghana. The amount of rainfall in the municipality has been generally declining since 1985. The municipality experiences a double maximum rainfall pattern. The major rainy season is between March and July while the minor one begins in September and ends in November. These coincide with the main and minor cropping seasons. (www.ghanadistricts.com, 2009).

1.5.6 Geology and Soil

The distribution of the main soil types in the Keta Municipal generally follows the major geographic units already identified. Along the coastal strip are the Oyibi-Muni and Keta Associations characterized by sandy soils often without any top layer of humus. Naturally, it supports coconut cultivation. When manured, it supports shallot, okro, pepper and other vegetables. This strip is the leading shallot producing area in

Ghana though it covers only about 11 per cent of the district (excluding lagoons). Soils in the lagoon basin (Ada-Oyibi Association) are very shallow, overlying a hard and compact clay formation.

The soil is generally alkaline and supports mangrove vegetation, sugar- cane, and grass for pasture. Due to the underlying clay, this area is liable to flood and not suitable for arable farming though it covers over 75 per cent of the total dry land of the municipality. The Toje-Alajo Association covers the Northern plains around Abor constituting about 14 per cent of the municipality (lagoon excluded). It is relatively deep and supports crops like cassava, maize and legumes. Thus, apart from severally constrained access to land, nearly 80 per cent of the land is covered by soils not suitable for cultivation. Besides, the ranges of crops cultivated are limited on account of poor soils and dry climatic conditions. The high average temperatures (about 30^{o}C), couple with low relative humidity, promotes high evapotranspiration (www.ghanadistricts.com, 2009).

1.5.7 Socio-economic environment

There is a number of large and small communities in the area with a total population of over 786,000 people as at the 2000 census. The communities are predominantly Ewe and Adangbe and their economic ventures are in the fishing, mat weaving and salt industries and crop farming. Crop farming is practiced around Whuti-Anloga areas where extensive shallot cultivation is done using water from very shallow hand

dug wells for irrigation. Agriculture is confined to the northern parts of the study area between the flood plains of the Keta lagoon and the tapered ends of the sand dunes because of lack of land due to sand dune covered areas.. Some farming activities are also carried out in furrows (depressions) located within the dunes. Thus, the rate of groundwater abstraction is relatively high in these areas. As a result, more lands virtually lying idle in the past have now been put under cultivation, farm sizes become larger and consequently, groundwater abstraction by pumping is much higher. The continuous and large-scale extraction of water from the fresh water lenses could result in significant depressions in the groundwater levels, a situation that can trigger seawater encroachment in the area (Hortor, 2005).

1.5.8 Drainage

The main drainage basins are the lagoons, which together constitutes about 362km^2. The major lagoons include Keta, Angaw Agbatsivi, Logui, Nuyi and Klomi. Tributaries of the Volta River and other smaller rivers and streams drain into this basin These include such streams as Angor, Avida, (near Hatorgodo), Awafla (near Awaflakpota), Nukpehui (in the north-western part of the district), Tordzie and Kplikpa. Many of the creeks are dwindling in size due to low rainfall, excessive evaporation and siltation. As a result, the volume of water in the lagoon has drastically declined and tends to fluctuate seasonally, leading to the emergence of several islands in the Keta, Angor and Agbatsivi lagoons. The biggest among the Islands are Seva and Dudu, which are partially inhabited (www.ghanadistricts.com, 2009).

1.5.9 Geological setting

The Keta basin is one of the fault-controlled sedimentary basins in West Africa along the southeastern coast of Ghana and is dominated by the Volta River estuary (Akpati, 1978). The surface geology of the basin is poorly exposed, being covered extensively by lagoons, marshes and thick undergrowth. Geologically, the Keta Basin is a continuous basin that spans from the eastern coastal areas of Ghana through Togo to the Republic of Benin and it is underlain by recent unconsolidated beach sands and lagoon clays, which deepen westwards towards the Volta River estuary and at depth by clay, gravels, and interlayers of varying thicknesses of limestone which forms the main deep freshwater resource of the whole basin. (Kesse, 1985; Banoeng-Yakubo et al, 2005; Hortor, 2005; Hilstrup, 2006).

The recent deposits rest on a series of continental beds of Middle Tertiary age. The rocks are unconsolidated limonitic argillaceous sands and gritty sands with persistent gravelly beds at their base. The gravelly beds are persistent from the Ghana-Togo border. A geological map of the Keta Basin is shown in Fig 1.10.

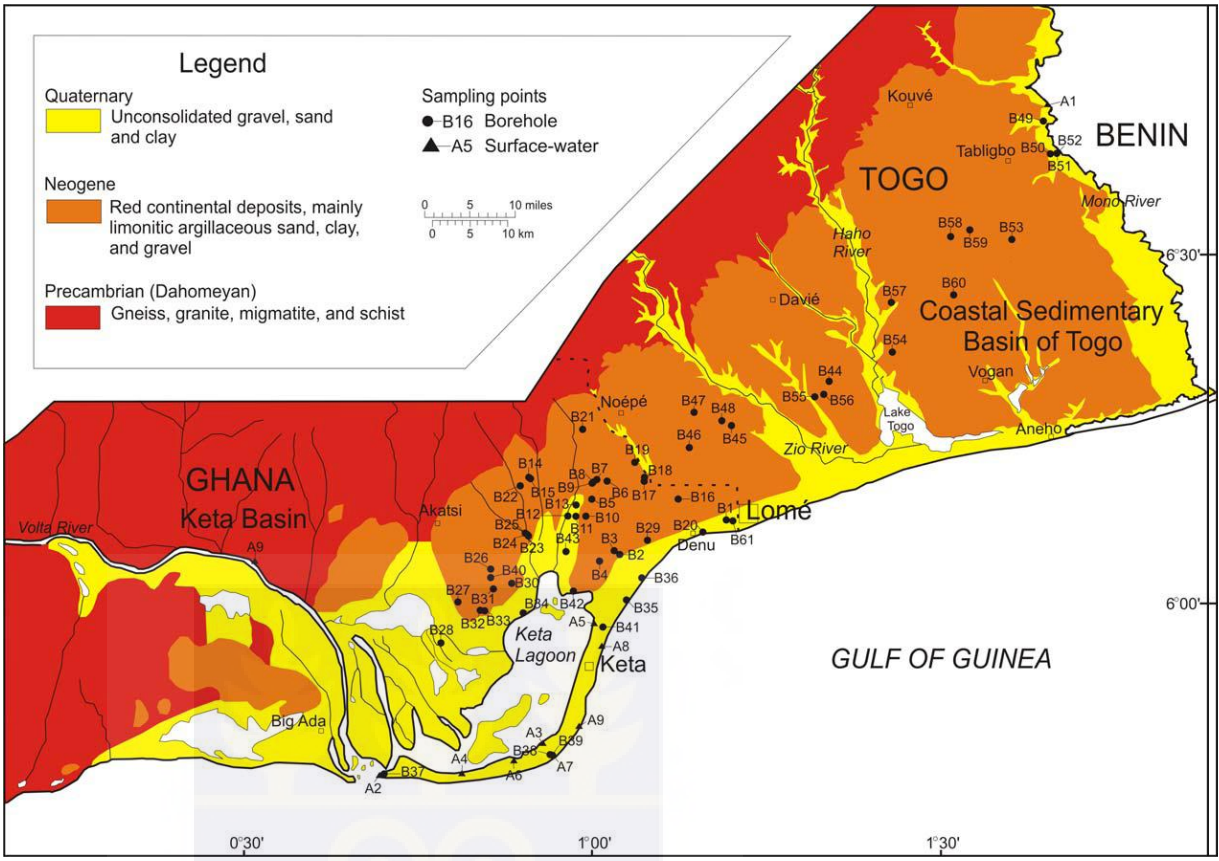

Fig. 1.10. Geological Map of Parts of the Keta Basin. Source: Helstrup (2006)

From drilling results, three main hydrogeological units have been identified in the Keta Basin (Nerquaye-Tetteh, 1993; Jorgensen and Banoeng-Yakubo, 2001)

1. Quaternary coastal marine sands and gravels in the Volta River estuary and the Keta Lagoon area.
2. Surficial Neogene continental deposits of argillaceous sands and gravels in the northeastern and central parts of the Keta Basin.
3. Upper Cretaceous-Eocene marine clay, shale, sand, sandstone, and fractured limestone. The limestone horizons of this interval are exploited for drinking water in the eastern parts of the Keta Basin. A composite stratigaphy in the Keta basin is shown in Table 1.1.

Table 1.1 Composite stratigraphic framework in the Keta basin

Depth (m)	**Lithology**	**Age**
0-67	Sand and Gravel	Pliocene-Recent
	UNCONFORMITY	
67-270	Glauconitic fossiliferous shale and sand	Miocene
	Limestone	
	UNCONFORMITY	
270-480	Greenish -grey shaley clays with layers of fossiliferous **limestone.**	Eocene
480-735	Greenish –grey, benthonitic, fossiliferous clay.	Paleocene
735-972	Dark grey calcareous, fossiliferous clay.	Maestrichtian
	UNCONFORMITY	
972 – 1189	Alternating shale and light grey medium-grained sandstone.	Campanian
1189-1554	Medium-grained, moderately well-sorted sandstone and micaceous grey shale.	Albian
1554-2134	Greyish-white, coarse-grained sandstone alternating with mudstone containing numerous plant fragments, coal traces.	Aptian undif. Lower Cretacous
2134-3574	Alternating fine, grey, bituminous sandstone and shale.	
3574-3620	Igneous intrusive-greenish grey dolerite	Jurassic
3620-4493	Dark brown, grey, micaceous shale and light grey sandstones and siltstonone. Fossiliferous in middle-lower unit.	Devonian
4493 -	**Basement.** Quartzite-biotite gneiss (Dahomeyan)	Precambrian

Source: Banoeng-Yakubo et al. (2005)

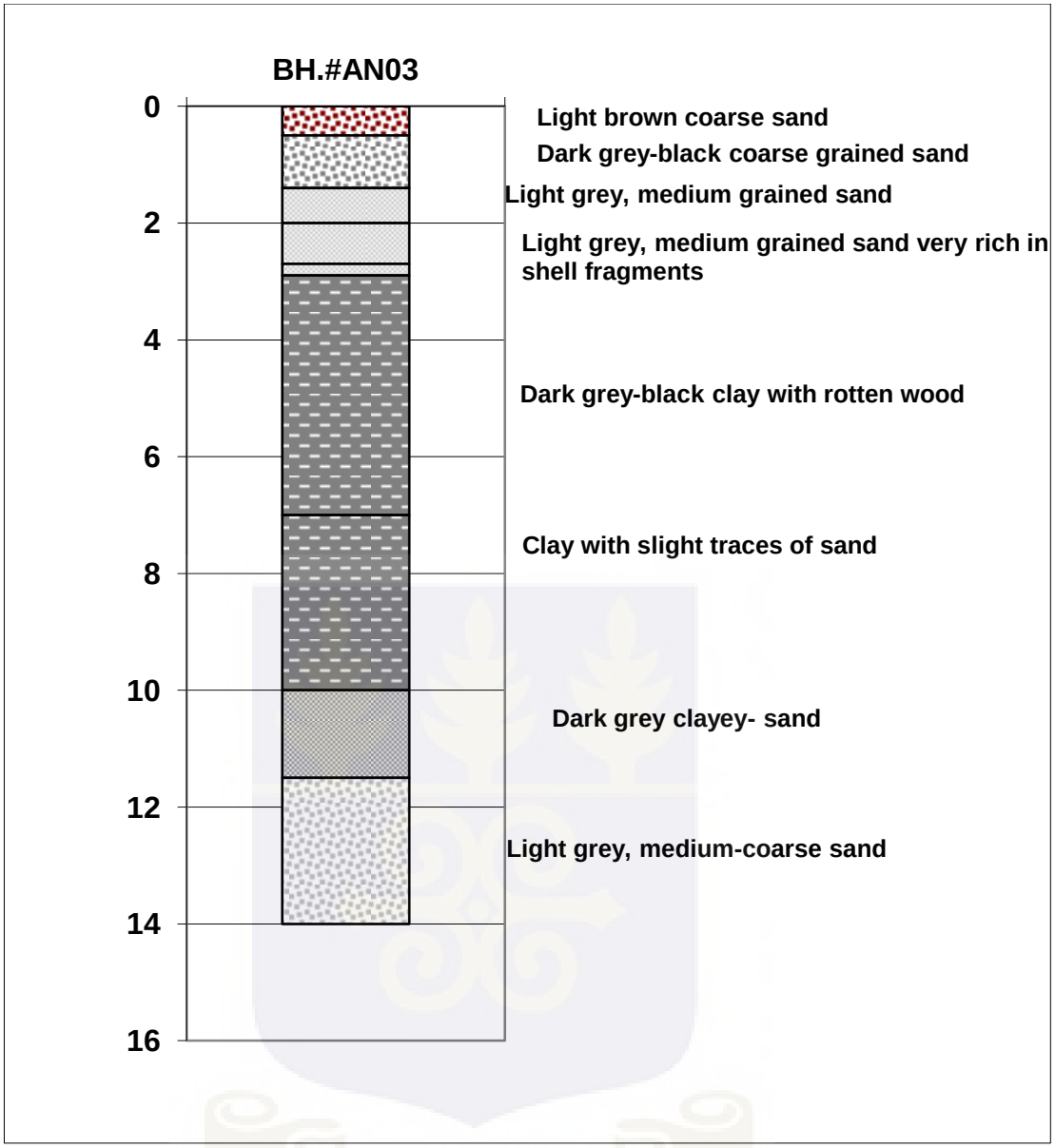

Figure 1.11 A representative composite graph of lithology near the hydrogeological station.

Source: Banoeng-Yakubo et al. (2005)

1.5.10.1 Aquifer types

According to Agyekum (2002) the Cenozoic and Mesozoic unconsolidated alluvial sedimentary rocks form about 1 % of the rock cover in the country. They consist of unconsolidated alluvial sediments, beach sand, red continental deposits of mainly alternating limonitic sand, sandy clay gravels, marine shale, limestone and glauconitic sandstone. The Cenozoic and Mesozoic sediments occur mainly in the extreme south eastern part of the country including the study area. Three aquifers occur in this formation. The first Quaternary aquifer is unconfined and occurs in the recent sand very close to the coast. It contains fresh meteoric water. The intermediate Neogene aquifer is either semi-confined or confined and occurs mainly in the red continental deposits of sandy clay and gravels. It contains mostly saline water. The third is the limestone aquifer. The groundwater in this aquifer occurs under artesian condition and is fresh.

1.5.10.1.1 The Quaternary aquifer

The shallow aquifer is exposed at the land surface, and is therefore recharged directly from precipitation. It provides recharge to deeper aquifers, either as leakage through intervening confining units or as direct infiltration where it directly contacts an underlying aquifer. Evaporation, transpiration to plants, and base flow to streams occur within the shallow aquifer (Jorgensen and Banoeng-Yakubo, 2001; Hortor, 2005). The Quaternary aquifer is the focus of this study. The shallow water aquifers generally consist of a series of lenticular/lenses to wedge shaped sand-gravel bodies interbedded with low permeability rocks like silt, clay and loose shells. Although the individual sand bodies that make up the aquifer form a series of discrete sub regional aquifers in the areas, they may be hydraulically interconnected to varying degrees on a regional scale (Hortor, 2005).

This aquifer lies at a mean depth of 6 m and contains fresh meteoric water. The mean depths of handdug wells and boreholes in this aquifer are extremely low, about 3 m and 12 m, respectively. The shallow, rain-fed aquifer constitutes the most prolific aquifer system in the Keta Basin. Aquifers in this formation have high transmissivity values, ranging between 0.7–1,624 m^2/d, with a mean of 22.2 m^2/d. In parts of the coastal strip, the surficial aquifer is underlain by semi-confined or leaky-type intermediate aquifer that contains brackish water (Agyekum, 2002).

1.5.10.1.2 The Neogene aquifer

This Intermediate aquifer according to Agyekum, (2002), is either semiconfined or confined and occurs mainly in the red continental deposits of sandy-clay and gravel. The depth of this aquifer varies from 18–120 m, and contains mostly saline water. Little research has been conducted in this aquifer probably because of its salinity levels.

1.5.10.1.3 The Limestone aquifer

The limestone and sandstone beds underlie an area of approximately 115 square kilometers and are believed to be a possible source of groundwater for the area. Relatively high yields of fresh water have been obtained from boreholes drilled within these beds. The limestone aquifer dips in the south west direction and reaches depths of over 200 metres around Ada. The average transmissivity of the limestone aquifer is 5.38 x 10-4 m^2/day. This is because, it is thought that the source of recharge to the limestone aquifer in the Keta area is from the Mono River of Togo as the limestone extends into Togo and even outcrops there (Hortor, 2005).

1.5.11 Groundwater use

The people living in the Keta basin depend heavily on groundwater for their water supply. Groundwater use for crop irrigation has increased substantially over the last decade. Traditionally, farmers draw water from the shallow aquifers with buckets and watering cans. Recent use of mechanised electrical pumping systems have enabled large volumes of water to be withdrawn for irrigation. Domestic use of water has increased with increase in population growth coupled with urbanisation. Majority of the people still depend on groundwater for washing and cooking purposes. Industrial use of water is minor. Actual data on the quantities of water usage in the study area are nonexistent.

1.5.12 Groundwater pollution sources

1.5.12.1 Land use

There are many sources of human activity that have the potential of polluting groundwater in the area. Agriculture, sewage, Septic tanks and solid waste disposal are the main pollution sources identified. Economic activities, especially active agriculture, continue to flourish with little consideration for groundwater protection measures. There is no centralised sewage system in the study area and residents have several household septic tanks and soak ways that discharge sewage directly into groundwater. Many old graves are unlined and pose a threat to water quality.

CHAPTER TWO

LITERATURE REVIEW

2.1 GROUNDWATER VULNERABILITY

Groundwater is a valuable natural resource used by mankind for life and economic development. In many areas of the world increases in population and demand for fresh water has led to overexploitation and pollution of aquifers from industrial and human waste. Pollution of groundwater impairs its use and poses a public health hazard through toxicity and the spread of disease (Samake et al., 2011). Once an

aquifer is contaminated it is costly and almost impossible to remediate completely. The loss of an aquifer through contamination puts stress on the remaining aquifers (Kaur and Rosin, 2009). As a result there has been a growing awareness in the field of groundwater management for the protection of groundwater resources (National Research Council, 1993; Focazio et. al., 2002; Soupios et. al., 2008). Groundwater protection strategies require the development of monitoring networks. Groundwater monitoring tools in the form of vulnerability maps are useful in an effective monitoring system. These maps have become essential tools for groundwater protection and environmental management (Al Hallaq and Abu, 2011).

The ease with which a contaminant introduced at the surface can travel to groundwater depends on the hydrogeological factors as well as its concentration (Technical Cooperation Project, 2003; Rahman, 2008). Hydrogeological conditions vary spatially. This means that the groundwater in some areas is more likely to be easily contaminated than others. This led to the concept of vulnerability (National Research Council, 1993).

The term 'vulnerability of groundwater to contamination' was introduced in 1968 by J. Margat, a French hydrogeologist (Jasem et. al. 2010). Several methods have since been developed for groundwater vulnerability assessment including those by Aller et al.(1987); Foster and Hirata, (1988); Civita, (1994); Panagopoulos et al., (2005). Vulnerability is not an absolute characteristic, but rather a relative, non-measurable, dimensionless property indicating where contamination is most likely to occur (Stigter et al., 2005). The term Vulnerability is not restricted to groundwater. It is a concept that can be used in a wider sense to describe the sensitivity of any kind of stress. It is technically feasible to assess the

vulnerability of groundwater to other hazards such as drought, flood, over- pumping and other subsurface disturbances (Ligget and Talwar, 2009; Voudouris et al., 2010).

Groundwater vulnerability to contamination is defined in agreement with the conclusion and recommendations of the international conference on "Vulnerability of Soil and Groundwater to Pollution", held in 1987 as "The sensitivity of groundwater quality to an imposed contaminant load, which is determined by the intrinsic characteristics of the aquifer" (Al Hallaq and Abu, 2011).

In this research work, groundwater vulnerability will be assessed using water quality degradation caused by contaminants as hazards. The concept of groundwater vulnerability is based on the assumption that the physical environment provides some natural protection to groundwater against anthropogenic impacts, especially with regard to contaminants entering the subsurface environment. There is no standardized definition for groundwater vulnerability; however, the concept describes the relative ease with which the groundwater resource could be contaminated. Many definitions that exist in literature are similar. In Appendix A., Carbonell et al., (1993) provide some definitions of vulnerability by various researchers to illustrate the diversity in terminology.

In this research, groundwater vulnerability is defined according to National Research Council, (1993) as the tendency or likelihood for contaminants to reach a specified position in the groundwater system after introduction at some location above the uppermost aquifer. From the definition of groundwater vulnerability two related dimensions that affect vulnerability emerge. First is the residence period of the contaminant as it travels from land surface to the groundwater. The second aspect is the contaminant attenuation. The first place of contact from contamination is the land surface and through the unsaturated or vadose zone.

It is in this zone that physical, chemical and biological processes can first occur to eliminate or render the contaminant benign before any contact with the groundwater. This makes the unsaturated zone an important factor during vulnerability assessment. Contaminants can either be released as a single event such as through spillage or as a continuous event over time as in the application of fertilizers on farm lands. Vulnerability cannot be measured directly but measurements or values of certain parameters may be used to infer vulnerability. Geologic settings, hydrological and hydrogeological conditions, land use parameters, environmental issues and soil parameters all vary from one aquifer to the other and from one area to another. These and other elements are used to determine intrinsic vulnerability.

Intrinsic vulnerability refers to susceptibility to contamination based on the hydrogeological parameters of the environment and not the nature of the contaminant. Specific vulnerability, on the other hand, considers both the physical characteristics of the environment as well as the transport properties (such as diffusion, dispersion, biodegradation) of a particular contaminant or a group of contaminants (Ligget and Talwar, 2009). Hazard considers types and concentrations of the contaminant as well as the level of toxicity.

Risk of groundwater contamination is closely related to specific vulnerability as both accounts for the pollutant. Risk is a function of vulnerability, hazard and consequence (Ligget and Talwar, 2009). In this study the consequence of losing the groundwater resource as a result of pollution is the main consideration. Parameters such as soil type, recharge by rainfall, depth to groundwater, slope of the topography, impact of the vadose zone, and aquifer media properties, in the area will be used to delineate vulnerability.

2.2 USES OF GROUNDWATER VULNERABILITY

The purpose for conducting any vulnerability assessment is important because the results will guide the kind of decisions to be made about groundwater resources protection. The National Research Council (NRC, 1993) has identified four general categories for the use of groundwater vulnerability analysis. These are:

(a) policy analysis and development: Vulnerability maps can assist decision and policy makers, land use planners and researchers to direct and prioritize resources for conservation of groundwater aquifers that are more vulnerable to pollution, and they are also helpful for educating and informing planners, managers, and decision and policy-makers about groundwater protection, risk of contamination, and contamination prevention

(b) programme management: For sustainable groundwater management, vulnerability maps are a good tool for local assessment of groundwater vulnerability potential and to identify areas susceptible to contamination. They can aid in the design of monitoring networks, and evaluation of groundwater contamination, particularly non-point contamination. Statistical probability maps may be used to assess vulnerability in areas of similar geological, hydrogeological and climatic conditions. The maps constitute a useful data source for further research either in the same area or in adjacent regions.

(c) to inform land use decisions: Vulnerability maps can help planners and regulators make informed, environmentally sound decisions regarding land use and groundwater protection.

(d) to improve general education and awareness of a regions hydrologic resources: The results can be used to educate and create the awareness with the view of increasing knowledge and understanding of the public in the study area about groundwater

resources which is a part of a large, interconnected ecological system (Bedane, 2008; Liggett and Talwar, 2009).

According to Rupert et al., (1991) typical programs that can use vulnerability maps include underground storage tanks, well (borehole) head protection, groundwater monitoring, public water supplies, agricultural chemicals, waste water management, best management practice implementation and development; harzardous waste management, land use planning and public information.

2.3 GROUNDWATER VULNERABILITY ASSESSMENT METHODS

Groundwater vulnerability assessments are a means to synthesize complex hydrogeologic information into a form useable by planners, decision and policy makers, geoscientists, and the public **(**Liggett and Talwar, 2009).They are used to analyze the effects of future human activities on groundwater resources and can be used for delineation of low, medium and high areas. Several methods and techniques have been developed to represent groundwater vulnerability either graphically or numerically including those by Aller et al (1987), Foster and Hirata (1988), Civita (1994), Panagopoulos et al.(2005).There are three broad categories of vulnerability assessment methods (National Research Council, 1993) namely:(1) Index-and- Overlay methods, (2) Process-based simulation models, and (3) Statistical models. The first category produces results that are appropriate for, water-resource decision makers who are more concerned with policy and management objectives. Process-based and statistical methods are more scientifically defensible as the results are more tied to scientific objectives. Process-based methods produce results delineating aquifer zones contributing water to the point of interest. Statistical methods produce probabilities of exceedence of set water quality targets. One characteristic of all methods is "uncertainty" in the methods and the data used for

the assessment **(**Liggett and Talwar, 2009). This research applies the first method for the characterization of vulnerability of the Keta strip.

2.3.1 Index-and-Overlay methods

These methods are used for assessing intrinsic vulnerability which considers only the hydrogeological characteristics of the area and not the contaminant factor. In these approaches data on hydrogeological parameters that are deemed to influence pollution are generated from the field or gathered from state agencies. Using Geographical Information Systems (GIS) a digital map of each parameter (for example depth to water table) is generated. Subjective numerical ratings are then assigned to each of the maps depending on how the parameter is perceived to influence pollution. The rated maps are then combined to produce an indication of spatial relative vulnerability of the area. The vulnerability is then categorised into a set number of categories (for example three categories: high, medium and low). According to Harter and Walker (2001) these methods have the advantage of being able to integrate large amounts of spatial data into maps of simple vulnerability indices. They are based on data that can readily be obtained from governmental agencies. The methods are suitable for use with Geographic Information System (GIS) and usually involve the overlaying and aggregation of multiple maps of the influencing parameters. The inclusion of many parameters in the model is more likely to increase the accuracy and decrease the probability of ignoring some important influencing parameters. It also minimises the effect of errors in the calculation of a parameter and so enhances the statistical accuracy of the model (Panagopoulos et al., 2006).

However, the subjective nature of the ratings limits this method of vulnerability characterization. Data availability and interpolation may lead to a poor representation of the

hydrogeological system, increase uncertainty and can affect the scale of the final map produced.

2.3.2 Process-based methods

Process-based methods are more elaborate than Index-Overlay processes. They do not provide output of simple relative values of low or high. These processes are mathematical simulations that take into account physical processes that govern groundwater movement and the fate and transport of contaminants in the environment. According to Liggett and Talwar, (2009) these models use deterministic approaches to estimate contaminant time of travel, concentration and duration of contamination to quantify areas of high and low vulnerability. Process based models may yield analytical solutions (e.g., Dupuit approximation under unconfined aquifer systems) or numerical approximations using computer models (e.g., MODFLOW SWAT and MIKE-SHE). Hasan et al., (1999) used MODFLOW code (McDonald and Harbaugh, 1988), the groundwater flow modeling and the USGS particle tracking code MODPATH (Pollock, 1994) to investigate the vulnerability of the Dupi Tila aquifer in the city of Dhaka, Bangladesh from induced recharge from polluted rivers and from enhanced vertical leakage from regions containing contaminated lands due to intensive abstraction. MODPATH was used to calculate particle movement and travel times within the calibrated steady-state groundwater flow field initially generated by MODFLOW. MODPATH simulations provided a demonstration of the aquifer vulnerability to contamination. They demonstrated the relative significance of each contaminant source by modeling. The results of the modelling have implications for aquifer protection, monitoring priorities and likely future trends in groundwater quality.

Results from process-based methods often require further interpretation to classify the results into specific categories such as, high, medium, low of vulnerability (Focazio et al., 2002). Process-based methods according to Evans and Maidment, (1995) have the advantage of being capable of predicting water quality spatially and with time. They however require a lot of data and are costly to develop especially if the model is to be used to assess vulnerability on a regional scale (Liggett and Talwar, 2009). Tesoriero et al., (1998) contend that though process-based methods are more sophisticated than Overlay and Index methods they do not necessary produce more accurate results. This is because process based methods often requires data that has to be extrapolated or estimated from other data, thus introducing large errors into the model. They are suitable for determining vulnerability for a source-receptor such as wells or small study areas. These models are therefore not used extensively for assessing groundwater vulnerability.

2.3.3 Statistical methods of assessing Groundwater vulnerability

These methods are based on the concept of uncertainty, which is described in terms of probability. Statistical methods correlate spatial variables with actual occurrence of contaminants in groundwater (Schleyer, 1994; Tesoriero and Voss, 1997; Tesoriero et al., 1998; Nolan et al., 2002; Twarakavi and Kaluarachchi 2005; Panagopoulos et al., 2006). Vulnerability involves the calculation of the probability of a particular contaminant exceeding a certain threshold concentration (e.g., WHO guideline limit or a national water quality guideline limit). Statistical methods usually start with an analysis and mapping of water quality from known sites e.g., samples from wells or soil. These maps can then be integrated with a set of pollution influencing factors such as geology, well depth and land use to develop a statistical model in the form of a linear regression equation (Schleyer, 1994; Evans and Maidment, 1995; Focazio et al., 2002; Nolan et al., 2002; Liggett and Talwar,

2009) These equations can then be used to predict probabilities of contamination. A further analysis allows for the elimination of insignificant influencing factors that bear little significance to the assessment process. The procedure produces weighting factors in the form of slope coefficients that optimize the use of important variables thereby removing the need for subjective influences of best professional judgment in determining the importance of each variable (National Research Council, 1993). These methods are typically used in places with diffuse sources of contamination, such as to detect nitrates over agricultural areas (Liggett and Talwar, 2009).

2.4 DRASTIC VULNERABILITY ASSESSMENTS

Many researchers have applied various techniques for the assessment of groundwater vulnerability to pollution (Carbonell et al., 1993; Schleyer, 1994; Maidment et al., 1995; Focazio et al., 2002; Stigter et al.,2005; Twarakavi and Kaluarachchi, 2005; Rahman, 2008; Ligget and Talwar, 2009; Jasem and Alraggad, 2010; Voudouris et al., 2010; Samake et al., 2011).

The DRASTIC method has been used widely by many researchers as a valuable tool for determining the sensitivity of aquifer systems (Ranjan.,2006; Rahman ,2008; Juan et al., 2009; Klug, 2009; Saidi et al., 2009; Jasem et al., 2010; Samake et al., 2011).

According to Manssone et al., (2010) the main limitation in the use of the index methods are (1) the use of qualitative definitions of groundwater vulnerability as opposed to a quantitative definition.

(2). Difficulties in gathering more information on uncertainty associated with vulnerability assessments and in developing ways to handle and display this uncertainty.

(3). Homogeneity in the results, which does not allow for discrimination and delimitation of areas of different vulnerability to pollution. This is of central importance in the development of aquifer protection strategies. Many areas around the world frequently show strong homogeneity in the results of aquifer vulnerability assessment.

Ranjan, (2006) successfully used the DRASTIC methodology in the Walawe basin in a semi-arid region of Sri Lanka to delineate five categories of vulnerability according to the hydrogeological conditions. GIS was used to develop vulnerability maps. The maps were then compared with the agricultural land use pattern of the area. It was found that areas with intense agricultural activities overlapped with the high DRASTIC index regions thus giving a good agreement between DRASTIC and polluting field activities. Such areas were then recommended to be prioritized for groundwater monitoring.

Kachi et al., (2007) successfully applied the DRASTIC method in the alluvial aquifer of the Tebessa-Morsott in Algeria. They used the principle of discretisation of the aquifer to generate detailed Vulnerability maps which compared well with water quality data of the study area. Similarly, Gougazeh and Sharadqah, (2009) used DRASTIC to assess the vulnerability of groundwater to contamination at two levels in Jordan. The first level involved calculating a DRASTIC index scale on a national scale where data was limited. Only depth to groundwater (D) and net recharge(R) parameters were considered. The result showed a category of moderate vulnerability in most parts of the country. The second level involved applying DRASTIC to the Ramtha region with a different climate and different hydrogeological conditions. The DRASTIC index corresponded to low vulnerability category.

They observed a limitation to the relative classification of the different zones based on vulnerability and questioned the effectiveness of the DRASTIC model to evaluate the vulnerability of groundwater to contamination in Jordan and other zones with similar conditions.

2.4.1 DRASTIC Model Modifications

Some studies have shown that vulnerability maps generated using DRASTIC do not compare well with water quality data from the same area. (Martinez-Bastida et al., 2009; Jasem et al., 2010; Samake et al., 2011). The subjective nature of the weighting and rating values assigned to the parameters sometimes result in DRASTIC vulnerability indexes which do not accurately represent aquifer susceptibility to pollution on the ground. Local hydrogeological settings may differ from those used by the proponents of DRASTIC. This may affect the calculated indexes. DRASTIC model results also depend on the type of overlay operation performed, the number of data layers and map units in each layer and the error or uncertainty associated with each map unit (Rahman, 2008; Samake et al., 2011).

Panagopoulos et al., (2006) listed the following criticisms by different authors on the DRASTIC method.

• So many variables are factored into the final index that critical parameters in groundwater vulnerability may be subdued by other parameters that have no bearing on vulnerability for a particular setting (Vbra and Zaporozec1994; Merchant 1994).

• The selection of the parameters is based on qualitative judgment and not quantitative studies (Garrett et al. 1989).

• Many important scientifically defined factors, e.g. sorption capacity, travel time and dilution are not taken directly into account (Rosen 1994).

• The system tends to overestimate the vulnerability of porous media aquifers compared to aquifers in fractured media (Rosen 1994).

• A test of the accuracy of the model is very difficult to carry out, because it requires that a pollutant with the properties assumed by the model (introduced into the ground surface, flushed into the groundwater via precipitation and the mobility of water) be deposited all over the test area with a uniform concentration and for a considerable time period of several years to allow the hydrogeological setting to respond (Rosen 1994).

In view of the shortcomings of the DASTIC method, some researchers have made modifications to the model (Rupert, 1999; Klug, 2009; Awawdeh and Jaradat 2009; Martinez-Bastida et al., 2009; Saidi et al., 2009; Jasem at al., 2010). Some have called for the reduction in the number of parameters (Foster and Hirata, 1988; Ruppet, 1999) while others have called for an inclusion of more factors such as land use intensity (Secunda et al., 1998). Others have yet questioned the accuracy of the DRASTIC method results (Garrett et al., 1989; Rosen L., 1994**;** Napolitano and Fabbri, 1996,). Javadi et al., (2011) state that the DRASTIC method usually gives satisfactory results in evaluation of groundwater intrinsic vulnerability to pollution, but cannot be used for accurate assessment of the groundwater pollution risk.

Piscopo (2001) conducted research in groundwater vulnerability in the Castlereagh Catchment area in Australia using DRASTIC and GIS .Due to lack of data the hydraulic conductivity parameter was not considered in the evaluation process. The researcher used a different approach from DRASTIC by replacing Net recharge with the potential of an area to receive recharge based on the amount of rainfall, slope and soil permeability. With these modifications to DRASTICS an accurate groundwater vulnerability map was produce for the area.

Awawdeh and Jaradat (2009) used a GIS based DRASTIC approach to determine areas where groundwater protection is critical. They found that though vulnerability was moderate in certain areas, nitrate concentrations were high in those areas and concluded that DRASTIC alone could not accurately depict the distribution of nitrate concentrations in the area.

In their research, vulnerability maps generated by DRASTIC were then integrated with lineaments and land use maps as a modification to assess more accurately the potential risk of groundwater pollution.

Saidi et al., (2009) using a GIS-based DRASTIC model in the assessment of groundwater vulnerability and risk mapping of the Hajeb-Jelma aquifer in Central Tunisia modified the DRASTIC parameters to reflect the local geology of the study area. Aquifer media (A) and the impact of the Vadose zone(I) were modified because some of the soil classes found in the study area do not exist in the original DRASTIC classification table by Aller et al., (1987) and there exist a wide heterogeneity of lithology in both aquifer and vadose zone.

Martinez-Bastida et al., (2009) investigated the vulnerability of groundwater in central Spain by using four methods namely DRASTIC, GOD, Composite DRASTIC index (CDI) developed by Secunda et al., (1998) and the Nitrate Vulnerability Index (NVI), a new approach based on a multiplicative model, to generate and compare maps showing specific vulnerability to nitrate pollution and to compare the intrinsic and specific vulnerability maps with the distribution of groundwater nitrate pollution. They also used the approach to analyse the reliability and the respective utilities of all the four vulnerability indexes to identify nitrate vulnerable zones. They concluded that all the four methods yielded similar results in the shallow Quaternary aquifer. The Nitrate Vulnerability index, however, showed the greatest statistical significance and offered a greater accuracy in estimating specific vulnerability with respect to the real impact of each type of land use.

Javadi et al., (2011) conducted research to assess the vulnerability potential of the Astaneh aquifer in northern Iran using the original and modified DRASTIC index. The study area mostly comprise of agricultural lands where irrigation is practiced with the use of fertilizers and pesticides. Nitrate concentration values were used to calibrate and optimise the rating values of the modified DRASTIC. Pearson correlation was used to find the relationship between the index and the measured pollution at each point. A correlation coefficient between vulnerability index and nitrate concentration was 68 percent for modified DRASTIC compared to 23 percent for the original DRASTIC. The results showed that the modified DRASTIC method is better than the original method for nonpoint source pollutions in agricultural areas. Their results further showed that nitrate concentration could be used as a modifying parameter with considerable improvement in the resulting index that could lead to more realistic management of groundwater quality.

Similarly, Samake et al., (2011) used DRASTIC with GIS to assess intrinsic vulnerability of aquifers in the Linfen basin in semi-arid northern province of China. Low indexes for vulnerability were calculated indicating less risk of pollution for groundwater. However contamination analysis indicates high levels of pollution. They concluded that the results for intrinsic vulnerability of the groundwater resource of the basin were not representative of the true levels of contamination. A sensitivity analysis was therefore performed to identify the most influential parameters on the vulnerability index. The modified DRASTIC compared well with water quality data.

2.4.1.1 Modifications from Land use

The land use system has an impact on how contaminants from the surface may travel to pollute groundwater. Land may be used for agriculture, industry or for urban settlement. Each of these land use types may influence groundwater vulnerability. The use of heavy duty

agricultural equipment for example has the tendency to either compact the soil media and make it less permeable or cut deep furrows that may enhance the transport of contaminants into the groundwater system. Burrows created by earthworms and rodents are not catered for in DRASTIC ratings. The amount of clay content and the presence of organic matter affect the soil permeability (Rupert, 2001). All these factors have the potential to influence contaminant transport.

Secunda et al. (1998) suggest that the type of agricultural practice will affect the transport of contaminants from the land surface to the aquifer. They developed a composite model along with DRASTIC by extending the number of factors to include intensive agricultural land use in their assessment of vulnerability of groundwater in Israel. They produced maps that better depicted vulnerability.

2.4.2 Model sensitivity

In order to limit the effects of subjectivity in the assigning of weights and ratings to the seven factors of the DRASTIC model, a sensitivity analysis is performed to determine the influence of the ratings assigned to each data layer (Napolitano, 1995). The outcome increases reliability and gives the actual weight of the data layer and those layers that significantly affect the vulnerability index. Many researchers (Napolitano and Fabbri, 1996; Hammouri and Kuisi, 2006; Al-Hanbali and Kondoh, 2008; El-Naqa et al., 2010) have applied sensitivity analysis to groundwater vulnerability models with the objective of reducing subjectivity and improving vulnerability maps. Napolitano and Fabbri, (1996) in the assessment of aquifer vulnerability using DRASTIC and SINTACS in the Piana Campana area near Napoli, southern Italy applied the single parameter and map removal sensitivity analyses. In their analysis the removal of each map layer generated a relevant variation in the

resulting vulnerability map. They concluded that all the seven DRASTIC parameters were significant for the area. The single parameter sensitivity was performed by first calculating the effective or real weights and comparing each weight to the theoretical weights assigned by the DRASTIC authors. They found that Net recharge was the parameter that most affected the vulnerability index as it had the highest average effective weight percentage of 26.59% compared to its theoretical weight of 17.4%. Its removal therefore greatly decreases the vulnerability index. The calculated effective weights were then used to calculate the effective DRASTIC Vulnerability index.

Babiker et al., (2004) estimated aquifer vulnerability by applying the DRASTIC model and utilized sensitivity analysis to assess the relative importance of model parameters for aquifer vulnerability in Kakamigahara Heights, Gifu Prefecture central Japan. They additionally sought to demonstrate the combined use of the DRASTIC model and Geographical Information System (GIS) as an effective method for groundwater pollution risk assessment. From the sensitivity analysis they observed that net recharge (R) has the largest impact on the intrinsic vulnerability of the aquifer followed by the soil media, topography, vadose zone media and hydraulic conductivity. Large variations in the vulnerability index were observed when net recharge (R), soil media (S) and topography (T) were removed. Net recharge and hydraulic conductivity were also found to highly influence aquifer vulnerability assessment than assumed for the DRASTIC model. The integrated vulnerability map revealed high risk on the eastern part where vegetable cultivation dominates in Land use. They concluded that land use is the dominant factor in determining groundwater contamination in the Kakamigahara Heights.

Al-Hanbali and Kondoh, (2008) evaluated the impact of human activity in the assessment of vulnerability in the Dead Sea groundwater basin, Jordan. Being an arid area, the recharge factor was modified to take into account fault lines and the intersection between the fault lines and the drainage system since these sources greatly influence the amount of water entering the aquifer system. Land use and land cover maps were used to assess the human activity impact. Human activities such as the use of fertilizers in agriculture, industries, leakages from septic tanks and sewerage systems are considered as hazards that have the effect of polluting groundwater. These human activities are categorized in the Human Activity Impact (HAI) parameter much the same way as the categorization of the depth to water ranges and ratings in DRASTIC. They verified the land use and land cover map with mean nitrate concentrations in groundwater associated with each land class (agricultural land, urban land etc.). Map removal sensitivity analysis introduced by Lodwick at al., (1990) and Single-Parameter sensitivity analysis introduced by Napolitano and Fabbri, (1996) were performed to reveal the hydrogeological factors that significantly influence vulnerability. The analyses showed that the depth to water table and hydraulic conductivity parameters have no significant impact on the model, whereas the impact of the vadose zone, aquifer media, and net recharge parameters have a significant impact on the DRASTIC model.

Similarly, Samake et al., (2010) in order to reduce subjectivity, applied sensitivity analysis to the DRASTIC parameters used in the development of vulnerability maps in the Datong basin in Northern China. Single parameter removal sensitivity analysis was performed in order to evaluate the influence of each of the seven DRASTIC parameters on the vulnerability index. Their results show that 32.5% of the total study area is under a “highly vulnerable zone”. Their results show that the seven hydrogeological parameters can be arranged in order of

importance different from the original weighting by Aller et al., (1987) in influencing vulnerability.

2.4.3 Model optimisation and calibration

Studies have shown that vulnerability maps developed using uncalibrated DRASTIC are generally poor at predicting groundwater contamination (Rupert, 1999; Rupert, 2001; Masonne at al. 2009; Awawdeh and Jaradat, 2009). The model has to be calibrated to fit the study area. Model calibration involves the use of statistical analysis as well as analytic hierarchy methods to optimize the weighting and rating values of the parameters used in the uncalibrated DRASTIC model. Calibration is done with existing water quality data. The resulting integrated model is envisaged to better predict specific vulnerability or pollution risk.

2.4.3.1 Analytic hierarchy process (AHP) and statististical methods

Analytical Hierarchy Process (AHP) sometimes referred to as the Saaty's method was developed by Saaty, (1980) and is one of a multi-criteria decision making method. It is a method to derive ratio scales from paired comparisons. In this approach the hierarchy of a set of criteria is used in a Multi-Criteria Decision Making process. A series of pair- wise comparison matrices which compares all the criteria to one another is constructed. The purpose of this is to estimate a weighting of each of the criteria that describes the importance of each of these criteria in contributing to the overall objective or final decision. The technique can be used to discriminate between competing options in the light of a range of objectives to be met (Coyle, 2004). The main advantage of the AHP is its ability to rank

choices in the order of their effectiveness in meeting objectives. Another strength of the AHP is its ability to detect inconsistent judgements (Coyle, 2004). For example, the DRASTIC factors used in the estimation of groundwater vulnerability are the criteria for arriving at vulnerability index values and subsequent maps.

Matkan et al. (2008) conducted an assessment of groundwater vulnerability to nitrate pollution in the Hamedan-Bahar plains in Iran. The objective of the study was to optimize the DRASTIC method using statistical methods and analytic hierarchy process by modifying the weights of the DRASTIC parameters. The criteria for optimization were the correlation coefficient of each of the parameters with groundwater nitrate concentrations. Pearson correlation factor was used with the aim of eliminating some factors from the DRASTIC equation. After normalizing by logarithmic transformation of the nitrate concentration data and on the basis of their statistical significance, net recharge, topography impact of the vadose zone and hydraulic conductivity were non-correlated and were eliminated from the DRASTIC equation. A new model, DAS was subsequently formed. The factor weightings were revised using Spearman's rho and Kendall's tau correlation coefficients. Using the revised weights and after eliminating the four factors, the DAS equation was modified as $\mathbf{V_{(intrinsic)} = 3.5\,D + 4\,A + 5\,S}$ Where $V_{(intrinsic)}$ is the intrinsic vulnerability, D is the depth to groundwater; A is the aquifer media and S the soil media.

Analytic Hierarchy Process (AHP) method was also applied to revise the weights. On the basis of the weights extracted from AHP method, the correlation between vulnerability indices and nitrate concentrations using AHP is 0.65. A comparison of the correlation coefficients from the various methods applied, the DAS model with deterministic layers was selected as the best model and was used to estimate intrinsic and specific vulnerability or the pollution risk of groundwater in the Hamedan-Bhar plains.

Elçi (2010) applied the optimisation method in the Tahtali stream basin in Iran. The main objective of the study was to optimize the conventional DRASTIC method and show the applicability of the optimisation method with a case study. Raster layers were constructed that represent the factors contributing to surface-originated groundwater contamination. The vulnerability of the stream basin to groundwater contamination was mapped using the original DRASTIC approach. The model was subsequently optimized using groundwater nitrate concentration measurements as surface-originated conservative contaminants for the basin. The author used statistical correlation method to calculate correlation coefficients between nitrate concentration values and the DRASTIC parameters. These coefficients were used to revise the conventional DRASTIC parameter weighting coefficients. The correlation coefficient between measured nitrate concentrations and corresponding vulnerability ratings increased from 0.589 (for the original DRASTIC) to 0.653 (for the optimised DRASTIC) Optimised vulnerability maps were produced which compared well with groundwater nitrate concentration data.

In this research the seven parameters of DRASTIC will be analysed using statistical and the Analytic Hierarchy methods in order to optimise the weights and ratings to be used for developing groundwater vulnerability maps for the study area.

2.4.4 Model validation

The efficacy of any model depends on its validation or verification. Traditionally DRASTIC results have been used to correlate field water quality data as a measure of validation of the model performance (Rupert, 1999; Antonakos and Lambrakis, 2006). Vulnerability maps are expected to show the potential for groundwater pollution from anthropogenic or natural sources. If groundwater is vulnerable then it is presumed that residues of the pollutant from

the type of activity on the land surface will be able to travel through the subsurface and reside in the groundwater (Jasem and Alraggad, 2010). For example, in urban areas, nitrate concentrations from laboratory analysis are used to determine the degree of water pollution in different parts of the aquifer (Jasem and Alraggad, 2010). In order to show the degree of accuracy of the vulnerability index for the various parts of the aquifer, pollutant concentration maps are drawn and compared with the vulnerability maps to indicate the correctness of the methods and parameters used in the vulnerability model (Jasem and Alraggad, 2010). The vulnerability map may also be compared to the land use map. Areas where intensive agriculture is practiced and residential areas have high potential for polluting groundwater resources.

2.5 CHOICE OF DRASTIC MODEL

From literature there are different methods by which groundwater vulnerability to pollution can be assessed. DRASTIC was selected based on the following reasons. Firstly, the DRASTIC model is best known and has been applied widely and is therefore well tested (Kachi et al. 2007; Atiqur, 2008; Yang and Wang, 2010; Voudoris et al. 2010). Data on parameters such as rainfall and depth to water are readily available over a large area making the model suitable for regional scale assessments (Yang and Wang, 2010). It is suitable for mapping vulnerability in porous media similar to the quaternary formations within the study area. Higher number of parameters is included in the DRASTIC model. It is, therefore, expected that this model will provide a greater degree of accuracy in the vulnerability maps that will be produced in this research.

2.6 THE DRASTIC VULNERABILITY MODEL

The most widely used index and overlay method is DRASTIC developed by Aller, et al. (1987). DRASTIC is an acronym for the parameters included in the method: **D**epth to groundwater, (Net) **R**echarge, **A**quifer media, **S**oil media, **T**opography (Slope) **I**mpact of vadose zone media, and hydraulic **C**onductivity of the aquifer. In this approach spatial data set on all the parameters are combined in a map to determine vulnerability. A brief description of the DRASTIC model parameters is presented below.

2.6.1 Depth to water, (D). This represents the depth to the water table from the ground surface. It determines the distance through which pollutants have to travel before reaching the water table. The deeper the water table, the lower the chance for pollution to occur.

2.6.2 Net recharge, (R). This represents the amount of water that penetrates the ground surface and reaches the water table. It acts as a vehicle for transporting pollutants to the water table through the leaching process.

2.6.3 Aquifer, (A). It refers to the saturated zone material properties which controls the pollutant permeability and attenuation processes.

2.6.4 Soil media, (S). This is the uppermost weathered portion of the unsaturated zone characterised by significant biological activity, which controls the amount of recharge that can infiltrate downward. It is also within this zone that natural biological processes may eliminate or render the pollutant benign.

2.6.5 Topography, (T). This represents the slope of the land surface and dictates whether or not precipitation runoff will remain on the surface to allow contaminant percolation to the saturated zone.

2.6.6 Impact of vadose zone, (I) It represents the type of material in the zone above the water table and below the typical soil horizon (unsaturated zone material), which controls the passage and attenuation of the contaminated material to the saturated zone.

2.6.7 Hydraulic conductivity of the aquifer, (C) It indicates the ability of the aquifer to transmit water, and, hence, determines the rate of the flow of contaminant material within the groundwater system.

According to Aller et al., (1987), the authors of the DRASTIC manual, the most important assumptions to be considered when using DRASTIC to assess vulnerability are that, the contaminant is introduced at the ground surface, it is flushed into the groundwater by precipitation and has the mobility of water and the area should not be less than one hundred acres (i.e. 0.4 km^2 or larger).

The DRASTIC approach provides a numerical ranking composite description of all the major geological and hydrological factors that affect and control groundwater movement into, through, and out across the vertical profiles of an area (Yang and Wang, 2010).

According to Aller et al., (1987) ratings and weights are assigned to the seven model parameters according to the significant media types or classes of each parameter. These classes and ranges are rated on a scale of 1 to 10 based on their relative impact on groundwater pollution potential.

The seven parameters which reflect the key mechanisms of the groundwater pollution pathways are then assigned weights ranging from 1 to 5 based on their relative importance in groundwater pollution process. The relative significance of each factor was determined using the Delphi approach which quantifies the opinions from single and multiple experts in the field of groundwater pollution. The most significant factor has a weight of 5 and the least significant one has a weight of 1. The DRASTIC Index **(DI)** which is a relative measure of groundwater pollution potential is then computed from equation 2.1.

$$\mathbf{DI=DrDw+RrRw+ArAw+SrSw+TrTw+IrIw+CrCw} \qquad \mathbf{2.1}$$

Where D, R, A, S, T, I and C are the parameters and the subscripts **r** refers to the rating value and **w** refers to the weight. A higher DI for a site means the site is more susceptible to pollution than a site with lower DI. According to Piscopo, (2001) similar hydrogeologic parameters therefore produce similar vulnerability.

The relative measure of this procedure requires that specific site investigations be conducted to assess the extent of pollution. The quantitative DRASTIC Index results (numbers) are converted back to qualitative risk categories after dividing the results into convenient ranges such as low, medium and high.

The weights of D, R, A, S, T, I and C in equation (1) are 5, 4, 3, 2, 1, 5 and 3, respectively, for general pollutant, while they are 5, 4, 3, 5, 3, 4 and 2 for pesticide groundwater pollution vulnerability calculation

CHAPTER THREE

MATERIALS AND METHODS

3.1 DATA ACQUISITION AND DESCRIPTION

Various data was collected in order to achieve the goal of this research. Data collection was done from field work, laboratory analysis and from previous reports of research conducted in the area. Governmental agencies were also contacted for data. Some of the data was used for this research. Data on depth to water, elevation, aquifer media, soil media and hydraulic conductivity were gathered from the field and combined with data from Banoeng-Yakubo et al., (2005) for this study. The type of data, what the data was used for, and the sources are shown in Table 3.1.

Table 3.1 Data used for construction of DRASTIC parameters

Data Type	Source	Used to produce
Well data (Static water level)	Field data and UNEP Reports	**D and R**
Soil sample analysis	Field data	**A, I, S and C**
Elevation data	Field data	**T**
Digital topographic map of study area	Ghana Survey Department	

3.1.1 Depth to water (D)

Depth to water was determined using data from Banoeng-Yakubo et al., (2005) on static water levels (SWL) from 108 dug wells measured for a period of two years (2003-2005) with known geographic coordinates in the study area. The static water levels were measured again in October, 2010 by the author. The Static water levels were measured with reference to the ground surface using an Elwa EL-30 well sounder for all the wells. In order to maintain a common altitude datum for the depth measurements, the elevations of 21 wells spatially distributed to cover the study area were measured with reference to the National Mean Sea Level (NMSL) datum located at Light house, James Town, Accra using two Trimble differential Geographic Positioning Systems (GPS). The differential GPS applied real time kinematics (RTK) processes to calculate the altitude of each well. The depth to water table was obtained by subtracting the mean static water levels measurements from the well elevation measurements.

3.1.2 Topography

The RTK elevation data used to determine the depth to water values were used for the determination of topography. The elevation data will be used to produce a digital elevation map (DEM) of the area. Percentage slope will be calculated from the DEM using ArcGIS and used in the evaluation of vulnerability.

3.1.3 Aquifer media (A)

The study area is located in a coastal Quaternary unconsolidated deposits made up of mainly sand, gravel and clay. Core rock samples were taken using a 3.5cm core barrel from one meter and two meter depth at each of the 16 sampling point and stored in polyethylene bags. Samples from one meter depth which were dry were considered soil media while samples

from two meter depths which were wet were considered aquifer material. Soil and aquifer media were taken for analysis at the Soil Research Institute laboratory, CSIR, Accra.

Sieve analysis was performed on the samples from 2 m depth to determine grain size distribution and aquifer media types for each sample location. A representative sample weighing 400 gm was taken in the laboratory from quartering. The weight was dried in an oven and placed on top of standard sieves with the coarsest at the top and the finest at the bottom. The top sieve was covered and the nest was shaken mechanically for 5 min. The soil material remaining on each sieve and the bottom pan was weighed. The percentage of material passing through each sieve was plotted against particle size in millimetres on a log normal graph sheet for each sample to give a grading curve. The samples were then classified into particle size classes such as sand, gravel etc. This procedure was used to determine aquifer and vadose zone media.

3.1.4 Soil media (S)

Soil analysis was carried out on soil samples from 1m depth to determine the soil types. A similar procedure that was used for determining aquifer material was followed. However soil samples suspected to contain carbon were further heated to about 550^{o}C for about four hours. The samples were allowed to cool in a desiccator and weighed before sieve analysis. Soil classification was based on particle size, carbon and clay content.

3.1.5 Influence of Vadose zone media (I)

The vadose zone in the study area is relatively thin when compared to the depth of the water table. This was evident from the core samples taken for soil and aquifer media. Under such thin vadose media conditions the aquifer media and vadose media are considered the same (Qamhieh, 2006). This condition was applied in the research.

3.1.6 Net recharge

Seasonal fluctuations in the water table in the study area were used to estimate net recharge. Determination of net recharge using water table fluctuations method is suitable for areas with thin vadose zones where the water levels respond quickly to precipitation (Saidi et al., 2009). The sandy Quaternary aquifer in the study area has a relative thin vadose zone and therefore the method can be used. The water table fluctuations were determined from measurements of static water levels for each of the 108 wells averaged over a two year-period. The difference between the maximum and minimum averaged static water level at each well location was considered as the value for the water table fluctuation. Core samples of aquifer material were taken at 16 of the well sites for soil analysis to determine the aquifer material type around each well. The water table fluctuation values were then multiplied by the specific yield of the aquifer media type at each of the well locations to obtain the net recharge for the location. The Specific yield of the aquifer media was determined from Anderson and Woessner (1992). The net recharge was calculated from equation 3.1.

$$R = WTF \times S_y \qquad 3.1$$

Where R is the recharge, WTF is the mean annual Water Table Fluctuation and S_y is the specific yield of the aquifer material at the well location.

3.1.7 Hydraulic conductivity

Hydraulic conductivity was determined from laboratory analysis of the aquifer media. For unconsolidated sand-size sediments hydraulic conductivity may be estimated from laboratory grain size analysis (Anderson and Woessner, 1992). Haven determined the aquifer media types, established empirical methods were used to calculate hydraulic conductivity of the

different aquifer media from grain-size analysis**.** From the grain-size distribution curves the samples were classified into media types. The diameters of soil particles at 10%, 20% and 50% cumulative weight were determined from the curves and the coefficients of uniformity, intercepts and porosity values were calculated. Hydraulic conductivities were then calculated using the Kozenzy-Carman, Slitcher and USBR empirical formulae which are suitable for this unconsolidated sediments (Odong, 2007). The kinematic coefficient of viscosity is also necessary for the estimation of hydraulic conductivity, a value of $0.0874 m^2$/day derived for a water temperature of 20^oC was assumed in this study (Odong, 2007).

3.1.8 Groundwater quality data

Groundwater quality data of the study area was derived from UNEP report (Banoeng-Yakubo et al., 2005) and from groundwater sampling by the author. The data provides information on residues of pollutants from ground surface which have travelled down into groundwater and will be used to validate and optimized the DRASTIC model.

Groundwater samples were collected from eighty one (81) hand dug wells during the duration of the study. The samples were analyzed to determine some water quality parameters and their spatial variation in the study area. Sample bottles were prepared at the Chemistry Department of the University of Ghana by washing with a diluted solution of hydrochloric acid and deionized water. The same procedure was followed before each sample was taken in the field. Prior to sampling, each well was purged by drawing from it five to six buckets (size 30) of water. The pH, temperature and electrical conductivity (EC) were measured in situ. The samples were stored in an ice chest and transported to Accra the same day for analysis. The samples were filtered through a 45 micron filter and analyzed for major and minor ions at Ghana Atomic Energy Commission (GAEC), laboratory Accra.

Major ions like K^+, Na^+ were determined using Sherwood flame photometer model 420. Ca^{2+}, Mg^{2+} were determined using the Varian 420 atomic adsorption spectrometer and Cl^-, SO_4^{2-}, NO_3^- were determined using the Dionex DX 120 ion chromatograph in milligram per liter (mg/l). About 0.3mls of the sample was introduced by means of a syringe into the ion chromatograph. The ionic and inorganic elements based on molecular weight and valence charge strength were separated.

The bicarbonate ion concentration in the water was determined by titration. 10ml of the sample was pipetted into a volumetric flask. One drop of methyl orange was added and titrated against a standard acid (0.02 M HCl) until the colour changed from yellow to orange and the volume of acid used was recorded. The bicarbonate ion concentration in milli mol per liter was then calculated from equation 3.2.

$$\left[HCO_3^-\right] = \frac{[V_{THCl}]\times[M]}{a} \times 1000 \qquad 3.2$$

where V_{THCl} =Total volume of HCl used. M = Concentration of HCl and a =Volume of groundwater sample

3.2 DEVELOPMENT OF DRASTIC MODEL

ArcGIS 9.3 (ESRI 2007) software package was adopted as a tool for the evaluation of the DRASTIC model because of its advantages for spatial data management and visualisation. It was used in data preparation, processing, and analysis of the raster layers. The raster approach was used in the preparation of the seven thematic maps of the DRASTIC factors. In this approach regularly shaped cells divided in equal fashion similar to spread sheet rows and

columns, are used to subdivide space and every object within the map is covered by a grid or cell. Geographical positions are defined to the nearest cell position. Each cell or pixel is assigned one attribute value even if there are different attributes present within the same pixel. For example, in a raster map of Aquifer media (A) one cannot assign values for conductivity in the same pixels. Two separate files will have to be created and stored separately for Aquifer media (A) and Conductivity (C) . The smallest size of objects that can be represented on the map will be governed by the size of the pixels (Haag and Haglund, 1998).

3.2.1 Conceptual model

The DRASTIC model describes aquifer vulnerability in terms of seven influencing hydrogeological parameters. The contaminant is generated at or near ground surface and is flushed down through the geological setting to the groundwater. The thickness and types of the geological material influence the degree to which the aquifer may be susceptible to pollution. The model attempts to predict vulnerability with an index outcome. The relation of the parameters to the index outcome is expressed as a mathematical equation. The index outcome is calculated from the parameters that go into the equation. The DRASTIC Index **(DI)** which is a relative measure of groundwater pollution potential is then computed from equation 3.3.

$$DI=D_rD_w+R_rR_w+A_rA_w+S_rS_w+T_rT_w+I_rI_w+C_rC_w \qquad 3.3.$$

where D, R, A, S, T, I and C are the parameters and the subscripts **r** refers to the rating value and **w** refers to the weight. A higher DI for a site means the site is more susceptible to pollution than a site with lower DI.

3.2.2 Model data Preparation

The data gathered was used to construct the various spatial distributions of the DRASTIC parameters. The data was evaluated by examining and eliminating very extreme values especially the water quality data. Statistical evaluation was conducted by plotting scatter diagrams and a test of normal distribution was done on the data. Thematic maps of each of the parameters were then developed by interpolation methods in GIS and used in the calculation of the final vulnerability Index. The final results of the study were then analysed using GIS and statistical methods. A flow chart of the GIS procedure followed in the preparation of the seven thematic maps and the final vulnerability index is shown in Figure 3.1.

The following are the steps followed in generating the raster map of each parameter

Step 1 Store raw field attribute data of parameter in Excel format

Step 2. Export data to GIS as a shape file

Step 3. Convert Coordinate system from geographic to national grid

Step 4. Interpolate feature to raster

Step 5. Classify

Step6. Convert raster to polygon

Step 7. Clip polygon with base map

Step 8. Convert map back to raster

Step 9. Reclassify to obtain raster map of parameter

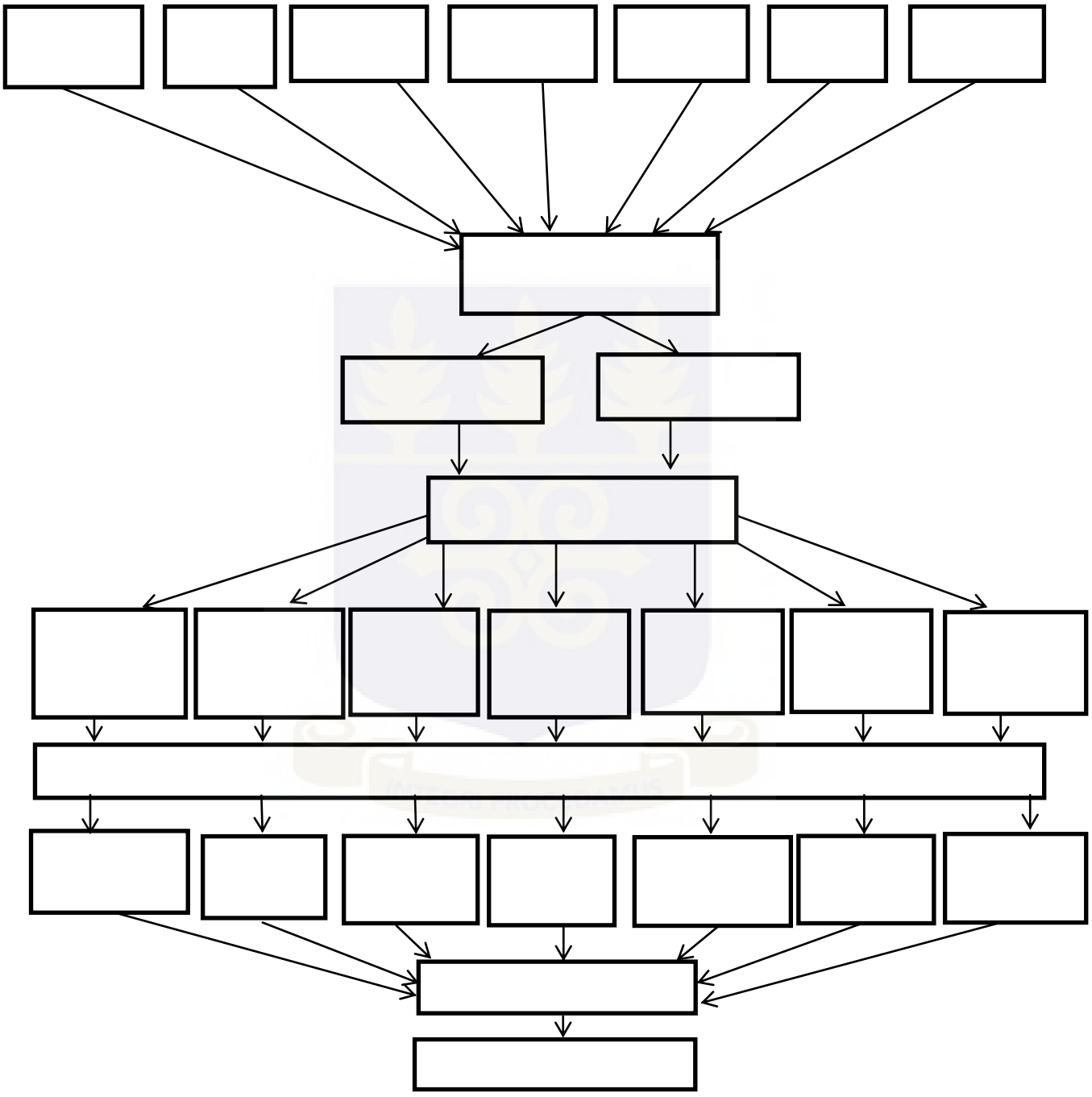

Figure 3.1 Flowchart of GIS methodology (Modified from Thapinta, 2002)

A map of the study area was clipped from a digital topographic map of Ghana in Computer Aided Design software (CAD) format obtained from Ghana Survey Department. The different data on the DRASTIC parameters was processed, and linked with the base map. Geographic features such as Depth to Water, topography and recharge values were calculated directly from static water levels and elevation measurements. Hydraulic conductivity was estimated from empirical formulae based on aquifer media grain size distribution for each sample. Geologic factors such as aquifer, soil and vadose zone media were assigned rating values following the DRASTIC manual (Aller et al., 1987). This was done to enable the conversion of the geologic factors to raster through interpolation. Attribute tables on all the seven parameters from the field were prepared and stored as separate files in excel format. Each excel file was then exported into GIS platform and stored as a shape file. These shape files were used to generate raster rating maps through interpolation.

3.2.3 Model data processing

Interpolation methods were used to convert the shape files into raster layers. The raster layers were classified and converted to polygon features. This conversion of raster feature to polygon was necessary because the base map was obtained from CAD as a polygon feature. Each of the factor feature polygon was then clipped with the base map of the study area. The clipped features were then converted back to raster to form the raster factor raster layers. The National grid coordinate system is used for geographical locations of all points in this research work. These raster layers or thematic maps were used as model input parameters.

3.2.3.1 Interpolation methods

The purpose of interpolation is to create raster surfaces for all the DRASTIC factors. This is achieved by, interpolating a spatially continuous variable from point samples. Spatial

interpolation assumes a field-based conceptual model of space; that a variable of interest varies continuously over the study area.

In general the larger the number of sampled points the more accurate the results of the interpolation. Interpolation techniques are necessary because of high cost and limited resources in data collection (Sutton et al. 2009).

Three interpolation methods available in ArcGIS 9.3 and used in this study to model spatially distribution from point data are Inverse Distance Weighting (IDW), Spline and Ordinary Kriging (OK). Deterministic and geostatistical techniques are the two main categories of interpolation. Deterministic methods create surfaces from measured points or from mathematical formulae (Sutton et al. 2009). The IDW and Spline methods belong to this category. Geostatistical techniques are based on statistics and include some measure of certainty or accuracy of prediction. The Kriging method belongs to this category (Sutton et al. 2009).

Data collection was done in a limited number of selected locations. The data obtained for each parameter was first evaluated by eliminating extreme values. Simple statistical test for normality by checking the skewness of the data and plotting of scatter diagrams were also applied to ensure that data used for the research was suitable. The three different interpolation methods were applied to each parameter data set and the results of each method were evaluated using the cross validation procedure. The procedure involved withholding a small subset of the sample points from the interpolation process. After interpolation, estimated values at withheld sample points were checked with the observed values at those locations. The predicted values were subtracted from the withheld (observed) values to give an error estimate of the interpolation method. The interpolation method that produced the least error was adopted for the data set.

The spatial analyst tool of ArcGIS 9.3 was used to interpolate the data and to create raster surfaces.

3.2.3.1.1 Inverse Distance Weighted (IDW)

The inverse distance weighting (IDW) is one of the most commonly used method of interpolation of scatter points (ESRI, 2010). It is fairly accurate under a wide range of conditions (Lam, 1983). The interpolating surface is a weighted average of the sampled points. To predict a value for any unmeasured location, IDW uses the measured values surrounding the prediction location. The measured values closest to the prediction location have more influence on the predicted value than those farther away. It assigns greater weights to points closest to the prediction location, and the weights diminish as a function of distance, hence the name inverse distance weighted (Esri, 2010)

A general form of finding an interpolated value Z(**x**) at a given point **x** based on **n** samples using IDW is given by the interpolating function:

$$z(\mathbf{x}) = \sum_i w_i z_i \Big/ \sum_i w_i \qquad \textbf{3.1}$$

where w is some function of distance (d), $w_i = 1/d^p$, $i = 1 \ldots\ldots n$, p is the weighted power.

It can be seen from the equation that the weighted power ***p*** in effect controls the region of influence of each of the sampled locations. As ***p*** increases the region of influence decreases until in the limit it becomes the area which is closest to point ***x***. When ***p*** is set to zero, the method is identical to averaging the sample values.The inclusion of more points for averaging means more distant points will have an influence or the local estimate and the overall surface is expected to be smoother. Some of the advantages of IDW include: IDW is an exact interpolator, where the maximum and minimum values in the interpolated surface occur at sample points. No interpolated value will be outside the observed range of sample values.

IDW can be used when the set of points is dense enough to capture the extent of the local variation needed for analysis (ESRI, 2010). Generally, the IDW method is particularly well suited to deal with abruptly changing data because it can incorporate barriers into its estimation process (Thapinta, 2003). The IDW interpolation method also has some disadvantages: The quality of the interpolation result can decrease, if the distribution of sample data points is uneven. Maximum and minimum values in the interpolated surface can only occur at sample data points. This often results in small peaks and pits around the sample data points (referred to as "bull's eye") and edgy surface. IDW does not provide prediction standard errors and so justifying the use of this model may be problematic (Sutton et al.,2009).

ArcGIS 9.3 uses the default value of p = 2 for a variable search radius using 12 points for averaging. This default settings were used to interpolate all the parameters except topography.

3.2.3.1.2 Spline

Spline is a deterministic interpolation method which fits mathematical function through input data to create smooth surface. The Spline method is an interpolation method that estimates values using a mathematical function that minimizes overall surface curvature, resulting in a smooth surface that passes exactly through the input points. Spline uses a piecewise polynomial to provide a series of patches resulting in a surface that has continuous first and second derivatives (Childs, 2004). There are two Spline methods: Regularized and Tension. The Regularized method creates a smooth, gradually changing surface with values that may lie outside the sample data range. The Tension method controls the stiffness of the surface according to the character of the modeled phenomenon. It creates a less smooth surface with

values more closely constrained by the sample data range (ESRI 2007). Spline can generate sufficiently accurate surfaces from only a few sampled points and they retain small features. Spline works best for gently varying surfaces (Renade et al.,2008). Spline interpolation is better for showing a gradually changing surface while the IDW method is better for showing extremes in the data. Spline interpolation would also be the better choice for irregularly spaced data. This method is best for gently varying surfaces such as elevation, water table heights, points or pollution concentrations (Thapinta,2009). The Spline method has some advantages namely: It produces a continuous surface with minimum curvature output on a raster. The maxima and minima do not necessarily occur at the data points. It is a local interpolator and can be exact and used to smooth surfaces. The method is however poor for surfaces which show marked fluctuations as this can cause wild oscillations in the spline (Renade et al.,2008).

The spline method was used to interpolate the topography data. This was after the IDW and kriging were dropped as a result of producing higher error margins.

3.2.3.1.3 Kriging

Kriging is a geostatistical interpolation method based on 3 main components of the sample data: the spatial trend, spatial autocorrelation, and random variation. These three are combined in a mathematical model to create an estimation function. The function is then applied to the data for the sample points and used to estimate values over

the surface of the study area. The basic tool of kriging is the semivariogram. The semivariogram is used to model the spatial autocorrelation (spatial relationships between sample points) instead of assuming a direct, linear relationship with separation distance to obtain estimates for the weighting parameters. (Renade et al.,2008). A simple variogram model is shown in Equation 3.5

$$\gamma(h) = \frac{1}{2N_h}\sum_{i=1}^{N_h}(z_i - z_{i+h})^2 \qquad 3.5$$

Z_i is the measurement of a regionalized variable taken at location i ,

Z_{i+h} is another measurement taken h intervals away from i

N_h is number of separating distance = number of points –Lag (if the points are located in a single profile)

The variogram yields the size of the zone of influence, the isotropic nature of the variable, and the continuity of the variable through space. It in effect controls the way that kriging weights are assigned to data points during interpolation and consequently controls the quality of the results. The Krige operation has been designed specifically for map layers that contain a sparse matrix of data.

One weakness of kriging is that the original data points are seldom honored. This is a common problem associated with grid based interpolation methods. It may lead to the dilemma that contours generated from the surface appear on the wrong side of observed data points. Another problem associated with kriging is the estimation of semivariogram. It is not always easy to ascertain whether a particular estimate of the semivariogram is in fact a true estimator of the spatial correlation in an area. The reasons for choosing a particular semivariogram to fit the given data set are often difficult to explain in terms of physical processes. They can only be rationalized in terms of a least-squares on maximum likelihood fit to the data set. Finally, kriging is not a suitable method for data sets which have anomalous pits or spikes, or abrupt changes such as breaklines.

In this research kriging interpolation was not applied because the margin of errors were higher for all the data sets.

3.2.3.2 Raster Layers and classification

Interpolation of the parameter shape files created raster layers for the seven parameters. This process generated a continuous grid from the sampled point values. The continuous grid contains a number of predicted values in which each of them represents an attribute value for a cell.

3.2.3.2.1 Rating layers

ArcGIS automatically classifies the raster map into ranges and class values. The classes were reclassified according to the DRASTIC manual to produce the rating maps.

3.2.3.2.1.1 Depth to water, (D)

The depth to water (D) shape file was converted to a continuous raster grid using the Inverse Distance Weighting (IDW) interpolation methods in ArcGIS. The depth to water table map was classified into ranges and assigned ratings according to the DRASTIC manual from 5 with minimum impact on vulnerability to 10 with maximum impact. In order to generate a depth to water rating map, the water table map was reclassified using the spatial analyst feature on ArcGIS. Each rating was multiplied by the factor weight to produce the factor Index. This procedure was repeated to generate factor indices for all the parameters.

3.2.3.2.1.2 Net Recharge

The IDW interpolation technique in was used to construct the net recharge map using the recharge shape file. The recharge map was classified into ranges and assigned ratings from 6 to 10 according to the DRASTIC manual. High recharge rates were assigned high numerical rates.. The recharge map was reclassified to generate net recharge rating map.

3.2.3.2.1.3 Aquifer Media

The IDW interpolation was applied to the aquifer media shape file to generate the rating map of aquifer media. The map was reclassified and rating values of 4 to 10 were assigned.

3.2.3.2.1.4 Soil media (S)

Similarly, the soil media shape file was interpolated to generate the soil media rating map using IDW interpolation techniques. The map was reclassified and rating values from 4 to 10 were assigned.

3.2.3.2.1.5 Topography

Using the spatial analyst in ArcGIS Spline interpolation was used to construct a spatial distribution of slope. The resulting slope distribution was divided into ranges and assigned ratings following the DRASTIC manual standards The slope map was reclassified to generate a topography (%slope) rating map.

3.2.3.2.1.6 Impact of vadose zone (I)

The vadose zone in the research area is thin and can therefore be considered the same as the aquifer media (Qamhieh, 2006). However the superior weighting of (5) of the impact of the vadose media will influence the overall vulnerability differently from the aquifer media. The rating map was generated from the vadose media shape file using IDW methods. The map was reclassified and ratings assigned from 4 to 10.

3.2.3.2.1.7 Hydraulic conductivity (C)

The IDW interpolation method was used to generate the hydraulic conductivity map from the conductivity shape file. The conductivity map was reclassified to generate the hydraulic conductivity rating map. The rating map was assigned rating values from 6 to 9.

3.2.3.2.2 Parameter vulnerability index

Parameter vulnerability index maps were created to evaluate the degree of vulnerability contributed by each parameter to the overall DRASTIC vulnerability of the area The maps were generated by interpolating the (multiplication of rate by weight) column in the attribute table. This procedure was done for all the parameters to produce seven parameter vulnerability maps.

3.2.3.3 Overlay process

The index raster layers generated from interpolation were combined to produce a composite layer. The layers were added arithmetically using the raster calculator feature on ArcGIS to produce an uncalibrated DRASTIC model referred to as intrinsic vulnerability map. This map delineates the groundwater intrinsic vulnerability to pollution.

3.2.4 Data analysis

Studies have shown that intrinsic vulnerability maps developed using uncalibrated DRASTIC models are generally poor at predicting groundwater contamination (Rupert, 1999; Rupert, 2001; Masonne at al. 2009; Awawdeh and Jaradat, 2009). The model was tested to establish its accuracy in predicting groundwater vulnerability in the study area or otherwise.

3.2.4.1 Model Test

The DRASTIC model provides vulnerability indices which indicate how susceptible the aquifer is to pollution from ground-surface activities. If the aquifer is indeed vulnerable then residue of the ground-surface pollutants should be able to penetrate and reside in the groundwater below. To test this statement samples of groundwater from the unconfined aquifer in the study area were taken and analyzed in the laboratory. Groundwater nitrate concentration was used as the pollution index in this research. Generally groundwater nitrate concentration of 3 mg/l and above is above naturally occurring concentration levels and the aquifer has been impacted by anthropogenic activities (Tesoriero and Voss, 1997). Agricultural activities and urban settlements are found in most parts of the study area. Nitrates from agricultural and domestic sources therefore constitute the main ground-surface contaminants in the study area. Nitrate concentrations above 10 mg/L in drinking water pose a potential health hazard to humans (USEPA, 1996a). The United States Environmental Protection Agency (USEPA) has therefore proposed nitrate as a representative indicator of groundwater quality degradation (US Environmental Protection Agency, 1996a). Many researchers (Babiker et al., 2004; Awawdeh and Jaradat, 2009; Saidi et al., 2010; Hasiniaina et al., 2010; Elçi, A., 2010; Javadi et al., 2011) have used groundwater nitrate concentration data to calibrate, optimize and validate Drastic based vulnerability models.

A study of data from the study area over two years shows that the water table levels rose to their highest in the month of April leading to a corresponding highest increase in the concentration if nitrates. April, 2004 nitrate concentration data from55 wells in the study area were therefore selected and compared with the intrinsic vulnerability map of the area.

3.2.4.2 Model Calibration

DRASTIC model results depend on the values of the weights and ratings, the type of overlay operation performed, the number of data layers and map units in each layer and the error or

uncertainty associated with each map unit (Rahman, 2008; Samake et al., 2011). Subjectivity is inherent in the selection of the number of parameters, their weights and rating values. Subjectivity leads to doubts about the accuracy of the DRASTIC results. One approach to addressing subjectivity is by the use of statistical correlations analysis and analytic hierarchy process. Statistical correlation was applied to the parameter rating values and nitrate concentration data from the study area to optimize the weights and rating values and to eliminate some parameters of groundwater vulnerability to pollution in the study area.

3.2.4.2.1 Statistical Correlation Methods

Correlation coefficients are a measure of the strength of association between two continuous variables. Correlation is performed to see if one variable generally increases as the second increases, whether it decreases as the second increases, or their patterns of variation are totally unrelated. It does not provide evidence for causal relationship between the two variables (Helsel and Hirsch, 1992).

Statistical correlation analyses were performed to establish whether the parameters of the intrinsic vulnerability methodology are statistically significant in explaining the variation in groundwater nitrate concentration. In this respect correlation was used to compare nitrate concentration values and the vulnerability scores of the seven parameters affecting groundwater vulnerability at each sampled points. The score values were determined by superimposing the raster layer of the nitrate sampled points on each of the factor vulnerability layer of the seven parameters. The vulnerability score value was then extracted at each nitrate point. The purpose of this is twofold; first the correlation coefficients were used to select effective parameters and secondly to determine the appropriate parameter weights. The criterion for selection was based on the value of the correlation coefficient. The weights were then used to revise the conventional DRASTIC parameter weighting coefficients. The

Microsoft excel XLSTAT 7.5.2 add-on statistical package was used for correlation. Pearson (r), Spearman(ρ) and Kendall (τ) are the three types of correlation methods applied in this research. Pearson is a parametric statistical correlation method that assumes that data is normally distributed (Matkan et al., 2008). Spearman's rho and Kendall's tau correlations are non-parametric and are more suitable for ranked values (Elci, 2010). The parameter ratings in this study are ranked values and therefore non-parametric correlation methods can be used. However a preliminary scatterplot of the nitrate concentration data indicates that the data is not normally distributed. The data had to be normalised by a log transformation before applying Pearson method. Where the correlation coefficient was not statistically significant, the parameter was eliminated from the DRASTIC equation. The new weightings for the remaining effective factors were calculated from the correlation coefficients of the effective parameters by reducing them to a linear scale with a maximum value of 5 and a minimum value of 1, as defined by the DRASTIC model.

3.2.4.2.1.1 Correlation to determine effective parameters and weights

In this section statistical correlation to compare nitrate concentration values and parameter rating values was used to determine which DRASTIC parameters had a significant influence in causing groundwater nitrate pollution and also to revise the weighting scheme of the parameters. Fifty five samples of nitrate concentration data in April, 2004 were plotted on each parameter rating map. The rating values were extracted at each of the nitrate points. This was done for all the seven parameters. The pair of nitrate values and corresponding rating values were used to perform the correlation tests. The criteria for effective parameters and the revision of weights was the value of the correlation coefficient. The range of correlation coefficient values obtained were rescaled by a linear transformation to a scale of 1 to 5 to obtain the modified weighting coefficients. Correlation coefficients of parameters that were

not statistically significant or were too low compared to the others were eliminated from the DRASTIC equation to obtain the optimized weights and effective parameters.

3.2.4.2.1.2 Correlation to revise rating values

After eliminating those parameter that were not statistically significant ,the rating values were modified by using the mean nitrate values and the original ratings. April 2004 nitrate concentration data was plotted on each of the effective parameter rating maps. Nitrate values were then extracted from all sections of the rating map. The mean value of nitrate in each category was then calculated. For example, after plotting the nitrate values on the depth to water rating map, nitrate values were extracted from all sections of the map with rating value of 10. The mean nitrate value was then calculated. The same procedure was followed for sections with rating values of 9, 7 and 5. Using the modified ratings, new raster rating maps were developed for each of the effective parameters.

3.2.4.3 Analytic Hierarchy Process (AHP)

The ratings and weights of the original DRASTIC factors are based on expert judgement. This therefore makes the use of AHP suitable for estimating values for factor weights. The procedure for calculating the weights is described below. A pair-wise matrix shown in Table 3.2 which expresses the relative values of the modified DRAI model factor weights was constructed following the method developed by Saaty (Saaty, 1980). The purpose of this is to estimate a value for each of the factor weights. The conventional DRASTIC weights (D = 5, R = 4, A = 3 and I = 5) were used as input values for the AHP analysis. The relative weight of each factor was then calculated as the eigenvector using matrix algebra.

Table 3.2 Pair-wise matrix of relative factor weights

					Product Of values	**n^{th} root of product of values**	**Eigen vectors**	**$A\omega=\lambda_{max}$**	**λ_{max}**
	D	R	A	I					
D	1.00	1.25	1.67	1.00	2.083	1.201	0.294	1.176	4
R	0.80	1.00	1.33	0.80	0.853	0.961	0.235	0.941	4
A	0.60	0.75	1.00	0.60	0.270	0.721	0.176	0.706	4
I	1.00	1.25	1.67	1.00	2.083	1.201	0.294	1.176	4
Totals	4.085	1.000							

n = the number of rows (4)

The eigenvector was calculated from multiplying together the entries in each row of the matrix and then taking the n^{th} root of that product. The n^{th} roots were summed and that sum was used to normalise the eigenvector elements. For example in the matrix of table 4.18 above the 4^{th} root for the first row is 1.201 and that was divided by 4.085 to give 0.294 as the first element in the eigenvector. The calculated eigenvector of the relative importance or value of D, R, A and I is (0.294, 0.235, 0.176, 0.294). D and I are the most valuable, R follows and A is less significant.

The next stage was to calculate λ_{max} in order to determine the Consistency Index (CI) and the Consistency Ratio (CR). The matrix of judgements was multiplied by the eigenvector, to obtain a new vector. The calculation for the first row in the matrix is done using equation 3.6.

1*0.294+1.25*0.235+1.67*0.176+1*0.294 = 1.176 3.6

and the remaining three rows give 0.941, 0.706 and. 1.176. This vector of four elements (1.176, 0.941, 0.706, 1.176) is, the product Aω and the AHP theory says that $A\omega=\lambda_{max}\omega$ so we can now get four estimates of λ_{max} by dividing each component of (1.176, 0.941, 0.706, 1.176) by the corresponding eigenvector element. This gives 1.176/0.294=4 together with 4., 4. and 4. The mean of these values is 4 and that is the estimate for λ_{max}. According to the theory of AHP if any of the estimates for λ_{max} turns out to be less than n, or 4 in this case, there has been an error in the calculation, which is a useful sanity check(Coyle, 2004). The Consistency Index for a matrix is calculated from $(\lambda_{max}-n)/(n-1)$ and, since n=4 for this matrix, the CI is 0. The final step was to calculate the Consistency Ratio for this set of judgements using the CI for the corresponding value from large samples of

matrices of purely random judgments using Table 3.3, derived from Saaty's book, in which the upper row is the order of the random matrix, and the lower is the corresponding index of consistency for random judgements.

Table 3.3 Saaty's Consistency scale of random judgments (Coyle, 2004).

1	2	3	4	5	6	7	8	9	10	11	12	13	14	15
0.0	0.0	0.5	0.9	1.1	1.2	1.3	1.4	1.4	1.4	1.5	1.4	1.5	1.5	1.5
0	0	8	0	2	4	2	1	5	9	1	8	6	7	9

For this analysis, that gives 0/0.90=0. Saaty argues that a CR > 0.1 indicates

that the judgements are at the limit of consistency. A CR as high as, say, 0.9 would mean that the pairwise judgements are just about random and are completely untrustworthy (Coyle, 2004). A CR of zero value is perfect consistency which is the situation in this analysis.

3.2.4.4 Model Validation

The optimized DRAI model was validated using July 2003 nitrate data from seventy five wells taken from the unconfined aquifer in the study area. The nitrate map was plotted on the AHP-DRAI vulnerability map for visual inspection and statistical correlation analysis. Vulnerability score values extracted from the nitrate points were correlated with the nitrate concentration values.

CHAPTER FOUR

PRESENTATION OF RESULTS AND DISCUSSIONS

4.1 PARAMETER RATING MAPS

The raster rating maps of the seven parameters were generated by interpolating each of the seven shape files and reclassifying the rating values. The ratings were multiplied by their corresponding weights to obtain the parameter vulnerability index shown. The data used for the interpolation of all the seven parameters is shown in Appendix 8.

4.1.1 Depth to water (D)

This factor determines the minimum distance through which pollutants have to travel before reaching the water table or saturated zone. The deeper the water table the more likely pollutant attenuation will occur before it reaches the saturated zone and therefore, the lesser the chance of pollution.

The elevation measurements, the mean static water level averaged over two years and the depth to water table calculated for the twenty one wells are shown in Table 4.1. The depth to water rating values were assigned using the DRASTIC manual and IDW method was used for interpolation to generate the depth to water raster map. The attribute table is shown in Table 4.2 and the depth to water raster rating map is shown in Figure 4.1.

Table 4.1 Depth to water table (D) and elevations above National Mean sea Level

Well ID	Longitude	Latitude	GPS Elevation	RTK Elevation.	5+RTK Elevation	Mean static water level (MSWL)	Depth to water (D)
AL15	0.93551	5.81015	16	0.306	5.306	2.94	**2.366**
AL2	0.93162	5.81181	13	-2.355	2.645	0.51	**2.135**
AL4	0.92804	5.80969	14	-2.375	2.625	0.62	**2.005**
AL19	0.92569	5.80355	14	-0.619	4.381	1.1	**3.281**
AL8	0.92201	5.80435	13	-1.878	3.122	1.14	**1.982**
AL12	0.91454	5.80089	14	-1.956	3.044	1.08	**1.964**
WE13	0.93533	5.81403	5	-2.472	2.528	0.83	**1.698**
WE28	0.94153	5.81312	6	-1.055	3.945	0.9	**3.045**
WE8	0.94919	5.82829	3	-2.077	2.923	0.96	**1.963**
WE21	0.95722	5.82952	6	-1.561	3.439	0.71	**2.729**
WE16	0.96497	5.83582	98	-1.547	3.453	0.99	**2.463**
TG16	0.97368	5.84093	15	-1.127	3.873	1.96	**1.913**
TG13	0.93533	5.81403	17	-1.255	3.745	1.8	**1.945**
TG11	0.91622	5.80243	17	-2.453	2.547	2.07	**0.477**
TG6	0.98638	5.86503	19	-1.335	3.665	2.03	**1.635**
TG1	0.97843	5.87552	15	-1.891	3.109	1.3	**1.809**
DN10	0.98744	5.89033	14	-0.988	4.012	1.62	**2.392**
KK35	0.99363	5.89947	10	-1.73	3.27	0.97	**2.3**
KK25	0.98813	5.90332	9	-0.222	4.778	2.38	**2.398**
KK9	0.98957	5.91155	6	-1.027	3.973	0.97	**3.003**
KET5	0.99267	5.92149	2	-0.801	4.199	3.16	**1.039**

Table4.2 Depth to Water attribute table

Depth to Water (D) and rating attribute table					
Well ID	Longitude	Latitude	Depth to water-(D) (m)	Rating	Index (D_r x D_w)
AL15	0.93551	5.81015	2.366	9	45
AL2	0.93162	5.81181	2.135	9	45
AL4	0.92804	5.80969	2.005	9	45
AL19	0.92569	5.80355	3.281	5	25
AL8	0.92201	5.80435	1.982	9	45
AL12	0.91454	5.80089	1.964	9	45
WE13	0.93533	5.81403	1.698	9	45
WE28	0.94153	5.81312	3.045	5	45
WE8	0.94919	5.82829	1.963	9	45
WE21	0.95722	5.82952	2.729	7	35
WE16	0.96497	5.83582	2.463	9	45
TG16	0.97368	5.84093	1.913	9	45
TG13	0.93533	5.81403	1.945	9	45
TG11	0.91622	5.80243	0.477	10	50
TG6	0.98638	5.86503	1.635	9	45
TG1	0.97843	5.87552	1.809	9	45
DN10	0.98744	5.89033	2.392	9	45
KK35	0.99363	5.89947	2.3	9	45
KK25	0.98813	5.90332	2.398	9	45
KK9	0.98957	5.91155	3.003	5	25
KET5	0.99267	5.92149	1.039	10	50

Weight: 5

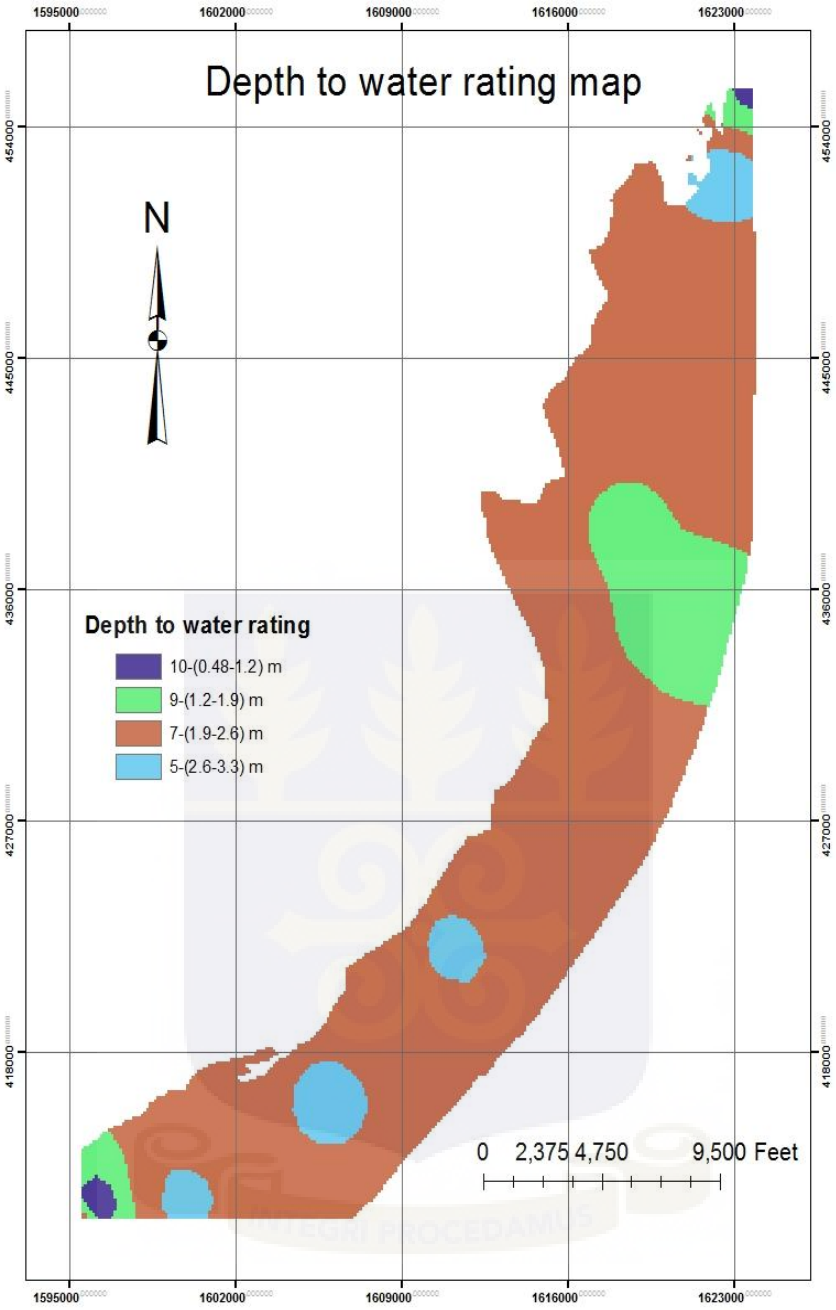

Figure 4.1 Depth to water rating map

The depth to water ranges from 0.48 to 3.3 m. The shallowest portions of the water table range from 0.48 to 1.2 m and occur around Anloga and Keta. The two locations may be in valleys and this could account for the low water table in these locations. A greater part of the study area however has the water table between 1.9 to 2.6 m and covers from Anloga through Woe to Keta. The highest depth to water rating (10) which has the greatest impact on

groundwater vulnerability are within the shallowest (0.48-1.2 m) areas around Anloga and Keta. The lowest rated (5) with least impact ranges between 2.6 to 3.3 m.

4.1.2 Net recharge

In the study area net recharge comes mainly from precipitation and represents the quantity of water that infiltrates through the ground surface and reaches the water table. It acts as a vehicle for transporting pollutants to the water table and within the aquifer through the process of leaching. An increase in net recharge increases the chances for contaminants to reach the water table. An increase in net recharge also raises the water table thus shortening the depth to water table and thereby increasing the chance of contamination. An excessive increase in net recharge may however tend to dilute the pollutant and reduce its contamination effect. Reliable rainfall data, soil moisture data and other data required for assessing the water balance in the study area were not available.

The annual recharge values varied between 70 mm and 1550 mm. It is assumed that water table fluctuations are due mainly to precipitation. Tidal and other effects on the water table variations are neglected. The calculated net recharge is shown in Table 4.3. The specific yield of the aquifer materials sourced from literature is shown in Appendix 5. The recharge attribute table is shown in Table 4.4. The recharge rating raster map is shown in Figure 4.2.

Table 4.3 Net recharge at sampled well locations

NET RECHARGE CALCULATIONS USING WATER TABLE FLUCTUATIONS (WTF)									
WELL ID	Long.	Lat.	Mean SWL (m)	Min (m)	Max (m)	WTF (m)	Aquifer media Type	Aquifer media Specific yield (S_y)	Net Recharge (m)

WE11	0.94242	5.81910	0.56	0.22	0.81	0.59	Medium Sand	0.32	0.1888
WE17	0.96222	5.83617	1.04	0.55	1.52	0.97	medium Sandy	0.32	0.3104
WE23	0.95188	5.82861	0.67	0.41	0.99	0.58	Gravely Sand	0.28	0.1624
TG 2	0.98145	5.87165	1.83	1.38	2.66	1.28	Fine Sand	0.33	0.4224
TG 18	0.96878	5.84512	0.73	0.57	0.88	0.31	Gravely	0.21	0.0651
AL1	0.93382	5.81227	0.46	0.15	0.78	0.63	Gravely Sand	0.28	0.1764
AL11	0.91622	5.80243	1.49	0.42	5.25	4.83	medium Sand	0.32	1.5456
AL12	0.91454	5.80089	1.08	0.1	5.3	5.2	Gravely Sand	0.28	1.456
AL14	0.91083	5.80032	1.07	0.03	5.26	5.23	Gravely Sand	0.28	1.4644
AL16	0.93305	5.80868	2.96	1.31	5.51	4.2	Fine Sand	0.33	1.386
AL23	0.91525	5.79883	3.72	3.51	3.96	0.45	Fine Sand	0.33	0.1485
AL24	0.91219	5.79820	2.42	1.42	3.48	2.06	Gravely Sand	0.28	0.5768
kk29	0.98765	5.90014	2.34	1.7	2.75	1.05	Medium sand	0.32	0.34
kk30	0.98505	5.89972	0.56	0.08	0.9	0.82	Gravely Sand	0.28	0.2296
kk38	0.98565	5.89550	2.08	1.11	2.78	1.67	Medium Sand	0.32	0.5344
ket 5	0.99267	5.92149	3.16	2.7	3.49	0.79	Medium Sand	0.32	0.2528

Table 4.4 Net recharge attribute table

Net Recharge (R)					
WELL ID	Lat.	Long.	Net Recharge (m)	Rating	Index (R_r x R_w)
WE11	0.94242	5.81910	0.1888	3	12
WE17	0.96222	5.83617	0.3104	3	12
WE23	0.95188	5.82861	0.1624	3	12

TG 2	0.98145	5.87165	0.4224	3	12
TG 18	0.96878	5.84512	0.0651	1	4
AL1	0.93382	5.81227	0.1764	3	12
AL11	0.91622	5.80243	1.5456	8	32
AL12	0.91454	5.80089	1.456	6	24
AL14	0.91083	5.80032	1.4644	6	24
AL16	0.93305	5.80868	1.386	6	24
AL23	0.91525	5.79883	0.1485	3	12
AL24	0.91219	5.79820	0.5768	6	24
kk29	0.98765	5.90014	0.34	3	12
kk30	0.98505	5.89972	0.2296	3	12
kk38	0.98565	5.89550	0.5344	6	24
ket 5	0.99267	5.92149	0.2528	3	12

Weight: 4

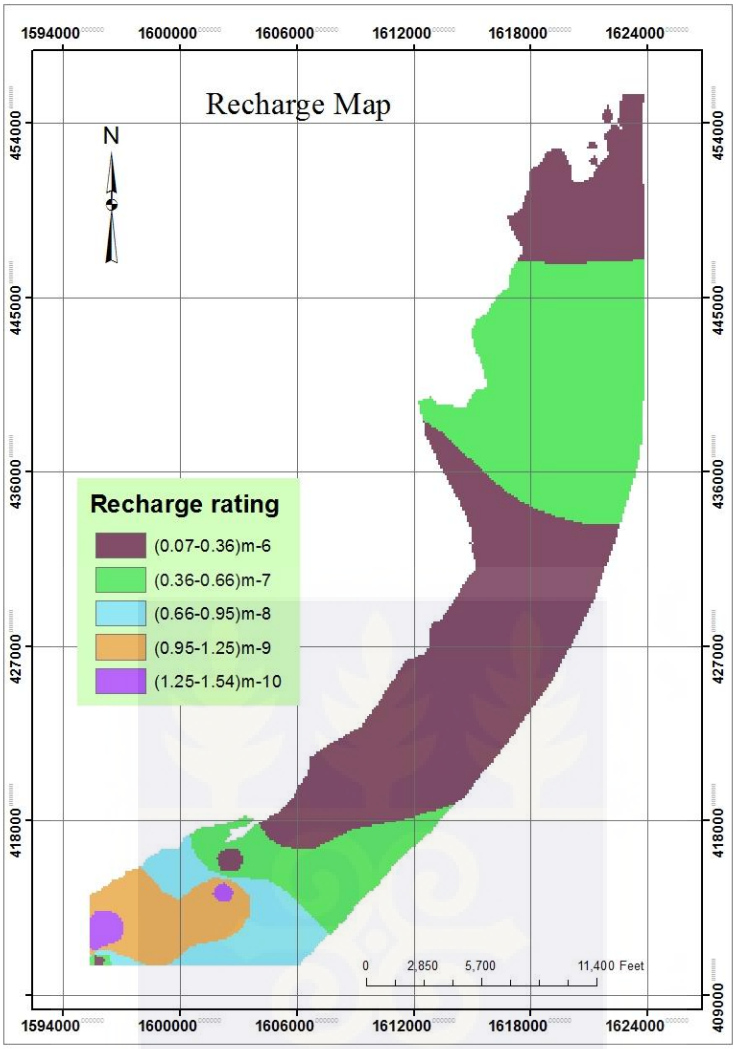

Figure 4.2 Net recharge rating map

The recharge map of the study area was divided into five ranges with the lowest range of recharge between 0.07 and 0.36 m and the highest range between 1.25 and 1.54 m. The average recharge rate is 0.81m. The relatively high recharge rates round Anloga may be due to the topographically low zones in the form of valleys and dug outs in those areas. As topography is almost zero, there will be no precipitation run-off hence there will be maximum infiltration. The coarse sands and gravel that form that portion of the study area may also account for the high infiltration rate. The relatively lower recharge rates observed around Keta and most parts of the farming areas may be due to residential and plants coverage impeding infiltration and enhancing evapotranspiration. The rating values were

assigned according to the impact on groundwater vulnerability with a rating value of 5 assigned to recharge range of 0.07-0.36 m and 10 to 1.25-1.54 m with the least and highest impact respectively.

4.1.3 Aquifer media

Aquifer media refers to the saturated zone material properties which controls the pollutant permeability and attenuation processes such as sorption, reactivity, and dispersion. This medium may be consolidated or unconsolidated rock. Larger grain size and fractured rock material increases the permeability and hence increases vulnerability. The media type was determined from soil analysis. The table of classifications and the particle size distribution curves are shown in Appendix 6 and 7. The aquifer media consists of fine sand, medium sand, coarse sand, gravel sand and gravel. The aquifer media types are shown in Table 4.5. The rating values shown in Table 4.6 assigned to the media types were determined from the classification shown in Appendix 2 from the DRASTIC manual.

The aquifer media was divided into five ranges according to the media type. The aquifer media in the study area consists of fine sand, medium sand, coarse sand, gravel sand and gravel. Most parts of the strip are composed of medium to coarse sands. Gravel and gravely sand occur mainly in the central and western parts of the strip. The fine sands occurring around Tegbi towards the sea side of the strip tend to reduce infiltration and may lead to a low vulnerability in that zone. Aquifer media ratings were assigned values from 4 to 10 with least and greatest impact on vulnerability to groundwater in the study area respectively.

Table 4.5 Aquifer media types

Aquifer Media

Sample ID	Lat.	Long.	Soil Class.
AL-SP1	5.79957	0.91163	Gravely Sand
AL-SP2	5.80074	0.91069	Gravely Sand
AL-SP3	5.7974	0.91423	Gravely Sand
AL-SP4	5.78957	0.91541	Fine Sand
AL-SP5	5.7867	0.91574	Medium Sand
AL-SP6	5.81272	0.93259	Fine Sand
AL-SP7	5.81004	0.93375	Gravely Sand
WE-SP1	5.8121	0.9424	Medium Sand
WE-SP2	5.81351	0.95076	Gravely Sand
WE-SP3	5.82342	0.96136	Medium Sandy
TG-SP1	5.84443	0.96689	Gravely
TG-SP2	5.84579	0.98104	Fine Sand
KET-SP1	5.8265	0.98415	Gravely Sand
KET-SP2	5.89668	0.98466	Medium Sand
KET-SP3	5.92148	0.99271	Medium Sand

Table 4.6 Aquifer media attribute table

Aquifer Media (A)					
Sample ID	Lat.	Long.	Media Class.	Rating	Index (A_r x A_w)
AL-SP1	5.79957	0.91163	Gravely Sand	9	27
AL-SP2	5.80074	0.91069	Gravely Sand	9	27
AL-SP3	5.7974	0.91423	Gravely Sand	9	27
AL-SP4	5.78957	0.91541	Fine Sand	4	12

AL-SP5	5.7867	0.91574	Medium Sand	6	18
AL-SP6	5.81272	0.93259	Fine Sand	4	12
AL-SP7	5.81004	0.93375	Gravely Sand	9	27
WE-SP1	5.8121	0.9424	Medium Sand	6	18
WE-SP2	5.81351	0.95076	Gravely Sand	9	27
WE-SP3	5.82342	0.96136	Medium Sandy	6	18
TG-SP1	5.84443	0.96689	Gravely	10	30
TG-SP2	5.84579	0.98104	Fine Sand	4	12
KET-SP1	5.8265	0.98415	Gravely Sand	9	27
KET-SP2	5.89668	0.98466	Medium Sand	6	18
KET-SP3	5.92148	0.99271	Medium Sand	6	18

Weight: 3

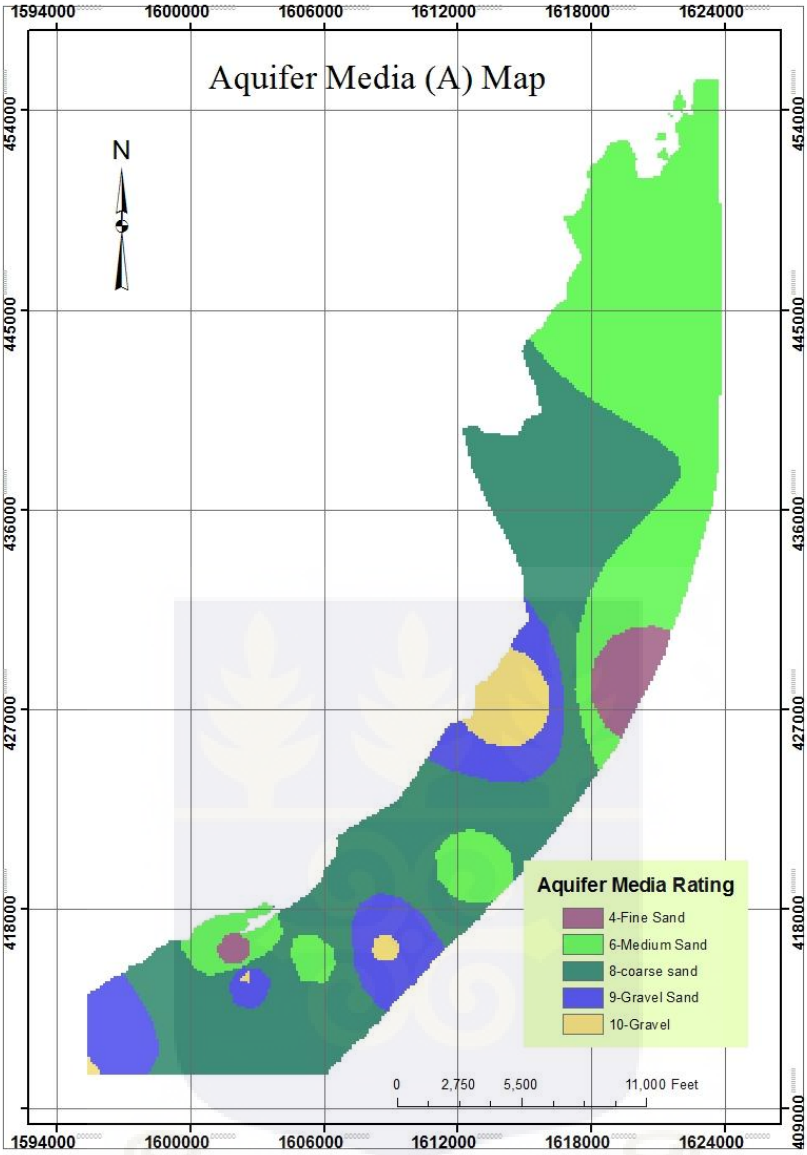

Figure 4.3 Aquifer media map

4.1.4 Soil media

This is made up of the uppermost weathered portion of the unsaturated zone characterised by significant biological activity, which controls the amount of recharge that can infiltrate downward. It is also within this zone that natural biological processes may eliminate or render the pollutant benign. The determination of the soil media was done from soil analysis at the Soil Research Institute laboratory, CSIR, Accra as described in chapter three. From the results the soil media was classified as shown in Table 4.7. The soil media consists of gravel,

sand, sandy loam, loam, silty loam and clay loam. Rating values of 3 to 10 were assigned. Clay loam, silt loam and sandy loam soils with their potential to attenuate contamination were rated low, while gravels and sandy soils with high permeabilities were rated high. The attribute table showing the ratings and index values is shown in Table 4.8. From Figure 4.4 most parts of the study area are composed of sandy soils. A small zone in Woe towards the lagoon where grass and farms crops abound is made up of silt loam. Gravely soils occur at the western areas around Anloga where there is little vegetation.

Table 4.7 Soil media types

Soil Media			
ID	Long.	Lat.	Media type
AL-SP3-1m	0.91423	5.7974	Gravel
AL-SP4-1m	0.91541	5.78957	Clay loam

AL-SP5-1m	0.91574	5.7867	Sand
AL-SP6-1m	0.93259	5.81272	Gravel
AL-SP7-1m	0.93375	5.81004	Sand
KET-SP1-1m	0.98415	5.8265	Sand
KET-SP2-1m	0.98466	5.89668	Sand
KET-SP3-Im	0.99271	5.92148	Sand
TG-SP1-1m	0.96689	5.84443	Silt Loam
TG-SP2-1m	0.98104	5.84579	Gravely
WE-SP1-1m	0.9424	5.8121	Sand
WE-SP2-1m	0.95076	5.81351	Sand
WE-SP3-1m	0.96136	5.82342	Sand

Weight 2

Table 4.8 Soil media attribute table

Soil Media					
ID	Long.	Lat.	Media type	Rating	Index (S_r x S_w)
AL-SP3-1m	0.91423	5.7974	Gravel	10	20
AL-SP4-1m	0.91541	5.78957	Clay loam	3	6
AL-SP5-1m	0.91574	5.7867	Sand	9	18

AL-SP6-1m	0.93259	5.81272	Gravel	10	20
AL-SP7-1m	0.93375	5.81004	Sand	9	18
KET-SP1-1m	0.98415	5.8265	Sand	9	18
KET-SP2-1m	0.98466	5.89668	Sand	9	18
KET-SP3-Im	0.99271	5.92148	Sand	9	18
TG-SP1-1m	0.96689	5.84443	Silt Loam	4	8
TG-SP2-1m	0.98104	5.84579	Gravely	10	20
WE-SP1-1m	0.9424	5.8121	Sand	9	18
WE-SP2-1m	0.95076	5.81351	Sand	9	18
WE-SP3-1m	0.96136	5.82342	Sand	9	18

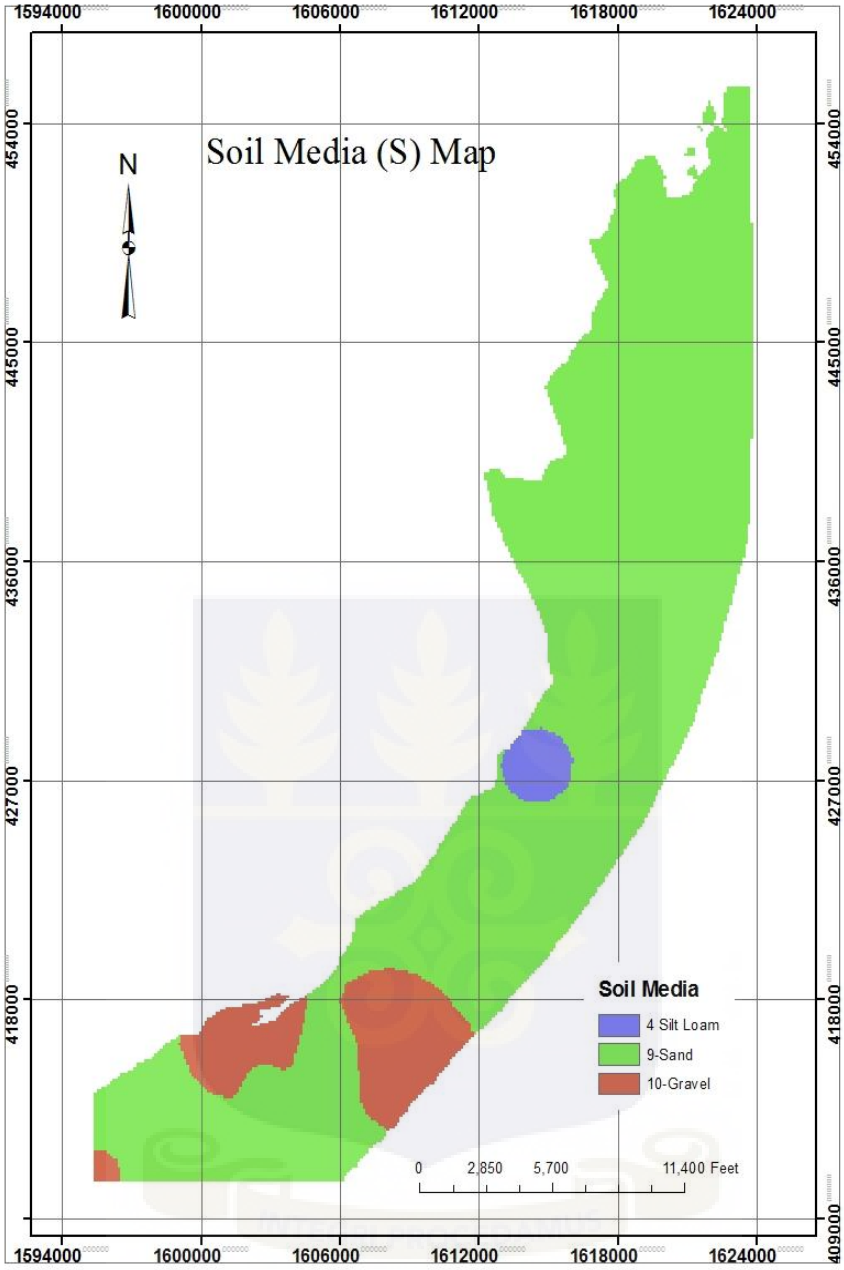

Figure 4.4 Soil media map

4.1.5 Topography

It is the slope of the land surface that dictates whether rainfall runoff will remain on the ground surface to influence contaminant percolation into the saturated zone. Topography may also give an indication of areas where contaminants will concentrate. Rainfall runoff will carry surface pollutants from topographically higher elevations to lower elevations. This

makes areas of lower slopes more vulnerable to contamination **(**Ahmed, 2009). The slope data was developed from the elevation data determined using the differential GPS in the previous section on depth to water (D) data. The elevation data is shown in Table 4.9. The attribute data with the assigned ratings is shown in Table 4.10. The slope percentage in Table 4.10 was calculated using the ArcGIS surface analysis feature. Except for well AL15 the rest of the wells were below the NMSL as indicated by their negative RTK elevation values. Since negative elevation values cannot be used for the model, the RTK elevation data was transformed by adding a minimum constant value of five metres to each well elevation value to yield positive elevation values and also to ensure that a positive depth to water value was maintained at well Ket 5.

Table 4.9 Elevation data

Topographic Data (T)

Well ID	Longitude	Latitude	GPS Elevation	RTK Elevation	5+RTK Elevation **(T)**
AL15	0.93551	5.81015	16	0.306	5.306
AL2	0.93162	5.81181	13	-2.355	2.645
AL4	0.92804	5.80969	14	-2.375	2.625
AL19	0.92569	5.80355	14	-0.619	4.381
AL8	0.92201	5.80435	13	-1.878	3.122
AL12	0.91454	5.80089	14	-1.956	3.044
WE13	0.93533	5.81403	5	-2.472	2.528
WE28	0.94153	5.81312	6	-1.055	3.945
WE8	0.94919	5.82829	3	-2.077	2.923
WE21	0.95722	5.82952	6	-1.561	3.439
WE16	0.96497	5.83582	98	-1.547	3.453
TG16	0.97368	5.84093	15	-1.127	3.873
TG13	0.93533	5.81403	17	-1.255	3.745
TG11	0.91622	5.80243	17	-2.453	2.547
TG6	0.98638	5.86503	19	-1.335	3.665
TG1	0.97843	5.87552	15	-1.891	3.109
DN10	0.98744	5.89033	14	-0.988	4.012
KK35	0.99363	5.89947	10	-1.73	3.27
KK25	0.98813	5.90332	9	-0.222	4.778
KK9	0.98957	5.91155	6	-1.027	3.973
KET5	0.99267	5.92149	2	-0.801	4.199

Table4.10 Topography Attribute table

Topography (T) **(% slope)**						
Well ID	Longitude	Latitude	Elevation	Topography % Slope (T)	Rating	Index (Tr xTw)

AL15	0.93551	5.81015	5.306	0.44	7	7
AL2	0.93162	5.81181	2.645	0.49	6	6
AL4	0.92804	5.80969	2.625	0	10	10
AL19	0.92569	5.80355	4.381	0.44	7	7
AL8	0.92201	5.80435	3.122	0	10	10
AL12	0.91454	5.80089	3.044	0	10	10
WE13	0.93533	5.81403	2.528	0	10	10
WE28	0.94153	5.81312	3.945	0	10	10
WE8	0.94919	5.82829	2.923	0	10	10
WE21	0.95722	5.82952	3.439	0	10	10
WE16	0.96497	5.83582	3.453	0	10	10
TG16	0.97368	5.84093	3.873	0.44	7	7
TG13	0.93533	5.81403	3.745	0.44	7	7
TG11	0.91622	5.80243	2.547	0	10	10
TG6	0.98638	5.86503	3.665	0	10	10
TG1	0.97843	5.87552	3.109	0	10	10
DN10	0.98744	5.89033	4.012	0	10	
KK35	0.99363	5.89947	3.27			
KK25	0.98813	5.90332	4.778	0	10	
KK9	0.98957	5.91155	3.973	0	10	
KET5	0.99267	5.92149	4.199			

Weight=1

Figure 4.5 is the topography rating map and it shows that the entire strip has virtually zero slopes except for a few relatively thin ridges which are topographically higher and cut across at different sections over the entire length of the strip. Even though the slope percentage was categorized into five ranges, the strip can be said to be almost flat with little or no possibility of precipitation run-off. This explains why most of the study area has been assigned the highest rating value of 10.

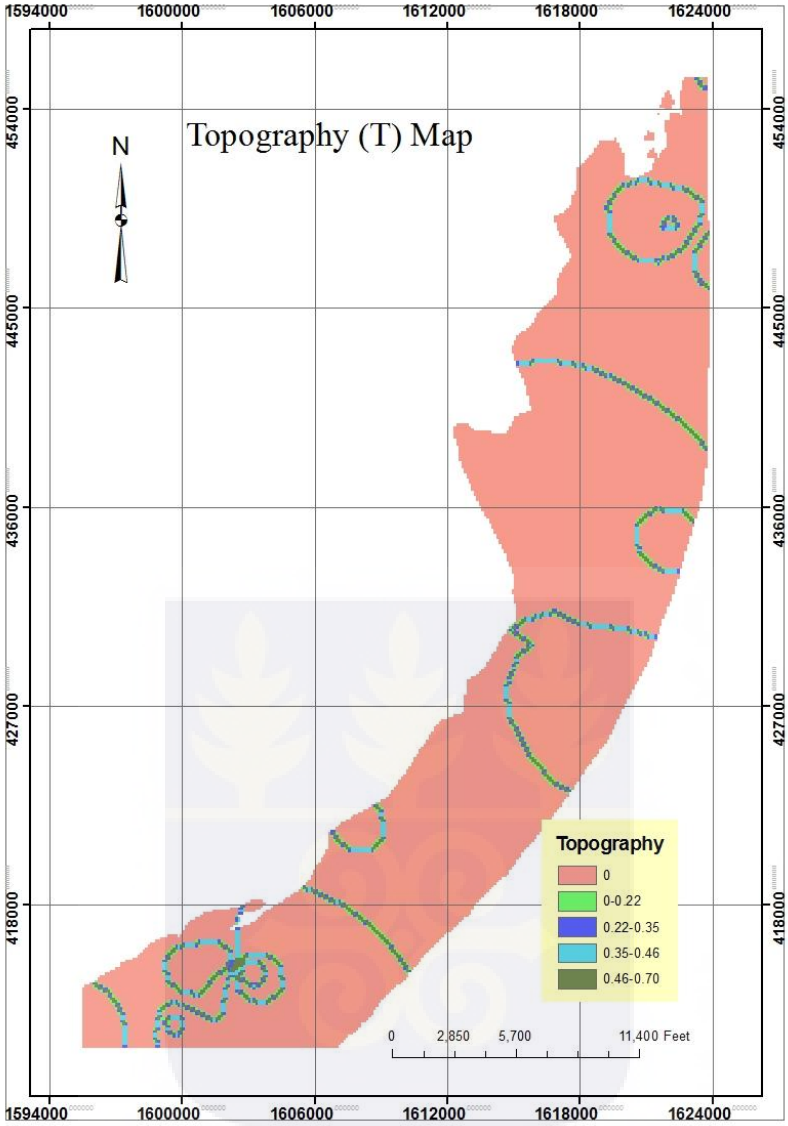

Figure 4.5 Topography map

4.1.6 Influence of the vadose zone

This represents the type of material in the zone above the water table and below the typical soil horizon, which controls the passage and attenuation of the contaminated material to the saturated zone by biodegradation, neutralization, mechanical filtration, chemical reaction, volatilization and dispersion processes. The Quaternary surficial aquifer in the study area is relatively shallow. In surficial aquifers, the ratings for the vadose zone are generally the same as the aquifer media (Qamhieh, 2006). This method was followed in this research. The

aquifer media is used to represent the vadose zone media. However the superior weighting of (5) of the impact of the vadose media will influence the overall vulnerability differently from the aquifer media. Table 4.11 shows the vadose media and Figure 4.6 shows the vadosemedia rating map. The vadose media therefore consists of fine sand, medium sand, coarse sand, and gravely sand.

Table 4.11 Vadose media types

Vadose media (I)				
Sample No.	**Sample ID**	**Latitude**	**Longitude**	**Soil Class.**
1	AL-SP1	5.79957	0.91163	Gravely Sand
2	AL-SP2	5.80074	0.91069	Gravely Sand
3	AL-SP3	5.7974	0.91423	Gravely Sand
4	AL-SP4	5.78957	0.91541	Fine Sand
5	AL-SP5	5.7867	0.91574	Medium Sand
6	AL-SP6	5.81272	0.93259	Fine Sand

7	AL-SP7	5.81004	0.93375	Gravely Sand
8	WE-SP1	5.8121	0.9424	Medium Sand
9	WE-SP2	5.81351	0.95076	Gravely Sand
10	WE-SP3	5.82342	0.96136	Medium Sand
11	TG-SP1	5.84443	0.96689	Gravely
12	TG-SP2	5.84579	0.98104	Fine Sand
13	KET-SP1	5.8265	0.98415	Gravely Sand
14	KET-SP2	5.89668	0.98466	Medium Sand
15	KET-SP3	5.92148	0.99271	Medium Sand

Table 4.12 Vadose media attribute table

Vadose Media Impact (I)					
Sample ID	**Longitude**	**Latitude**	**Media Class.**	**Rating**	**Index (A_r x A_w)**
AL-SP1	5.79957	0.91163	Gravely Sand	9	45
AL-SP2	5.80074	0.91069	Gravely Sand	9	45
AL-SP3	5.7974	0.91423	Gravely Sand	9	45
AL-SP4	5.78957	0.91541	Fine Sand	4	20
AL-SP5	5.7867	0.91574	Medium Sand	6	30
AL-SP6	5.81272	0.93259	Fine Sand	4	20
AL-SP7	5.81004	0.93375	Gravely Sand	9	45
WE-SP1	5.8121	0.9424	Medium Sand	6	30

WE-SP2	5.81351	0.95076	Gravely Sand	9	45
WE-SP3	5.82342	0.96136	Medium Sandy	6	30
TG-SP1	5.84443	0.96689	Gravely	10	50
TG-SP2	5.84579	0.98104	Fine Sand	4	20
KET-SP1	5.8265	0.98415	Gravely Sand	9	45
KET-SP2	5.89668	0.98466	Medium Sand	6	30
KET-SP3	5.92148	0.99271	Medium Sand	6	30

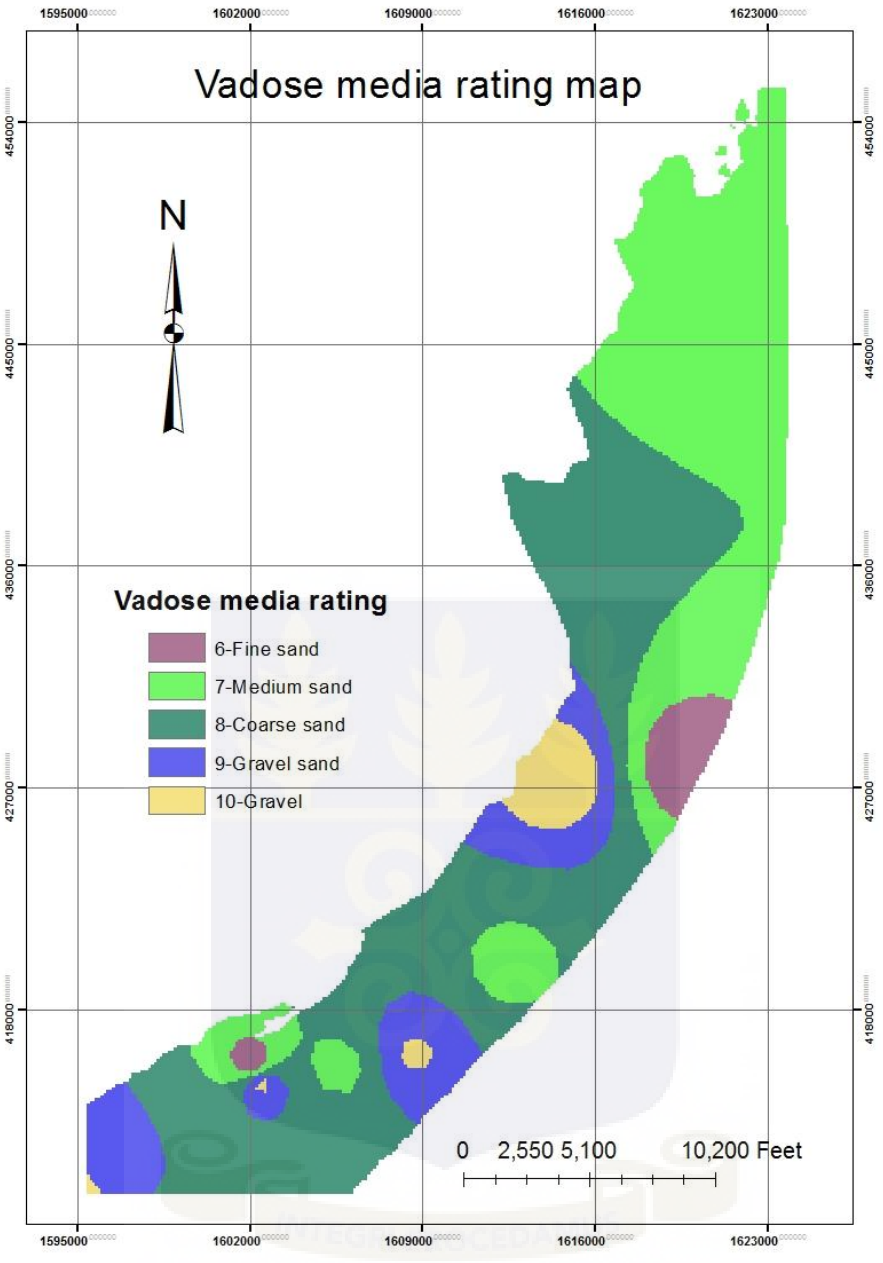

Figure 4.6 Vadose zone media rating map

4.1.7 Hydraulic conductivity

Hydraulic conductivity indicates the ability of the aquifer to transmit water, and hence it determines the rate of the flow of contaminant material within the groundwater system. The higher the conductivity, the faster contaminants will travel within the aquifer. Reliable pumping test data for the study area were not available. Observations of drawdowns in two

separate surface centrifugal irrigation pumps delivering over 500l/min showed no significant drawdown of the water table. Conducting constant discharge pumping test for the purpose of determining hydraulic conductivity will be extremely difficult in the terrain. The surficial aquifer is very prolific and acquiring suitable pumps of very high delivery capacity will be costly. The perverse sandy nature of the area may make it difficult to discharge the pumped water without recharging the aquifer instantly. Hydraulic conductivity values were therefore estimated from grain sizes following experiments from sieve analysis of aquifer material sampled from the field as described in chapter three. Calculated hydraulic conductivity values were compared with values of the same geologic material from literature. The media particle diameters, uniformity coefficient and other particle characteristics are shown in Table 4.13. The Kozeny-Carman empirical equation used for calculating hydraulic conductivity values (K) is:

$$K = \frac{g}{v} \times 6 \times 10^{-4} [1 + 10(n - 0.26)] d_{10}^2 \qquad 4.1$$

1

Where n is porosity, d_{10} is the diameters of soil particles at 10% cumulative weight on the grading curve and v is kinematic viscosity of water at 20°C.

The Conductivity values calculated from Kozeny-Carman method are shown in Table 4.14. The grading curves for all the sample points are shown in Appendix 6. The hydraulic conductivity values range from 26 m/d to 150 m/d. Figure 4.7 shows the hydraulic conductivity map. The map was divided into four ranges. The maximum conductivity values occur in limited zones (0.8% of the area) where gravel and very coarse sands are the dominant media type. A greater portion (67%) of the area which is made up of medium sands has conductivity values less than 40 m/day. Areas with lower conductivity values were

assigned lower rating values. A maximum rating value of 10 was assigned to the highest conductivity values as these values impact most on groundwater vulnerability.

Table 4.13 Aquifer media particle characteristics

Sample ID	**D_{10} (mm)**	**D_{20} (mm)**	**D_{30} (mm)**	**D_{50} (mm)**	**D_{60} (mm)**	**(U) D60/D10**	**Porosity (n)**	**g/*v* (/ms)**
AL-SP1	0.191	0.23	0.25	0.32	0.4	2.094	0.428	9761194.03
AL-SP2	0.18	0.22	0.24	0.33	0.4	2.222	0.424	9761194.03
AL-SP3	0.29	0.36	0.4	0.51	0.55	1.897	0.434	9761194.03

AL-SP4	0.26	0.34	0.39	0.49	0.54	2.077	0.428	9761194.030
AL-SP5	0.21	0.31	0.39	0.5	0.58	2.762	0.407	9761194.030
AL-SP6	0.14	0.2	0.22	0.32	0.39	2.786	0.407	9761194.030
AL-SP7	0.2	0.26	0.3	0.4	0.45	2.250	0.423	9761194.030
WE-SP1	0.21	0.28	0.32	0.43	0.49	2.333	0.420	9761194.030
WE-SP2	0.24	0.31	0.35	0.45	0.5	2.083	0.428	9761194.030
WE-SP3	0.21	0.29	0.31	0.42	0.48	2.286	0.422	9761194.030
TG-SP1	0.18	0.27	0.38	1.6	3.3	18.333	0.263	9761194.030
TG-SP2	0.18	0.21	0.23	0.29	0.31	1.722	0.440	9761194.030
KET-SP1	0.205	0.29	0.35	0.5	0.6	2.927	0.403	9761194.030
KET-SP2	0.2	0.24	0.28	0.36	0.41	2.050	0.429	9761194.030
KET-SP3	0.21	0.28	0.32	0.42	0.49	2.333	0.420	9761194.030

Key: K-C=Kozeny-Carman, U=Uniformity coefficient, g= acceleration due to gravity (m/s^2),v = kinematic viscosity

Table 4.14 Calculated Hydraulic Conductivity values using Kozeny-Carman Method

Hydraulic conductivity (C)				
Sample ID	**Latitude**	**Longitude**	**Soil Class.**	**K-C (m/day)**
AL-SP1	5.79957	0.91163	Slightly Gravely Sand	60.94369
AL-SP2	5.80074	0.91069	Slightly Gravely Sand	51.85657

AL-SP3	5.7974	0.91423	Gravely Sand	150.3586
AL-SP4	5.78957	0.91541	Slightly Silty Sand	113.594
AL-SP5	5.7867	0.91574	medium Sand	59.452
AL-SP6	5.81272	0.93259	very Fine Sand	26.232
AL-SP7	5.81004	0.93375	Gravely Sand	63.435
WE-SP1	5.8121	0.9424	Medium Sand	68.052
WE-SP2	5.81351	0.95076	Gravely Sand	96.580
WE-SP3	5.82342	0.96136	medium Sandy	69.120
TG-SP1	5.84443	0.96689	Fine sand	67.636
TG-SP2	5.84579	0.98104	Fine Sand	61.607
KET-SP1	5.8265	0.98415	Gravely Sand	53.909
KET-SP2	5.89668	0.98466	Medium Sandy	67.833
KET-SP3	5.92148	0.99271	Medium Sand	68.052

Key: K-C=Kozeny-Carman

Table 4.15 Hydraulic conductivity attribute table

Hydraulic Conductivity (C)						
Sample ID	Longitude	Latitude	Media class.	Hydraulic Conductivity (C) (m/d)	Rating	Index R_c x W_c
AL-SP1	5.79957	0.91163	Slightly Gravely Sand	60.94369	6	18
AL-SP2	5.80074	0.91069	Slightly Gravely Sand	51.85657	6	18
AL-SP3	5.7974	0.91423	Gravely Sand	150.3586	9	27
AL-SP4	5.78957	0.91541	Slightly Silty Sand	113.594	8	24

AL-SP5	5.7867	0.91574	medium Sand	59.452	6	18
AL-SP6	5.81272	0.93259	very Fine Sand	26.232	6	18
AL-SP7	5.81004	0.93375	Gravely Sand	63.435	7	21
WE-SP1	5.8121	0.9424	Medium Sand	68.052	6	18
WE-SP2	5.81351	0.95076	Gravely Sand	96.580	8	24
WE-SP3	5.82342	0.96136	medium Sandy	69.120	6	18
TG-SP1	5.84443	0.96689	Fine sand	67.636	6	18
TG-SP2	5.84579	0.98104	Fine Sand	61.607	7	21
KET-SP1	5.8265	0.98415	Gravely Sand	53.909	6	18
KET-SP2	5.89668	0.98466	Medium Sandy	67.833	6	18
KET-SP3	5.92148	0.99271	Medium Sand	68.052	6	18

Weight=3

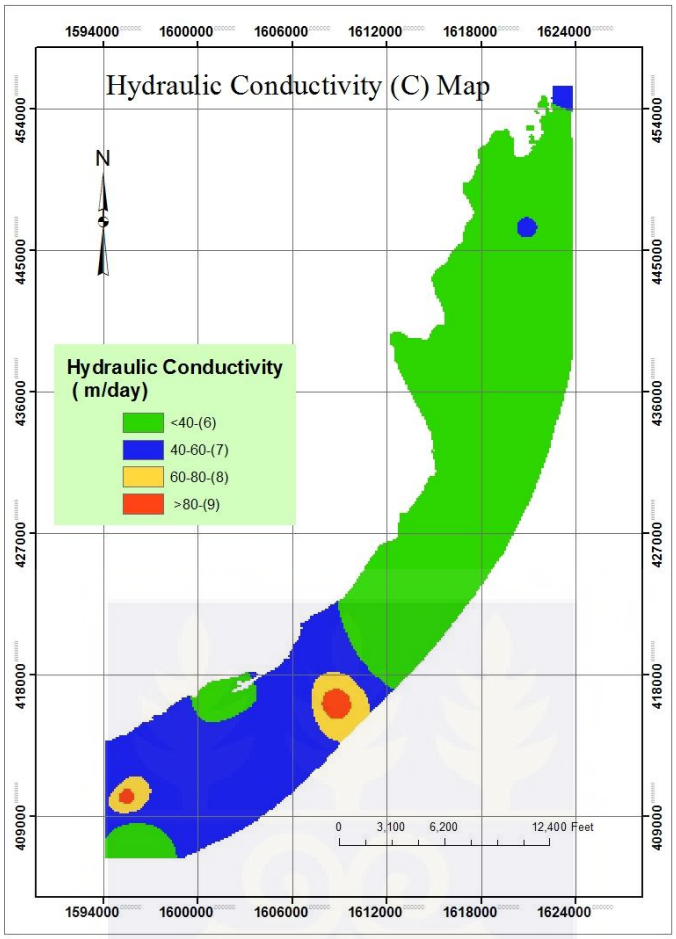

Figure 4.7 Hydraulic conductivity map

4.2 PARAMETER VULNERABILITY INDEX MAPS

The parameter vulnerability index (a multiplication of rating and weight at a point) was calculated for each parameter as a measure of vulnerability the parameter contributes to the final DRASTIC vulnerability index. The IDW interpolation method was used to generate the seven raster parameter vulnerability maps.

4.2.1 Depth to water

The depth to water parameter vulnerability index is shown in Figure 4.8. The index is divided into four classes with the greatest impact having an index value of 50 and the least 35. If depth to water was the only criterion for vulnerability then only a small proportion (0.62%) of the area will fall under very high vulnerability. High, moderate and low vulnerabilities cover 11.9%, 81.3% and 6.1% respectively. Very high and low vulnerabilities which represent danger and safety respectively together cover only 6.7% and occur only at Anloga and Keta. These areas have shallow water tables and probably account for the high index values. Moderate vulnerability dominates and covers 81.3%. This means that depth to water contributes moderately to the final vulnerability index of the area.

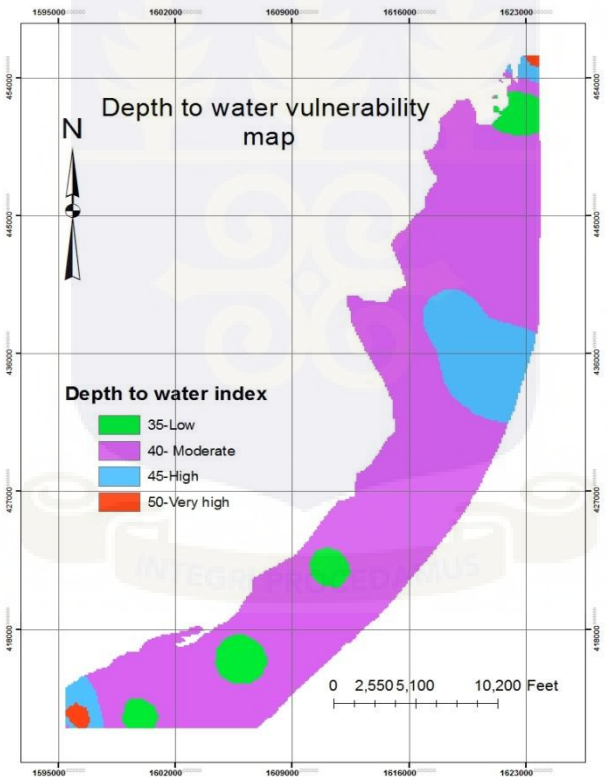

Figure 4.8 Depth to water vulnerability index map

4.2.2 Recharge

The recharge vulnerability index shown in Figure 4.9 is divided into five classes with the highest scores occurring at only Anloga areas. The lowest scores occur in Keta, Dzelukope, Kedzikope, Tegbi and a small portion of Woe. Very low vulnerability forms 47.6% of the

area while very high forms only 0.9%. Low, moderate and high scores have areal coverage of 38.0%, 6.9% and 6.6% respectively. Very low vulnerability dominates. Very low and low constitute 85.6% of the area. This is due to the fact that 75% of the area (inferred from the recharge map, Figure 4.2) receives less than 0.5m of recharge annually while the remaining receives over 1.0 m of recharge. The recharge parameter emphasises low groundwater vulnerability.

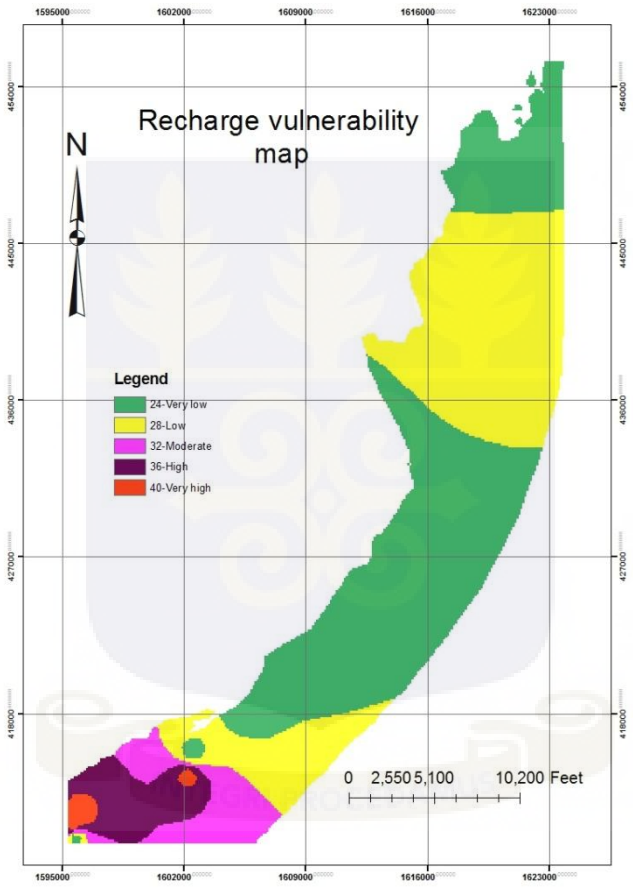

Figure 4.9 Recharge vulnerability index map

4.2.3 Aquifer media

Figure 4.10 shows the aquifer media vulnerability map. It is divided into five classes ranging from a score of 12 to 30. The areal coverage for the vulnerability classes are, 3.3%, 37.7%, 44.1%, 11.3% and 3.5% for very low, low, moderate high and very high respectively. Moderate and low vulnerability classes together form 81.8 %. Thus the aquifer media

parameter emphasises relatively low vulnerability in the study area. This is due to a greater part of the aquifer media being medium sand. The parameter considers Tegbi as the area having both the highest and lowest risk if a pollutant exists.

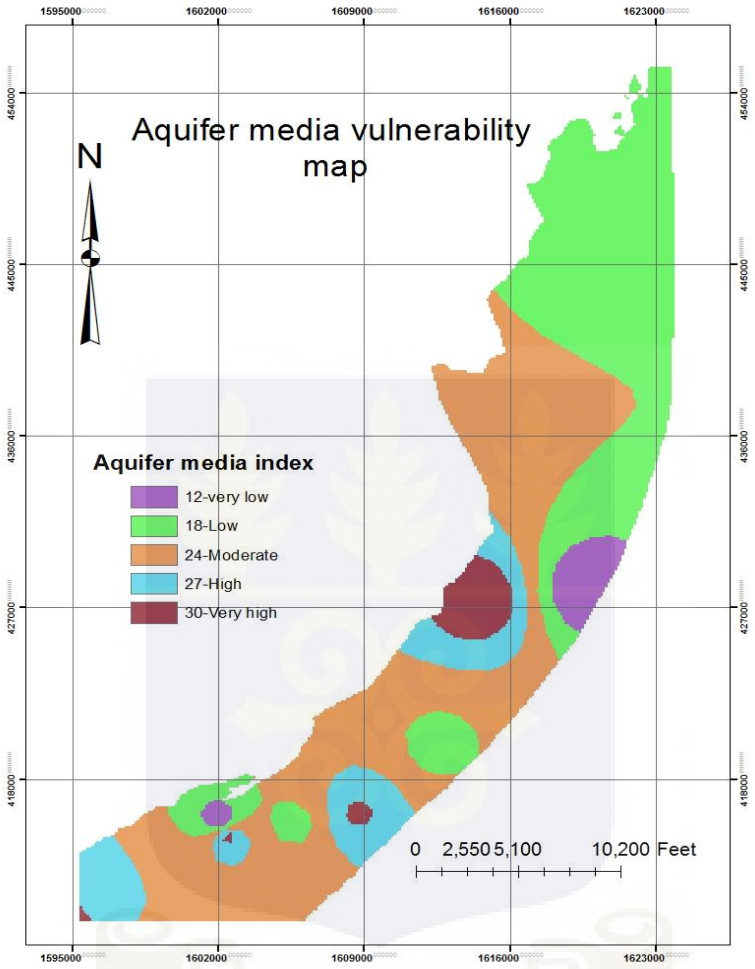

Figure 4.10 Aquifer media vulnerability index map

4.2.4 Soil media

The soil media vulnerability map is shown in Figure 4.11. Moderate vulnerability dominates with low occupying a very small portion around Woe and Tegbi. High follows moderate but is still low compared to moderate. Thus the soil parameter indicates moderate vulnerability to groundwater pollution. This is due to the dominance of medium sandy soils in the study area which tend to increase vulnerability. Most of the agricultural areas however have silt loam and clay loam soils. They tend to reduce vulnerability because of the contaminant attenuation

characteristics of these soils. The balance between the effects of these soils results in a moderate vulnerability coverage. Low, moderate and high classes have 1.9%, 87.8% and 10.3% areal coverage respectively.

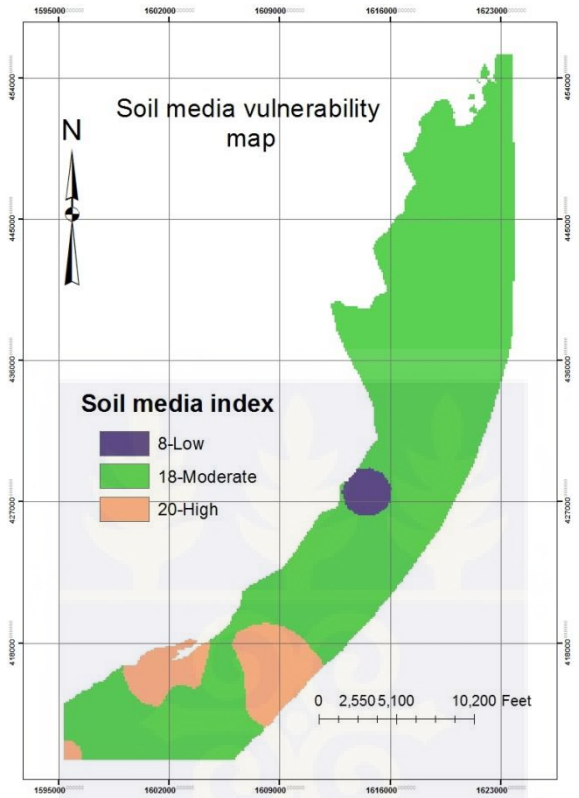

Figure 4.11 Soil media vulnerability index map

4.3.5 Topography

The topography vulnerability index of the study area is shown in Figure 4.12.The entire strip is highly vulnerable. Even though the index is divided into four classes in effect classes 7, 8 and 9 are negligible. The RTK elevation data of the entire study area showed it is below the National mean sea level. There are also no significant differences in the elevation data used for interpolation of the rating map and subsequently the topography vulnerability map. Ninety five per cent (95%) of the study area is highly vulnerable with regard to topography.

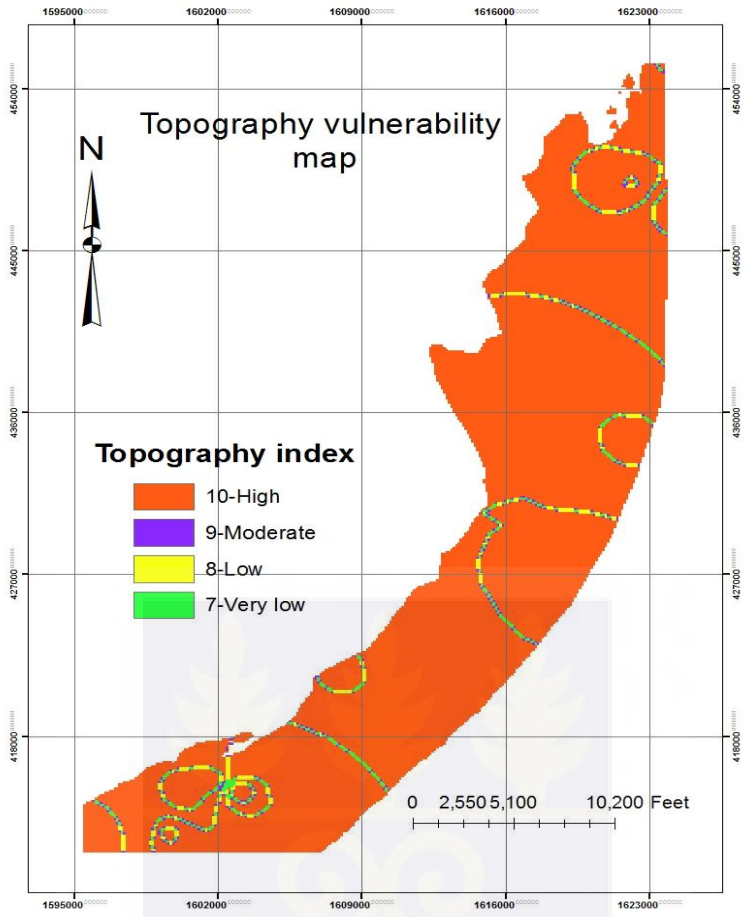

Figure 4.12 Topography vulnerability index map

4.2.6 Influence of the vadose media

The vadose vulnerability index map is a multiplication of the aquifer rating map and the weight of the vadose media. The superior weight of 5 makes the vadose media impact differently from the aquifer media with weight 3. Figure 4.12 shows the vadose media vulnerability index map. The map is divided into five classes with class 45 being the highest vulnerable area and class 20 the lowest. Low to moderate vulnerability classes dominate. Very high and very low both occur in Tegbi. The vadose media indicates the area is low risk. Very high, high, moderate, low and very low vulnerability classes have areal coverage of 1.8%, 3.2%, 15.5%, 75.6%, And 3.8% of the study area.

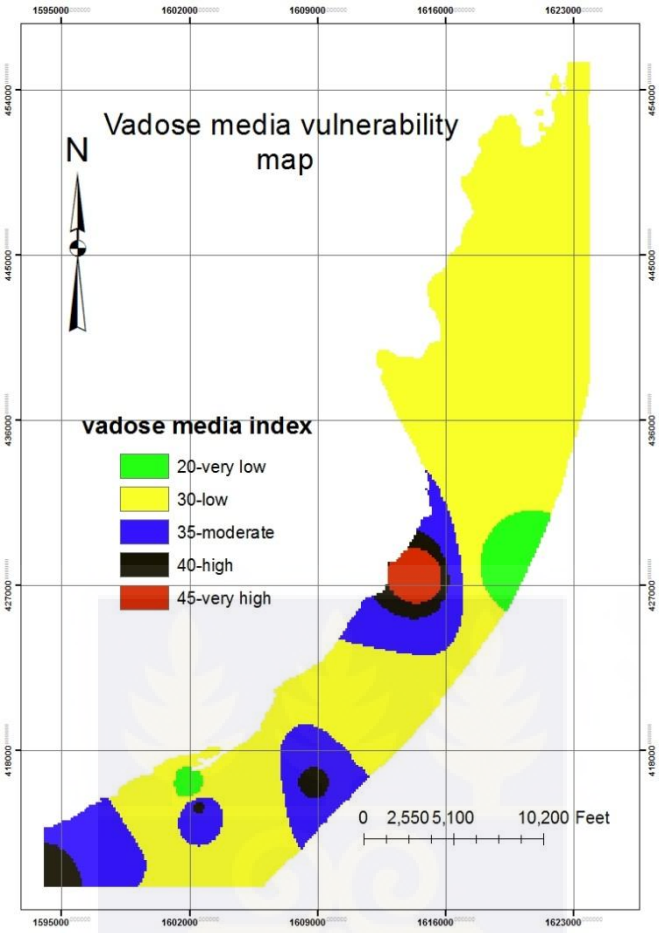

Figure 4.13 Influence of vadose zone media index map

4.2.7 Hydraulic conductivity

The hydraulic conductivity vulnerability index map in Figure 4.14 shows five classes. Low and moderate classes dominate forming 95.8% of the study area. Very high, high, moderate and low vulnerability classes have 0.8%, 2.8%, 24.6%, and 71.8% areal coverage of the study area. Most of the study area has conductivity values between 30 to 60 m/day which are quite moderate for such sandy environments. Conductivity values of 100 m/day and above are found in the few gravely zones around Woe and Tegbi but they donot contribute much to conductivity vulnerability.

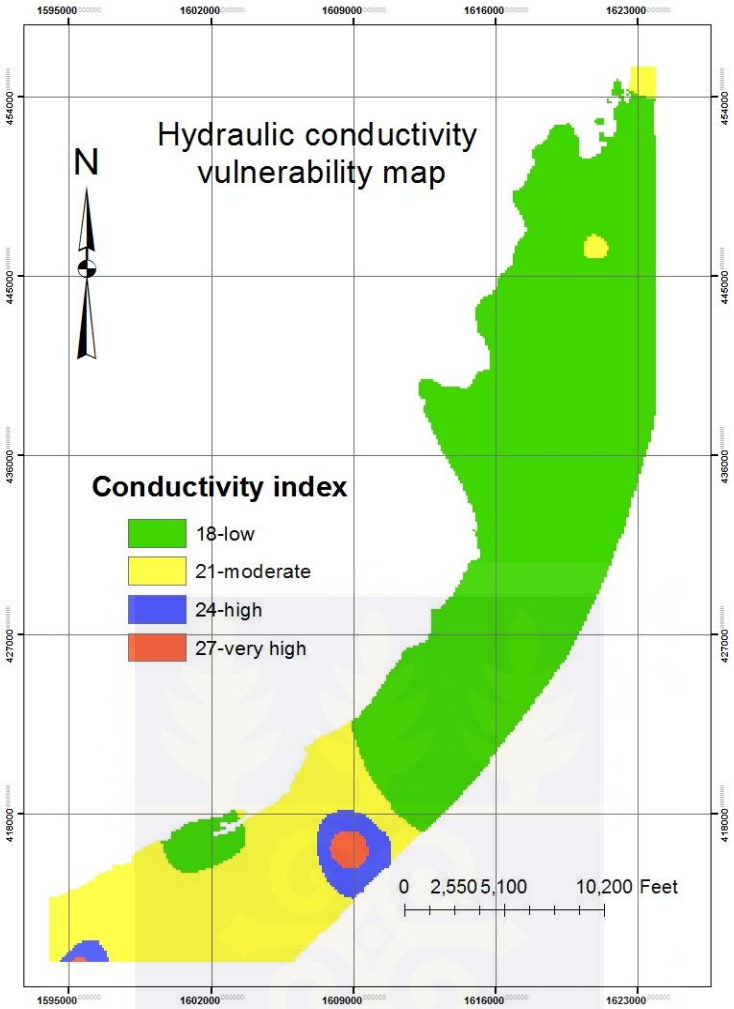

Figure 4.14 Hydraulic conductivity index map

4.3 OVERLAY PROCESS

The seven index raster maps were added using the raster calculator feature on ArcGIS to produce a variable quantitative DRASTIC index (DI) values. These DI values delineate the potential vulnerability to groundwater pollution due to anthropogenic activities. The quantitative index values were then categorized and converted to qualitative indices to produce an intrinsic groundwater vulnerability map of the Keta strip as shown in Figure 4.15. The map shows the sensitivity of the aquifer to ground-surface contamination. The intrinsic vulnerability map for the area has index values of 131 to 198. The map shows areas

delineated into classes of very low to very high potential vulnerabilities. Table 4.16 shows the classifications, ranges and percentages of areas covered by each class.

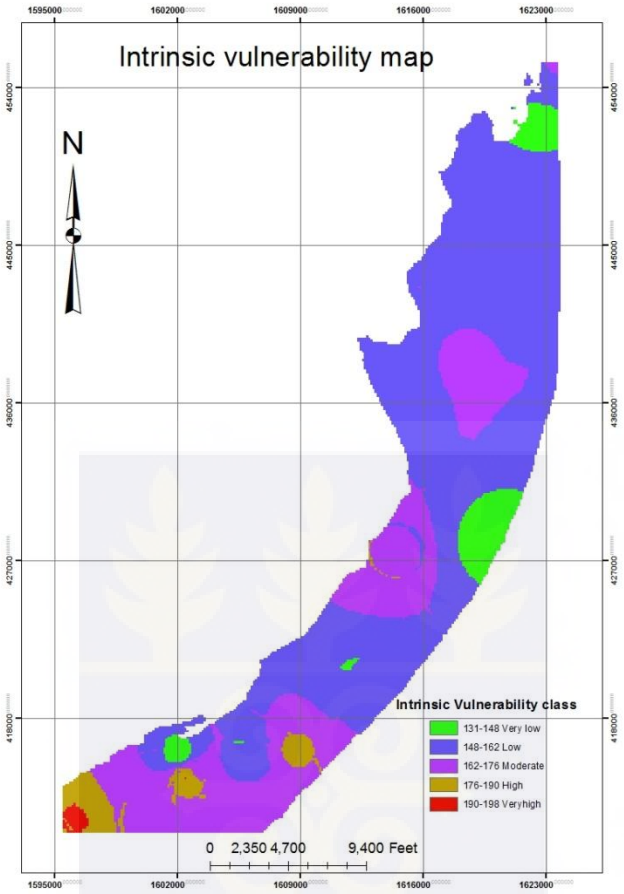

Figure 4.15 Intrinsic vulnerability map

Table 4.16 DRASTIC Index map analysis

DRASTIC index	DRASTIC range	Pixel Count	Area (Km^2)	% of the total area
VERY LOW	131 - 148	1341	1.84	5.57
LOW	148 - 162	15154	20.82	62.97
MODERATE	162 - 176	6585	9.05	27.36
HIGH	176 - 190	866	1.19	3.60
VERY HIGH	190 - 198	118	0.16	0.49
Total		24064	33.06	100

Pixel size = (37.1 x 37.1) m. Unit Pixel area = 1373.7m^2. Total Area = 33.1km^2

The map shows that low vulnerability class dominates (62.97% areal coverage) and mainly covers sections of Anloga, Woe, Tegbi, Dzelukope, Kedzikope and Keta. This is due to the relatively deeper water tables (1.9-2.6 m) in these zones. Very low vulnerability class has an areal coverage of 5.6%. This class occurs around the northern fringes of Anloga, close to the Keta lagoon and around Woe and Tegbi and Keta closer to the sea. The low class closer to the lagoon is probably due to the clay and loamy (containing some organic material) soils which possess good contaminant attenuation characteristics. Very high vulnerability class has the lowest areal coverage (0.5%) and covers a very small section of the study area around Anloga. This is due to the coarse sands and gravelly nature of the soils to the southern parts of Anloga which help increase infiltration. High to very high vulnerability classes have together an areal coverage of 4.1% and occur around Anloga, Woe and Tegbi. These vulnerability classes are also due to the gravels and porous vadose zone and aquifer media especially around Woe and Tegbi.

4.4 GROUNDWATER NITRATE CONTAMINATION

Groundwater nitrate concentration was used as the pollution index in this research. Generally groundwater nitrate concentration of 3 mg/L and above is above naturally occurring concentration levels and the aquifer has been impacted by anthropogenic activities (Tesoriero and Voss, 1997). Agricultural activities and urban settlements are found in most parts of the study area. Nitrates from agricultural and domestic sources therefore constitute the main ground-surface contaminants in the study area. According to Evans and Maidment (1995) nitrates form one of the most widespread contaminants of health significance in groundwater

and occur naturally from nitrogen-rich rock minerals, atmospheric deposition and as by-products of anthropogenic activities such as agriculture, human wastes and land disposal of municipal and industrial wastes. The sources of nitrate contamination in an agricultural setting are shown in Figure 4.16.

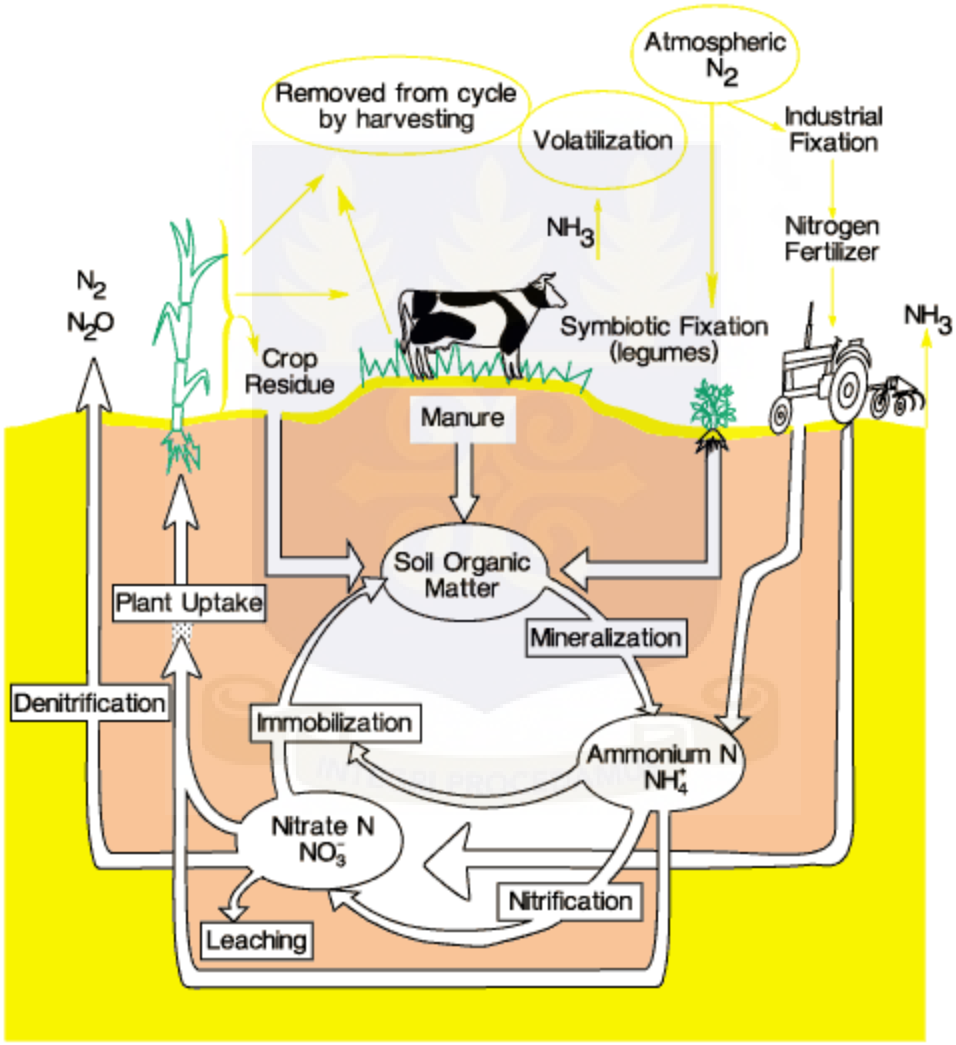

Figure 4.16 Nitrogen cycle in the soil and vadose zone in an agricultural setting.

(Source: Esser et al. 2002)

Nitrate concentrations above 10mg/l in drinking water pose a potential health hazard to humans (USEPA, 1996a). The United States Environmental Protection Agency (USEPA) has ,therefore, proposed nitrate as a representative indicator of groundwater quality degradation (US Environmental Protection Agency, 1996a).

Nitrate in drinking water can cause methemoglobinemia, a fatal oxygen-deficient condition in babies called the "blue baby" syndrome. Other health risks include a link to cancer and spontaneous abortions in some women (Gurdak and Qi, 2006). In order to address the health risks associated with the ingestion of nitrates many countries and the World Health Organisation (WHO) have established the maximum concentration limit for nitrates in drinking water. The U.S. Environmental Protection Agency (USEPA) established a Maximum Contaminant Level (MCL) of 10 mg/L nitrate as N (measured as Nitrogen) in drinking water (U.S. Environmental Protection Agency, 2004).

In groundwater nitrogen occurs as nitrate or nitrite anions and as ammonium cations. Nitrite is unstable in aerated water while nitrates are readily transported in water and are stable over a wide range of conditions (Evans and Maidment, 1995). There are a wide range of contaminants in groundwater. The DRASTIC model assumes a generic contaminant which has the following characteristics: The contaminant is highly soluble and has the mobility of water. It is chemically stable over a wide range of conditions. It comes from a wide range of natural non-point sources and sources associated with land use practices (Aller et al., 1987). Nitrate is chosen in this research as the indicator for groundwater vulnerability because it has the characteristics of the generic contaminant as suggested by the authors of DRASTIC. It is one of the most widely measured water quality parameters.

The use of nitrate as a generic contaminant for groundwater vulnerability assessments has been tested by many researchers including Tesoriero and Voss (1997); Nolan, (1998); Rupert, (2001), Nolan et al., (2002); Babiker et al., (2004); Stigter et al., (2005); Panno et al.,(2006);

Nolan and Hitt (2006); Antonakos and Lambrakis; (2006); Rahman (2008); Awawdeh and Jaradat, (2009); Saidi et al., **(**2010); Hasiniaina et al., (2010); Elçi , (2010); Javadi et al., (2011).

Nitrate concentration values are measured and reported in milligrams per litre (mg/l). Concentration measurements may be expressed as nitrate-NO_3 or nitrate –N. Nitrate measured as NO_3 refers to nitrate with a molecular weight of 62. Nitrate measured as nitrogen has a molecular weight of 14. Thus the minimum nitrate concentration level of 10 mg/l nitrate-N is equivalent to 44.3mg/l nitrate-NO_3.

A study of the UNEP water quality data over two years reveals that nitrate concentrations are highest during the month of April and corresponds with the highest water table rise. The highest water table rise increases the vulnerability of the groundwater. Hence nitrate data for April, 2004 was used to test the DRASTIC model. The nitrate concentration data measured as Nitrate-Nitrogen from fifty five (55) wells is shown in Table 4.17.

Table 4.17 April, 2004 nitrate concentration data (UNEP, 2005)

April, 2004 nitrate concentration values			
ID	Longitude	Latitude	NO_3 (mg/l)
AL1	0.93382	5.81227	0.09
AL2	0.93162	5.81181	0.69
AL6	0.925	5.80588	13.49
AL7	0.92315	5.80662	1.25
AL8	0.92201	5.80435	0.04
AL9	0.92067	5.80879	0.05
AL11	0.91622	5.80243	0.07
AL12	0.91454	5.80089	34.95
AL15	0.93551	5.81015	21.92
AL17	0.92962	5.80765	4.06
AL18	0.92799	5.80507	42.06
AL19	0.92569	5.80355	20.44
AL20	0.92315	5.80624	8.73
AL23	0.91525	5.79883	30.44
WE1	0.96481	5.839	0.64
WE3	0.96357	5.84132	0.55
WE12	0.93932	5.81582	0.48
WE14	0.96717	5.83982	11.53
WE15	0.9669	5.83766	0.09
WE16	0.96497	5.83582	0.13
WE19	0.95971	5.8338	33.48
WE20	0.9579	5.83162	449.42
WE21	0.95722	5.82952	20.07
WE24	0.94941	5.82565	62.48
WE29	0.93729	5.81235	24.29
kk1	0.98955	5.90896	140.53
kk5	0.98883	5.90831	41.59
kk7	0.99034	5.91076	447.8
kk11	0.9901	5.90538	200.71

kk14	0.99141	5.90491	138.92
kk17	0.98874	5.90578	80.57
kk25	0.98813	5.90332	164.02
kk30	0.98505	5.89972	15.54
kk33	0.99105	5.919	143.62
kk37	0.99069	5.89518	50.39
kk38	0.98565	5.8955	52.48
ket 1	0.99122	5.92131	24.45
ket 5	0.99267	5.92149	63.9
ket 6	0.99181	5.92022	51
ket 10	0.99021	5.92148	16.27
ket 16	0.99125	5.9164	134.69
ket 20	0.99054	5.91314	4.13
TG 2	0.98145	5.87165	0.33
TG 3	0.97988	5.87214	0.41
TG 6	0.98638	5.86503	0.96
TG 7	0.9829	5.86106	5.99
TG 8	0.97512	5.85751	2.71
TG 10	0.98478	5.85414	2.5
TG 12	0.97631	5.84831	1.4
TG 16	0.97368	5.84093	0.23
DN 4	0.98279	5.88746	25.43
DN 6	0.9786	5.89176	1.36
DN 9	0.98195	5.88294	2.09
DN 11	0.99076	5.88863	1.88
DN 14	0.99062	5.88063	1.8

4.5 MODEL CALIBRATION

Fifty five wells sampled in April, 2004 for nitrate concentration in the study area were plotted using graduated symbols on the intrinsic vulnerability map. A visual inspection of the

resulting map shown in Figure 4.17 indicates that most of the high nitrate concentration data are found in areas delineated as low and very low vulnerability. However, the area delineated as very high vulnerability contained no high values of nitrate concentration. Statistical correlation was used to test if the model is an accurate representation of vulnerability in the study.

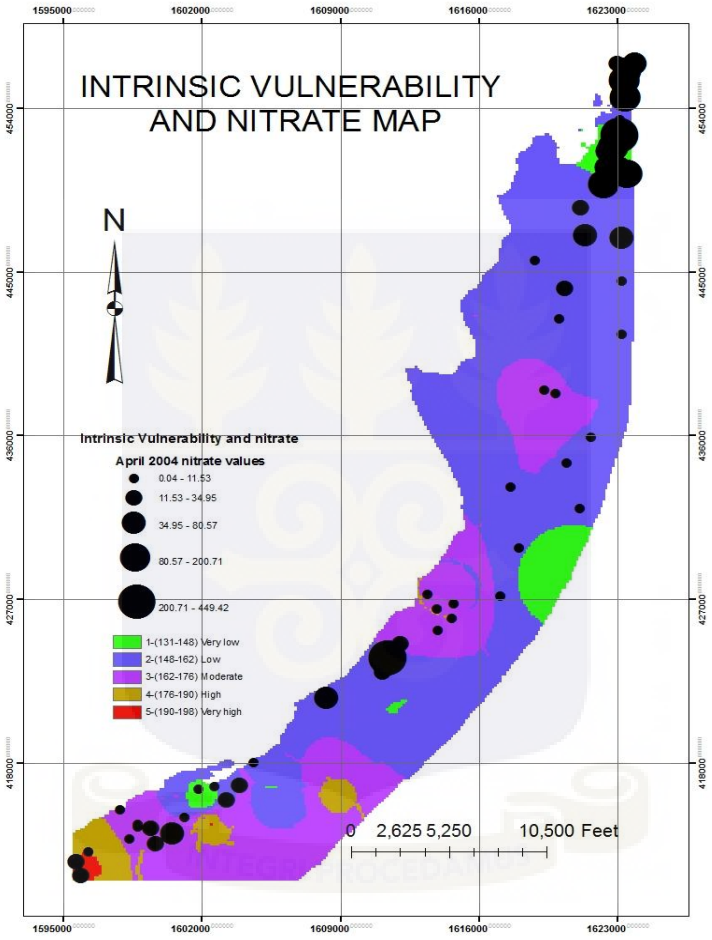

Figure 4.17 Map of April, 2004 nitrate concentrations plotted on intrinsic vulnerability map

4.5.1 Statistical correlation to determine effective parameters and optimal weights

After plotting the nitrate data on the intrinsic vulnerability map, the corresponding vulnerability values were extracted from the nitrate points. Table 4.18 shows the nitrate values and the vulnerability classes. The correlation between the nitrate values and the

extracted vulnerability values were calculated for Pearson (r), Spearman (ρ), and Kendall (τ) as -36.4%, -36.3% and -27.0% respectively. The correlation coefficients are low. The low coefficients may be due to the subjective approach to the selection of the rating and weight values of the parameters. The DRASTIC model in this form is therefore not an appropriate representation of the groundwater vulnerability of the area. In order to reduce subjectivity and address the low coefficients, the model was modified by optimizing the weights and ratings of the parameters. The modifications are envisaged to lead to improvement on model accuracy in predicting groundwater vulnerability to pollution in the study area.

In order to optimise the weights, nitrate concentration values sampled from 55 wells in April 2004 were plotted on each parameter rating map. The corresponding rating value for each point was extracted and the correlation coefficients between rating and nitrate values were calculated. Table 4.19 shows the nitrate concentration values and the rating values used for the correlation.

Table 4.18 Data used for correlation of DRASTIC intrinsic vulnerability class with Nitrate values

Well ID	NO_3 value (Mg/L)	DRASTIC vulnerability class
AL1	0.09	2
AL2	0.69	1
AL6	13.49	3
AL7	1.25	3
AL8	0.04	4
AL9	0.05	3

AL11	0.07	5
AL12	34.95	4
AL15	21.92	3
AL17	4.06	3
AL18	42.06	3
AL19	20.44	3
AL20	8.73	3
AL23	30.44	4
WE1	0.64	3
WE3	0.55	3
WE12	0.48	3
WE14	11.53	3
WE15	0.09	3
WE16	0.13	3
WE19	33.48	2
WE20	449.42	2
WE21	20.07	2
WE24	62.48	2
WE29	24.29	3
kk1	140.53	1
kk5	41.59	1
kk7	447.8	1
kk11	200.71	2
kk14	138.92	2
kk17	80.57	2
kk25	164.02	2
kk30	15.54	2
kk33	143.62	2
kk37	50.39	2
kk38	52.48	2
ket 1	24.45	3
ket 5	63.9	2

ket 6	51	3
ket 10	16.27	2
ket 16	134.69	2
ket 20	4.13	1
TG 2	0.33	3
TG 3	0.41	3
TG 6	0.96	2
TG 7	5.99	2
TG 8	2.71	2
TG 10	2.5	1
TG 12	1.4	2
TG 16	0.23	2
DN 4	25.43	2
DN 6	1.36	2
DN 9	2.09	2
DN 11	1.88	2
DN 14	1.8	2

Table 4.19 Data of Correlation of DRASTIC parameter ratings with Nitrate values

	Parameter rating values						
NO_3 concentration (mg/L)	**D**	**R**	**A**	**S**	**T**	**I**	**C**
0.09	7	3	4	10	10	4	6
0.69	7	3	6	10	10	6	6
13.49	7	8	8	8	10	8	8
1.25	7	8	8	8	10	8	8
0.04	7	8	9	8	10	8	8
0.05	7	8	8	8	10	8	8
0.07	5	8	9	8	10	9	8

34.95	10	8	9	8	10	9	8
21.92	7	3	6	10	10	6	6
4.06	7	6	6	10	10	6	8
42.06	7	8	8	10	10	8	8
20.44	5	8	8	8	10	8	8
8.73	7	8	8	8	10	8	8
30.44	10	10	9	8	10	9	8
0.64	7	1	10	4	10	10	6
0.55	7	1	10	4	10	10	6
0.48	7	1	6	8	10	6	8
11.53	7	1	10	4	5	10	6
0.09	7	1	10	4	10	10	6
0.13	7	1	9	4	10	9	6
33.48	7	1	9	8	10	9	6
449.42	7	1	8	8	10	8	6
20.07	5	1	8	8	10	8	6
62.48	7	1	8	8	10	8	8
24.29	7	3	6	10	10	6	8
140.53	5	1	6	8	10	6	6
41.59	5	1	6	8	10	6	6
447.8	5	1	6	8	10	6	6
200.71	5	1	6	8	10	6	6
138.92	5	1	6	8	10	6	6
80.57	5	1	6	8	10	6	6
164.02	7	1	6	8	10	6	6
15.54	7	1	6	8	10	6	6
143.62	5	1	6	8	10	6	6
50.39	7	3	6	8	10	6	6
52.48	7	1	6	8	10	6	6
24.45	5	1	6	8	10	6	6
63.9	5	1	6	8	10	6	6
51	5	1	6	8	10	6	6

16.27	5	1	6	8	10	6	6
134.69	5	1	6	8	10	6	6
4.13	5	1	6	8	10	6	6
0.33	9	3	8	8	10	8	6
0.41	9	3	8	8	10	8	6
0.96	9	3	6	8	10	6	6
5.99	9	3	6	8	10	8	6
2.71	7	1	8	8	10	8	6
2.5	9	1	6	8	10	6	6
1.4	7	1	6	8	10	6	6
0.23	7	1	8	4	10	8	6
25.43	7	3	6	8	10	6	6
1.36	7	3	6	8	10	6	6
2.09	7	3	6	8	10	6	6
1.88	7	3	6	8	10	6	6
1.8	7	3	6	8	10	6	6

Table 4.20 shows the correlation coefficients and the revised weights of the seven parameters. Spearman non parametric correlation coefficients were chosen for this analysis. This is because the DRASTIC rating values are ranked data from 1 to 10 and the nitrate data is not normally distributed. These conditions make the use of rank correlation methods such as Spearman (ρ) and Kendall (τ) suitable for these kinds of data (Elçi, A., (2010). Spearman (ρ) was chosen because the coefficients for each parameter were averagely larger than those obtained for Kendall (τ). From the table it can be deduced that topography is statistically insignificant and does not influence pollution. Soil media and conductivity are statistically significant but have lesser influence on pollution as compared to the remaining parameters. Topography, soil and conductivity parameters were therefore eliminated from the DRASTIC equation (equation 4.1). Depth to water (D), aquifer media (A), recharge (R) and influence of the vadose zone media (I) are the effective parameters to obtain the acronym DRAI. The

correlation coefficients are generally low probably because of the relatively low nitrate concentration values in the study area. They however provide the basis for the elimination of some parameters and the revision of the weights to achieve higher coefficients. The effective DRAI parameters and revised weights are shown in table 4.21. The revised weights differ from those of the original DRASTIC. Depth to water (D) has maintained its weight of 5. Recharge (R), and aquifer media (A) have been upgraded from 4 to 4.2 and from 3 to 4 respectively indicating that they are more important in contributing to groundwater pollution than was initially thought. Influence of the vadose zone (I) has however been downgraded from 5 to 4, placing a lower importance to this parameter.

Table 4.20 Correlation coefficients of DRASTIC parameter ratings and Nitrate

Factor	Pearson (r)	Spearman(ρ)	Kendall (τ)
D	-0.349	**-0.428**	-0.486
R	-0.245	**-0.339**	-0.239
A	-0.317	**-0.326**	-0.221
S	0.290	0.199	0.201
T	-0.030	-0.009	-1.00
I	-0.317	**-0.326**	-0.221
C	-0.145	-0.147	-0.288
	P_r<0.05	P_r<0.05	P_r<0.05

P_r is the probability of correlation

In order to determine the revised weights, the highest correlation coefficient value is assigned to the highest DRASTIC possible weight (5). The lowest correlation value is assigned to the

lowest possible weight (1). The corresponding revised weights of the remaining coefficients are then calculated from the linear equation

$$RW=9.55\rho+0.91 \qquad 4.2$$

Where RW is the revised weight and ρ is the Spearman correlation coefficient.

Table 4.21 Effective parameters and revised weights as obtained from Spearman (ρ) correlation

Parameter	Original Weight	Spearman(ρ)	Revised Weight
D	5	**-0.428**	**5.0**
R	4	**-0.339**	**4.2**
A	3	**-0.326**	**4.0**
I	5	**-0.326**	**4.0**
		P_r<0.05	

4.5.2 Determination of optimal rating values

The rating values were modified by using the mean nitrate values and the original ratings. April 2004 nitrate concentration data was plotted on each of the DRAI parameter rating maps. Nitrate values were then extracted from all sections of the rating map. The mean value of nitrate in each category was then calculated. For example, after plotting the nitrate values on the depth to water rating map, nitrate values are extracted from all sections of the map with rating value of 10. The mean nitrate value is then calculated. The same procedure is followed for sections with rating values of 9, 7 and 5. Table 4.22 shows the mean nitrates concentration and the modified ratings of every range and media type. Using the modified

ratings, new raster rating maps were developed for each of the DRAI parameters. These maps were developed sorely to enable the use of the raster calculator feature on ArcGIS to calculate the final DRAI vulnerability map and are not shown here.

Table 4.22 Original and modified ratings based on mean nitrate concentrations

Depth to Water (D)			
Range (m)	Original Rating	Mean NO_3^- (mg/L)	Modified rating
0.48-1.2	10	26.47	**2.6**
1.2-1.9	9	37.37	**3.6**
1.9-2.6	7	24.51	**2.4**
2.6-3.3	5	103.42	**10.0**
Recharge (R)			
Range (m)	Original rating	Mean NO_3^- (mg/L)	Modified rating
0.07-0.36	6	51.42	**10.0**
0.36-0.66	7	14.67	**2.9**
0.66-0.95	8	21.92	**4.3**
0.95-1.25	9	11.27	**2.2**
1.25-1.54	10	43.48	**8.5**
Aquifer media (A)			

Media type	Original rating	Mean NO_3^- (mg/L)	Modified rating
Fine Sand	4	no data	**4.0**
Medium Sand	6	49.69	**10.0**
Coarse Sand	8	31.14	**6.3**
Gravel and Sand	9	19.2	**3.9**
Gravel	10	27.82	**5.6**
Influence of vadose media (I)			
Media type	Original rating	Mean NO_3^- (mg/L)	Modified rating
Fine Sand	4	no data	**4.0**
Medium Sand	6	49.69	**10.0**
Coarse Sand	8	31.14	**6.3**
Gravel and Sand	9	19.2	**3.9**
Gravel	10	27.82	**5.6**

Using the revised weights and modified ratings the DRAI equation for a point in the study area becomes

V (intrinsic) = 5.0D+4.2R+4A+4I ***4.3***

Where V (intrinsic) is the intrinsic vulnerability and D, R, A and I are the modified depth to water (D), recharge (R), aquifer media (A) and influence of the vadose media (I) rating values at that point.. The optimised DRAI vulnerability map was developed using the above equation with the raster calculator feature on ArcGIS to produce a variable quantitative DRAI index (DI) values These DI values delineate the potential vulnerability to groundwater

pollution. The quantitative index values were then categorized and converted to qualitative indices to produce an optimized intrinsic groundwater vulnerability map of the Keta strip as shown in Figure 4.18. A comparison of nitrate data with the DRAI model was done by plotting April 2004 nitrate concentration data on the DRAI vulnerability map as shown in Figure 4.19. The Spearman rho correlation coefficient between nitrate concentrations and vulnerability classes after optimizing the factor weights and ratings improved from 36 % to 62 %. This is an improvement in the prediction capacity of the model. Table 4.23 shows the data used for the correlation.

Table 4.23 Data used for correlation of DRAI intrinsic vulnerability class with Nitrate values

ID	NO_3 concentration (Mg/L)	Optimized DRAI vulnerability Class

AL1	0.09	1
AL2	0.69	1
AL6	13.49	2
AL7	1.25	1
AL8	0.04	1
AL9	0.05	1
AL11	0.07	2
AL12	34.95	2
AL15	21.92	1
AL17	4.06	2
AL18	42.06	2
AL19	20.44	1
AL20	8.73	1
AL23	30.44	2
WE1	0.64	2
WE3	0.55	2
WE12	0.48	2
WE14	11.53	1
WE15	0.09	2
WE16	0.13	2
WE19	33.48	3
WE20	449.42	4
WE21	20.07	3
WE24	62.48	3
WE29	24.29	1
kk1	140.53	5
kk5	41.59	5
kk7	447.8	5
kk11	200.71	5
kk14	138.92	5
kk17	80.57	5
kk25	164.02	5

kk30	15.54	4
kk33	143.62	5
kk37	50.39	4
kk38	52.48	4
ket 1	24.45	5
ket 5	63.9	5
ket 6	51	5
ket 10	16.27	5
ket 16	134.69	5
ket 20	4.13	5
TG 2	0.33	2
TG 3	0.41	2
TG 6	0.96	4
TG 7	5.99	4
TG 8	2.71	3
TG 10	2.5	4
TG 12	1.4	4
TG 16	0.23	2
DN 4	25.43	4
DN 6	1.36	4
DN 9	2.09	4
DN 11	1.88	4
DN 14	1.8	4

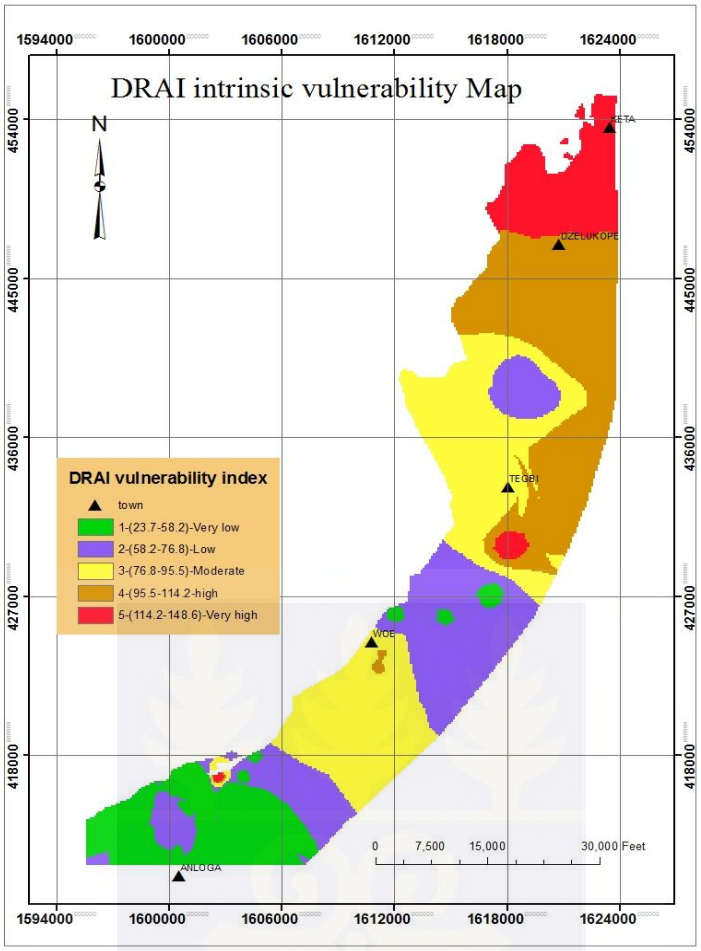

Figure 4.18 Optimised DRAI intrinsic vulnerability map as obtained from correlation

Table 4.24 shows the classifications, ranges and percentages of areas covered by each class. The map shows that low vulnerability class although reduced, still dominates (36.97% areal coverage). It covers mainly sections of Anloga and Woe. Tegbi, Dzelukope, Kedzikope and Keta are no longer considered as low vulnerability areas under this model as was the situation in the first DRASTIC intrinsic map (Figure 5.14). Very low vulnerability class areal coverage has reduced from 5.6% to 5.3% and has the lowest areal coverage. This class still occurs around the northern fringes of Anloga, close to the Keta lagoon and around Woe but no longer at Tegbi and Keta. Very high vulnerability class has areal coverage (10.7%) and covers maily Kedzikope, Dzelukope and Keta. This is due to the shallow water tables around these area and pollution of groundwater from septic tanks and other domestic sources. Very low, low and moderate vulnerability classes together form 65.6% of the area. Thus, despite

the active agricultural activities in the study area especially around Anloga and Woe groundwater vulnerability is still relatively low.

Table 4.24 Optimised DRAI index as obtained from correlation.

Optimised DRAI Index map analysis of the study area				
Index	Range	Pixel Count	Area (Km^2)	% of the total area
VERY LOW	1.0-51	1480	1.78	5.3
LOW	51-103	10236	12.34	36.9
MODERATE	103-152	6486	7.82	23.4
HIGH	152-204	6582	7.93	23.7
VERY HIGH	204-255	2957	3.56	10.7
Totals		27741	33.44	100

Pixel size = (34.7 x 34.7) m. Unit Pixel area = 1205.3m^2. Total Area = 33.44km^2

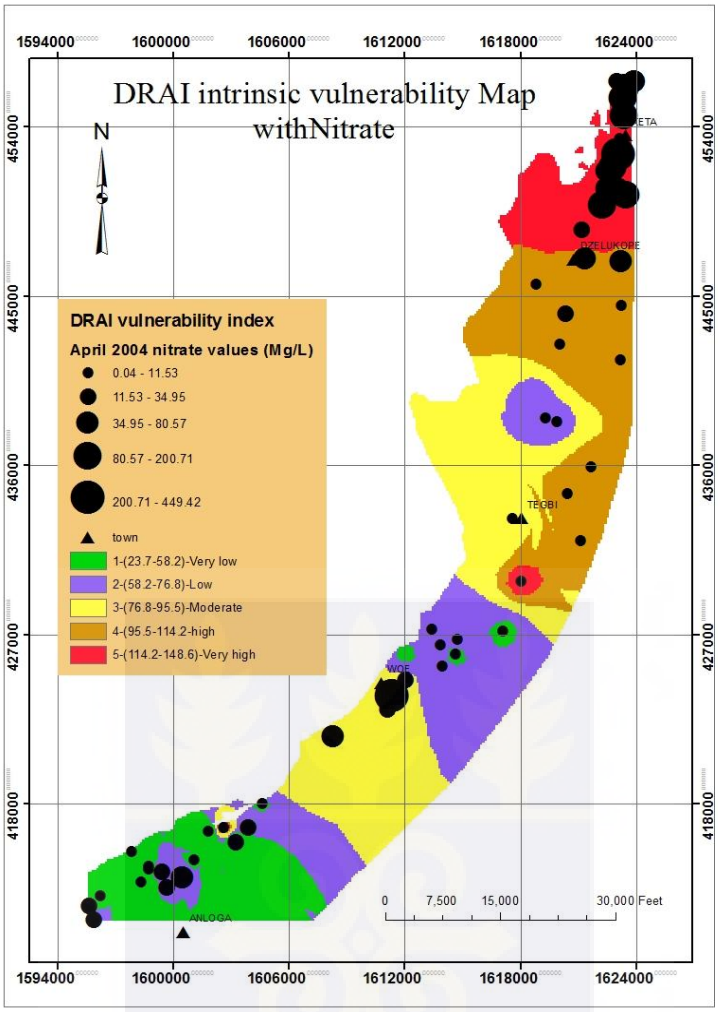

Figure 4.19 DRAI intrinsic vulnerability map and nitrate

The composite vulnerability map in Figure 4.19 shows that most high nitrate values (201.19-462.2) mg/l are located in areas designated as high and very high vulnerability classes. This map is an improvement over the original DRASTIC intrinsic vulnerability map of Figure 4.15. Most of the low nitrate values are located in zones demarcated as moderate to low vulnerabilities. A few high nitrate values are located in the area designated as moderate vulnerability. The model was therefore modified in a bid to make it more accurate using the analytic hierarchy process.

4.5.3 Analytic hierarchy process (AHP)

The AHP was used to estimate a value for each of the factor weights for the DRAI parameters in an attempt to further refine the model. The conventional DRASTIC weights (D = 5, R = 4, A = 3 and I = 5) were used as input values for the AHP analysis to determine weights for the DRAI parameters. The relative weight of each factor was then calculated as the Eigen vector using matrix algebra. Table 4.25 shows the pairwise matrix and the calculated Eigen vectors

Table 4.25 Pair-wise matrix of relative factor weights

					Product Of values	n^{th} root of product of values	Eigen vectors	$A\omega=\lambda_{max}$	λ_{max}
	D	R	A	I					
D	1.00	1.25	1.67	1.00	2.083	1.201	**0.294**	1.176	4
R	0.80	1.00	1.33	0.80	0.853	0.961	**0.235**	0.941	4
A	0.60	0.75	1.00	0.60	0.270	0.721	**0.176**	0.706	4
I	1.00	1.25	1.67	1.00	2.083	1.201	**0.294**	1.176	4
Totals						4.085	1.000		

The calculated eigenvector of the relative importance or value of D, R, A and I is (0.294, 0.235, 0.176, 0.294). D and I are the most valuable, R follows and A is less significant. The Eigen vectors form the new weight determined from the AHP method.

The new DRAI equation from the AHP analysis as described in chapter three is

$$IV=0.294D+0.235R+0.176A+0.294I \qquad 4.4$$

The intrinsic vulnerability map was produced by arithmetic overlay process. It was reclassified to five vulnerability classes and is shown in Figure 4.20. The map was tested with nitrate concentration map of the area as shown in Figure 4.21. There was a significant

improvement in the correlation coefficient from 39.4% to 66% after correlation between nitrate concentration data and the vulnerability class at the nitrate locations.

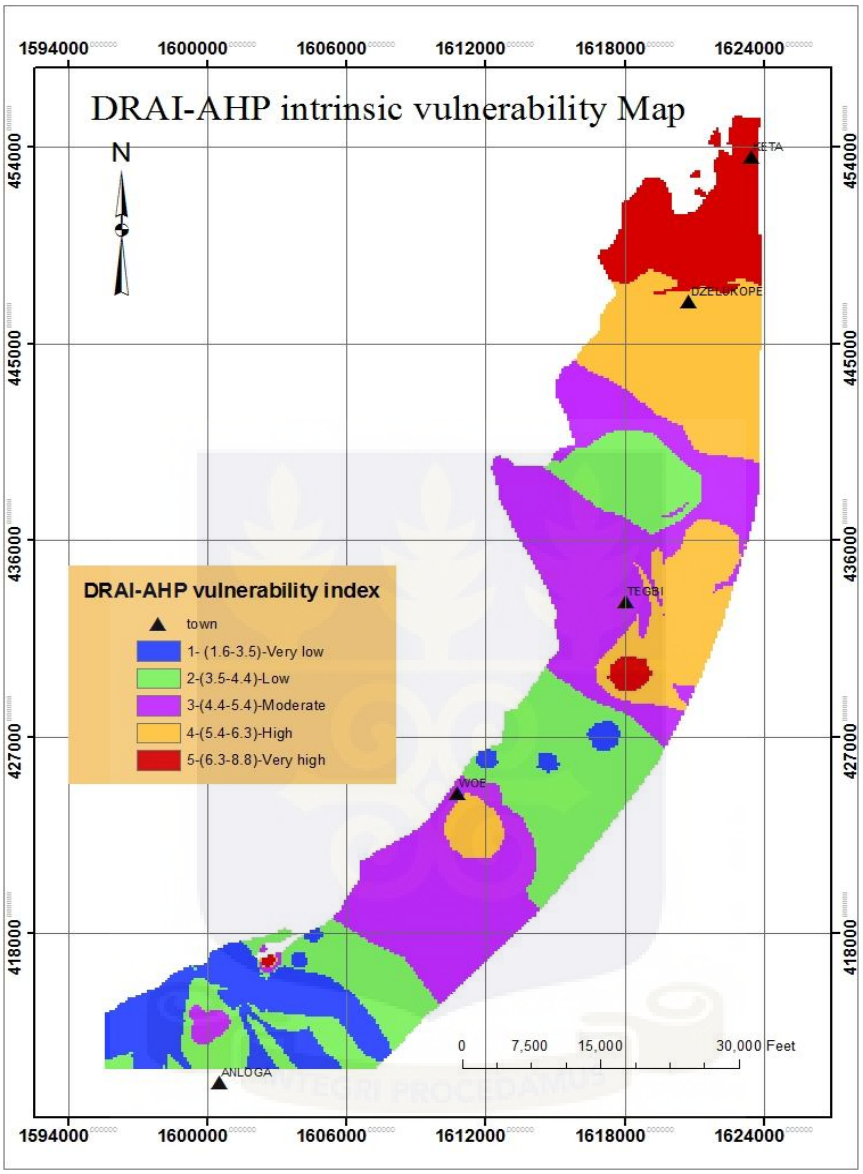

Figure 4.20 DRAI optimized Vulnerability map as obtained from AHP

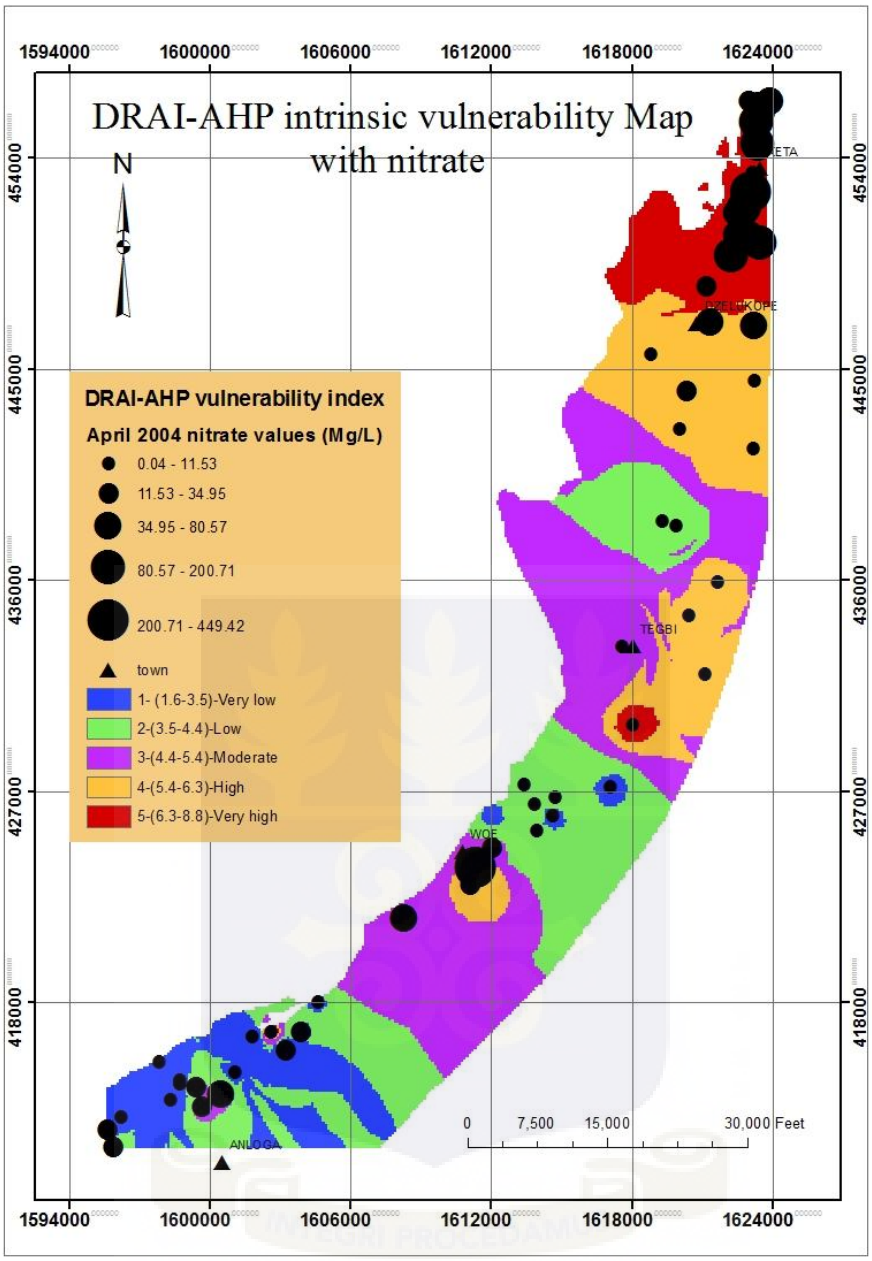

Figure 4.21 Intrinsic vulnerability map with Nitrate as obtained by AHP

4.6 COMPARISON OF MAPS

Figure 4.22 shows a visual comparison of the maps produced from the three vulnerability models. There is a significant shift of very low vulnerability index (green legend colour in figure 4.22a) from Keta and areas in Tegbi to an area in Anloga (green legend colour in Figure 4.22b). However very high vulnerability values (red legend colour in figure 4.22a) has

shifted from a small portion in Anloga to a large area in Keta (red legend colour in Figure 4.22b). These shifts and changes in areal coverages reflect improvements in the vulnerability map of the study area as evidenced by improvement in the correlation coefficients of vulnerability values and nitrate concentration data.

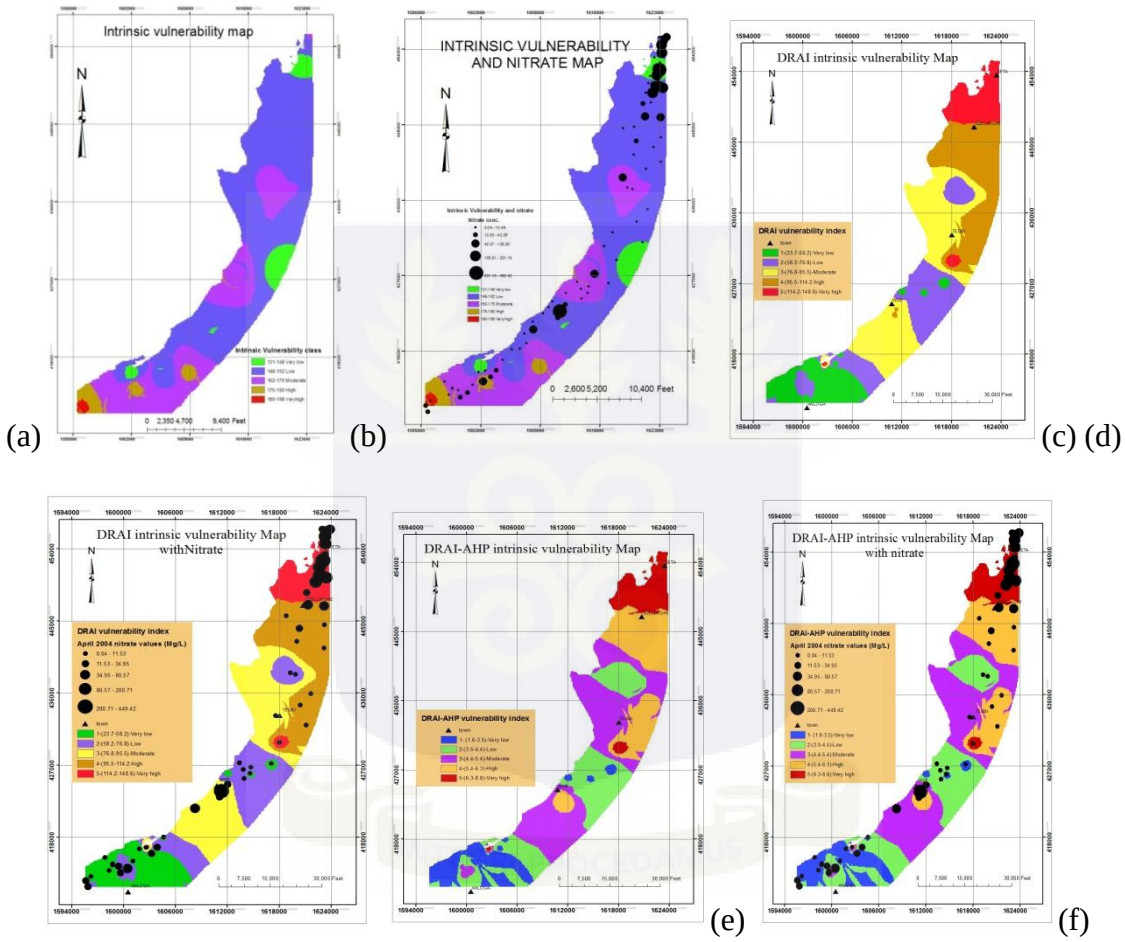

Figure 4.22 Aquifer vulnerability maps with nitrate as obtained by (a)&(b) DRASTIC, (c)&(d) DRAI with statistical correlations, (e)&(f) DRAI with analytic hierarchy Process

A comparison of map (b) and (c) shows there is little difference between the two maps. Very high vulnerability zones in both maps correlate with high nitrate values. The application of the analytic hierarchy process has reduced the high vulnerability area in map (b) to a smaller area in map (c). The percentage of total area covered for the vulnerability classes under each

method is shown in Table 4.26. Generally, vulnerability of groundwater increases from Anloga to Keta.

Table 4.26 Comparison of percentage of total area vulnerability coverage

Vulnerability Class	Original DRASTIC (% of total area)	Correlation DRAI (% of total area)	AHP DRAI (% of total area)
Very low	5.57	13.1	10.6
Low	62.97	21.7	26.8
Moderate	27.36	30.7	30.1
High	3.60	24.3	22.6
Very High	0.49	10.1	9.9

4.7 SELECTION OF VULNERABILITY MODEL

The analytic hierarchy process (AHP) produced the highest improvement in the Spearman rank correlation coefficient between nitrate values and vulnerability values from 0.36 to 0.66. The optimized DRAI intrinsic vulnerability map as obtained by the AHP method shown in Figure 5.18 will therefore be adopted as the vulnerability model for the area. The large nitrate values lying in the ranges (106.81-201.18) mg/l and (201.19-482.43) mg/l occur mostly in the

urban settlements around Dzolukope and Keta where agricultural activities are almost absent. Septic tanks, manholes and poorly lined old graves are common in the area and may be the cause of these high nitrate values.

4.8 MODEL VALIDATION

Nitrate concentration values measured the previous year in July 2003 but not used for developing the model were used to validate the DRAI model. Figure 4.23 shows July 2003 nitrate values plotted on the AHP optimized DRAI vulnerability map. It can be inferred from the map that no well with high nitrate levels (90.47-567.85) mg/l can be found in the areas classified as very low and low risk. Most of the high nitrate values are located in the high risk areas around Kedzekope and Keta. Thus the map and nitrate values compare well. The spearman correlation coefficient between the nitrate data and vulnerability class values is 74%. Thus the AHP method provides a suitable estimation of groundwater pollution risk for the study area. The use of AHP is therefore an effective method to modify the DRASTIC model in order to achieve better correlation with nitrates concentration data.

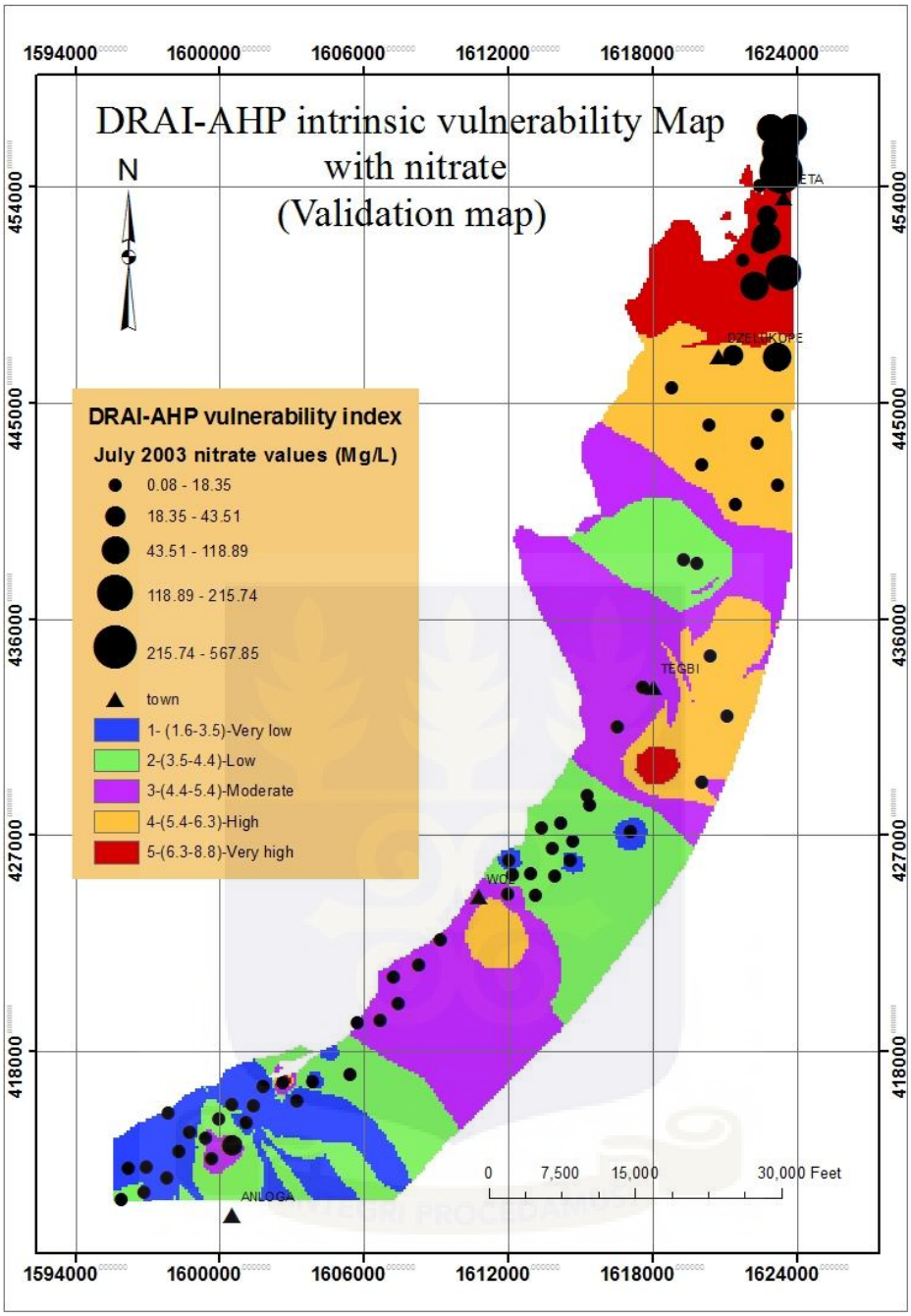

Figure 4.23 DRAI-AHP intrinsic vulnerability validation map.

4.9 DISCUSSION OF MODEL RESULTS

The DRAI indices identify areas that are more likely to be susceptible to ground water pollution from near ground surface anthropogenic activities. The index provides a relative

vulnerability between vulnerability classes and not an absolute numerical value. The higher the DRAI index, the greater the potential risk to groundwater pollution. The DRAI index has values ranging from 1.6 to 8.8. Using a colour coding system from ArcGIS, the vulnerability maps of the three models were colour coded using ranges as shown on the map legends. The color codes were chosen to represent the colors of the spectrum, with warm colors (red, orange, and yellow) for areas with higher potential for groundwater pollution (higher vulnerability indexes) and cool colors (greens, blues, and violet) for areas of lower vulnerability.

4.9.1 Vulnerability classification

The map in Figure 4.20 shows areas delineated into five ranked classes of very low, low, moderate, high and very high potential vulnerabilities. Table 4.26 shows the classifications, ranges and percentages of areas covered by each class. Moderate vulnerability class dominates (30.1% areal coverage) and mainly covers small sections of Anloga and significant sections of Woe and Tegbi.

4.9.2 Very high vulnerability class

Very high vulnerability class has the lowest percentage areal coverage (9.9%) and covers small sections of Anloga and Tegbi but covers a significant area around Dzelukope and Keta. The very high potential for groundwater pollution in these areas is due to the porous vadose zone and aquifer media especially around Keta and very permeable gravels around Tegbi. The relatively shallow water tables and high recharge around Anloga may also account for the very high vulnerability class in these zones.

4.9.3 High vulnerability class

This class has 22.6% percentage coverage of the study area. The coverage progresses from a relatively small portion in Woe through to Tegbi to a greater portion of the land around Dzelukope.

The High vulnerability may be due to high recharge potential, shallow depth to water table, permeable gravel and porous vadose media around Woe and Tegbi. Another reason for the high value is that the areas all have almost zero slopes and recharge is through direct local infiltration from the surface.

4.9.4 Moderate vulnerability class

Moderate ranked vulnerability has the largest percentage areal coverage of 30.1% and occurs in Anloga, Woe and Tegbi only. According to Sunil et al. (2008) groundwater resources of moderate class are areas made up of unconsolidated sediments, low slope, relatively deep water tables and moderate to slow soil permeability. Depth to water is relatively deeper in areas around Woe and Tegbi (1.9-2.6) metres. Slopes in the entire area are virtually zero.

4.9.5 Low vulnerability class

Low vulnerability class is dominated by sandy soils with small sections closer to the lagoon in Anloga made up of loamy soils. 26.6% of the study area falls within this class of vulnerability. The class is characterized by relatively deeper water table (2.6-3.3) metres. Clay rich and alluvial sediments which reduce permeability of the sediments occur around Anloga and Woe towards the lagoon. This accounts for the low groundwater pollution potential in these zones.

4.9.6 Very low vulnerability

This class occurs mainly around Anloga and covers 10.6% of the study area. The groundwater table in these areas is relatively deeper (1.9-3.3 m). The very low class around the northern fringes of Anloga and closer to the lagoon is probably due to the clay and loamy soils (containing some organic material) which possess good contaminant attenuation characteristics and hence reduce the potential for groundwater contamination.

It must be emphasized that sites with very low vulnerability index are not free from groundwater contamination, but are less susceptible to contamination compared with the sites with higher index values. Only site specific investigations can determine the level of groundwater pollution.

4.10 APPLICATION OF DRAI VULNERABILITY MAP

The DRAI optimized Vulnerability map as obtained from AHP in Figure 5.18 can be used for a wide variety of applications. Vulnerability maps are usually prepared to assist land use planners, managers of state agencies such as Community water and Sanitation Agency (CWSA), Water resources Commission (WRI) and local non-governmental organizations involved in evaluating the relative vulnerability of areas to ground water pollution. An important application of this pollution potential map in the study area is land use planning in determining site suitability for solid waste disposal. The present situation of indiscriminate waste disposal does not auger well for the protection of groundwater in the study area.

Other important applications that require the use of the vulnerability map include underground fuel storage tanks, well head protection public water supplies, groundwater

monitoring, agricultural chemicals, waste water management, best management practice implementation and development; hazardous waste and public information. Since the map delineates areas according to how susceptible they are to pollution, ground water protection strategies can be developed such that special attention is paid to those areas identified as low to very low vulnerability zones. More resources can therefore be channeled to these areas in the form of increased frequency of groundwater monitoring. Community animation programs can be developed to inform and educate people about ground water resources. New development projects will be carefully sited based on this map. Groundwater protection plans may need to be developed for existing and new projects.

The map constitutes a useful data source for further research either in the same area or in adjacent regions for groundwater contamination evaluation from non-point sources.

4.11 THE DRAI MODEL LIMITATIONS

The limitations of the present vulnerability map are those that pertain to maps generated by the use of the general DRASTIC model.

(a) The use of the DRAI to assess groundwater vulnerability is limited to areas greater than 0.4 km^2. The study area is greater than 30 km^2 and hence justifies the use of this model to generate valid vulnerability maps.

(b) The Neogene aquifer is believed to underlie the Quaternary aquifer under investigation. It is not very clear however if over the entire study area the Neogene may not be as shallow as 3 m. Under such scenario the study area may actually consist of major and minor aquifers, and will therefore not be considered as one aquifer.

(c) The DRAI vulnerability map shows average relative vulnerability values for the study area. Thus while the map is valid for evaluating relative vulnerability of the area, it should not be substituted for site-specific assessments.

(d) The model does not consider contaminant loading and toxicity effects. The map therefore cannot show areas that will be contaminated or areas that cannot be contaminated.

(e) The map cannot be permanent for the depiction of vulnerability in the area. The vulnerability assessment was based on field data generated by the author. These data may change with changing climatic and other conditions over time. The vulnerability map will then need to be updated as additional or new information becomes available.

4.12METHODOLOGY LIMITATIONS AND SOURCES OF ERROR

(a) The static water levels are not a true reflection of the "static" water table because the wells in the study area are used frequently throughout the day.

(b) The assumption that the sea tide has no influence on the water table fluctuation is unlikely especially for those wells closer to the sea.

(c) It would have been best to have taken the RTK elevations of all points using the differential GPS. This was not possible because clouds, trees and building coverage blocked view and the GPS could not function.

(d) Another major source of error is from the equipment used for the research. The water level indicator may introduce errors in the measurement of static water levels especially as the dry cell batteries get weaker. The Trimble dual frequency differential GPS used in this research already has a manufacturers' specified error of ±0.04metres in its measurements.

(e) Experimental errors in the analysis and determination of the soil, vadose, hydraulic conductivity and aquifer media may be introduced from the use of instruments from the Laboratory. Errors may also arise from the Judgement in classifying soil and aquifer samples into the various media types. Spatial interpolation to estimates values of un-sampled points may under or overestimate the values.

CHAPTER FIVE

SUMMARY, CONCLUSIONS AND RECOMMENDATIONS

5.1 SUMMARY

The focus of this research was to assess the intrinsic vulnerability to pollution of the unconfined aquifer in the Keta strip. The broad objectives were

1. To evaluate vulnerability using DRASTIC (Depth to water, net Recharge, Aquifer media, Soil media, Topography, Impact of vadose zone, and hydraulic Conductivity) model and GIS technology.
2. To provide a spatial analysis of the parameters and conditions under which groundwater may become contaminated.
3. To evaluate the relative importance of the DRASTIC model parameters using statistical correlations and analytical hierarchy process
4. To determine groundwater vulnerable zones to contamination and produce groundwater vulnerability maps of the study area within GIS environment capable of predicting pollution risk of the aquifer under environmental stress.

In order to meet these broad objectives, data was gathered from public institutions and from field work in the area. Specifically, data was gathered on all the seven DRASTIC parameters which include static water levels, soil sampling to determine soil media and aquifer media types, hydraulic conductivity, elevations and water quality.

Using GIS methods the data was prepared, processed and analysed. Interpolation techniques were used to generate raster layers of the parameters. The seven raster maps were combined using ArcGIS ESRI (2007) arithmetic overlay process to produce a composite vulnerability map. The map was reclassified into five classes namely, very low, low; moderate, high and very high pollution potential. The resulting map shows the relative intrinsic vulnerability of the unconfined aquifer to pollution in the study area.

The map was tested to determine if it is an accurate representation of vulnerability in the study area. Using nitrate concentration in groundwater as a pollution index, nitrate data measured in April, 2004 was plotted on the map. Statistical correlation between nitrate values and vulnerability class values extracted from the nitrate points yielded a Spearman rho correlation coefficient of 36.3%. The coefficient is low. The model was therefore calibrated using statistical correlations between each parameter and nitrate values. Seven correlation coefficients were thus produced. Soil media, topography and hydraulic conductivity parameters were not significantly correlated to nitrate pollution and were eliminated from the model parameters leaving depth to water (D) recharge (R), aquifer media (A) and influence of the vadose media (I) to form the acronym DRAI. The weights of the parameters were revised based on the seven correlation coefficients. The rating values were also revised based on the mean nitrate values for each rating class of the original DRASTIC. The new equation for the DRAI model using the modified weights and rating values was determined as

$$\mathbf{V_{(intrinsic)} = 5D+4.2R+4A+4I}$$

Where V (intrinsic) is the intrinsic vulnerability and D, R, A and I are the revised depth to water, recharge, aquifer media and influence of the vadose media rating values.

The model accuracy was tested by applying correlation to the vulnerability classes and nitrate concentration data. A correlation coefficient of 62 % was obtained. A further attempt was made to improve the accuracy of the model by using the analytic hierarchy process (AHP) to calibrate the model by determining a different set of parameter weights. A pair-wise matrix which expresses the relative values of the modified DRAI model factor weights was constructed following the method developed by Saaty (1980). The Eigen values derived from matrix analysis formed the calibrated weights. The new DRAI equation from the AHP analysis is

$$\mathbf{V_{(intrinsic)} =0.294D+0.235R+0.176A+0.294I}$$

The model accuracy improved to 66% after correlation between nitrate values and intrinsic vulnerability classes.

The models generated from the three different weighting and rating schemes were compared and on the basis of statistical correlation coefficients .The AHP model had the highest coefficient of 66% and was therefore selected for the study area. The AHP optimized intrinsic vulnerability map shows that 10.6%, 26.8%, 30.1%,22.6% and 9.9% of the study have very low, low, moderate, high and very high vulnerability to groundwater pollution respectively.

Nitrate concentration values from seventy wells sampled across the entire study area in July 2003 were used to evaluate validation of the AHP model. First, the nitrate values were plotted as graduated symbols on the AHP vulnerability map and a visual evaluation showed that high nitrate values corresponded to areas demarcated as high risk and low nitrate concentration values correspondeded to areas delineated as low risk. A further statistical correlation test between nitrate values and vulnerability values yielded a correlation coefficient of 75%, confirming a close agreement between model values and actual nitrate pollution on the ground.

Anloga and Woe area where agriculture is predominant has the lowest intrinsic vulnerability. The low pollution potential is probably due to a low nitrate loading from the use of limited inorganic and organic fertilizers. Soils in these areas also contain some organic matter that has good contaminant attenuation properties. Dzelukope, Kedzikope and Keta are heavily populated residential areas and have very high groundwater pollution potential. Nitrate concentration values follow the same trend as concentration values increases progressively from the western to eastern part of the study area.

5.2 CONCLUSIONS

The use of DRASTIC and GIS as a tool has proved to be an effective method in the evaluation of groundwater vulnerability in the study area. Large data sets involving numerous operations such as the overlay operations were automatically processed. These reduced data processing time and immensely improved efficiency. GIS has an added advantage of maintaining a database of each map layer in the form of an attribute table. A layer can easily be updated by modifying the attribute data. The digital vulnerability maps produced during this research can be combined with, land use maps, data on pollution sources and groundwater quality to evaluate groundwater pollution risk.

The validation evaluation indicates that the obtained results are realistic and representative of the actual groundwater pollution on the ground. Therefore, the DRAI model is applicable in the study area.

The spatial variation in pollution potential makes the vulnerability map suitable for identifying areas which must have high priority in terms of groundwater protection and pollution prevention. Land use planners and managers of state agencies involved in managing groundwater resources may also use the map. An important application of this pollution potential map in the study area is land use planning in determining site suitability for solid waste disposal. Other important applications that require the use of the vulnerability map in the area include underground fuel storage tanks, well head protection especially public water supplies, groundwater monitoring, agricultural chemicals, waste water management, hazardous waste and public information.

Since the map delineates areas according to how susceptible they are to pollution, ground water protection strategies involving frequent groundwater monitoring can be developed for those areas identified as high to very high vulnerability zones. Community animation programs can be developed to inform and educate people about ground water resources. New

development projects will be carefully sited based on this map. Groundwater protection plans may need to be developed for existing and new projects.

The vulnerability DRAI-AHP model developed can be used for further research either in the same area or in regions with similar hydrogeological conditions for groundwater contamination evaluation from non-point sources. Areas with similar hydrogeological conditions include the unconsolidated alluvial deposits of river Bia and Tano, located at Half Assini; river Pra at Sekondi; river Amisa at Cape Coast and river Densu at Accra.

The vulnerability equation is suited to predict the degree of groundwater susceptibility at any location within the study area. The vulnerability score for a location within the study area can be calculated directly from the model equation (5.2) if the values of the parameters are known.

5.3 RECOMMENDATIONS

The recommendations from this research are in two categories.

- General recommendations that will mitigate groundwater pollution in the study area and
- Recommendations for further research that will improve on the method of groundwater assessment used in this research.

5.3.1 General recommendations

The following recommendations are made based on the vulnerability class for actions to mitigate pollution in the short, medium and long term.

(a) Very high and high vulnerability zones

Responsible authorities should give priority to zones demarcated as very high and high risk areas during the planning of land use for development projects. The very

high nitrate values in these areas imply the groundwater resource has reached unacceptable limits to pollution. An immediate plan to stop further pollution should be designed and implemented. Tegbi, Dzelukope and Keta are heavily populated areas and therefore specific activities such as the use of unlined graves, direct discharge of sewage into the shallow aquifer should be stopped. Septic tanks should be lined. Any existing refuse dumps should be either relocated or given the necessary protection to avoid any direct contact of effluent or leachate from reaching groundwater. A programme involving groundwater level monitoring should be designed and implemented immediately. Permits for the siting of industries should be strict and only those very vital with less hazardous by-products may be permitted in the area. If financial resources are available a remediation plan to clean up the resource should be considered.

A detailed near surface site investigation should be carried out to reveal the type of geologic material and their vertical extent. Monitoring programs involving frequent sampling and analysis of groundwater should be implemented. The use of fertilisers on farmlands in the area especially in the depressions around the southern parts of Tegbi should be monitored.

(b) Moderate and low vulnerability zones

There is a risk to groundwater pollution as indicated on the vulnerability map. This requires a limited site investigation. Seasonal water level monitoring, soil and water sampling, hydrochemical analysis of pollution indicators are recommended for further validation of the vulnerability map. The use of fertilisers on farms in the area should be monitored. A programme should be established to estimate pollutant loading by gathering information on the quantities of fertilizers and types of herbicides used

annually. This information can be used to determine toxicity levels and help in a risk assessment for the study area.

(c) Very Low vulnerability zones

The concerns for groundwater pollution are not high. Therefore most measures here should be proactive in order to prevent pollution. There should be animation programmes to create awareness and educate policy makers, chiefs and the general public on groundwater vulnerability to pollution.

5.3.2 Recommendations for further research

(a) This research considered intrinsic vulnerability based only on the hydrogeologic features in the area. From the water quality data, there is a high groundwater nitrate concentration. A specific vulnerability evaluation should be conducted to address the risk of nitrate pollution.

(b) The results of this research depend heavily on the geologic material in the study area. Soil sampling was used to determine six (6) out of the seven (7) DRASTIC parameters. It is therefore recommended that further detailed research be conducted on the geologic material, to improve these parameters and enable further validation of the vulnerability map.

(c) The methodology considered the hydraulic conductivity of the aquifer media but did not consider the horizontal direction of flow of contaminants. This is important especially if the flow direction is from high pollution sources to areas with low pollution. Groundwater flow directions for the shallow aquifer should be

established from a simple groundwater flow model. Data from a well-planned constant discharge pumping test and static water level measurements will help provide information on the hydraulic regime.

(d) Nitrate was used as the only pollution indicator in this research. Specific vulnerability mapping should be conducted using different pollution indicators from anthropogenic sources such as herbicides which are used on farm lands in the area.

(e) The impact on groundwater vulnerability from land use related activities was not considered in the research. Agriculture forms a major land use type in the area and the use of fertilisers has an impact on vulnerability. The inclusion of nitrogen loading in the DRASTIC model in future studies will improve the vulnerability map.

(f) The hydraulic conductivity parameter was determined from grain size analysis and compared with values from literature. An alternative method involving a constant discharge pumping test should be conducted properly to calculate hydraulic conductivity.

(g) In the calculation of the recharge it was assumed the water table fluctuation is due entirely to recharge from only precipitation. In coastal areas variations in water levels are influence also by tides and barometric pressures. These factors should be considered in any future research in order to calculate more accurately the net recharge value. A different approach to recharge estimation such as using water

balance should be considered for further validation of the vulnerability map produced.

REFERENCES

Agyekum, W.A. (2002). Groundwater resources of Ghana with focus on international shared aquifer boundaries. Proceedings of the International Workshop, Tripoli Libya.

Ahmed, A.A. (2009). Using generic and pesticide DRASTIC GIS-based models for vulnerability assessment of the Quaternary aquifer at Sohag, Egypt. Hydrogeology Journal 17: 1203–1217.

Al Hallaq, A. and Abu, E. B. (2011). Assessment of Aquifer Vulnerability to Contamination in Khanyounis Governorate, Gaza Strip Palestine, Using the DRASTIC Model within GIS environment. An - Najah Univ. J. Res. (N. Sc.) 25: 1-48

Al-Hanbali, A. and Kondoh, A. (2008). Groundwater vulnerability assessment and evaluation of human activity impact (HAI) within the Dead Sea groundwater basin, Jordan. Hydrogeology Journal 16: 499–510.

Aller, L., Bennet, T., Lehr, J.H., Petty, R.J. and Hackett, G. (1987). DRASTIC: A standardised system for evaluating groundwater pollution potential using hydrogeological settings. US Environmental Protection Agency, Ada, Oklahoma.

Anderson, M.P. and Woessner, W.W. (1992). Applied groundwater modeling: Simulation of flow and advective transport. Academic Press Inc. 381p New York U.S.A.

Antonakos, A.K. and Lambrakis, N.J. (2006). Development and testing of three hybrid methods for the assessment of aquifer vulnerability to nitrates, based on the drastic model, an example from NE Korinthia, Greece. Journal of Hydrology 333: 288–304.

Asiamah, R.D. (1995). Soils of the Keta-Ho Plains, Volta Region, Ghana. Memoir No. 10. Soil Research Institute. Kumasi, Ghana.

Awardzi, T.W., Ahiabor, E., Breuning-Madsen, H. (2008). The Soil-Land Use system in a sand spit area in the semi-arid coastal savannah region of Ghana-Development, sustainability and threats. West African Journal of Applied Ecology 13: 181-194.

Awawdeh, M.M. and Jaradat, R.A. (2009). Evaluation of aquifer vulnerability to contamination in the Yarmouk River basin, Jordan, based on DRASTIC method. Saudi Society for Geosciences 3:273–282.

Babiker, I.S., Mohamed M.A.A., Hiyama T. and Kato K. (2004). A GIS-based DRASTIC model for assessing aquifer vulnerability in Kakamigahara Heights, Gifu Prefecture, Central Japan. Science of the Total Environment 345: 127– 140.

Bannerman, R. R. (1994). Appraisal of the limestone aquifer of the Keta Basin, Ghana. Future Groundwater Resources at Risk (Proceedings of the Helsinki Conference. IAHS Publ. no. 222.

Banoeng-Yakubo, B., Danso, S., and Tumbulto, J. (2005). Assessment of Pollution Status and Vulnerability of Water supply Aquifers in Keta, Ghana. UNEP/UNESCO/UN-HABITAT/ECA.

Bedane, E. (2008). Aquifer vulnerability assessment in Modjo River Catchment ,Central Main Ethiopian Rift). MSc Thesis, School of Graduate Studies, University of Addis Ababa.

Dickson, K.C. and Benneh, G. (1980). A New Geography of Ghana. Longmans Group Ltd. London.

Carbonell, A.J., Alley, W.M., Batten, L.G.,Contant, C.K., Doctor, P.G. and Donigian, A.S. (1999). Impact of urban growth on surface water and groundwater quality. Dhaka, Bangladesh. IAHS Publ. 259: 91-98

Childs, C. (2004). Interpolating Surfaces in ArcGIS Spatial Analyst. ESRI education sevices. www.esri.com

Coyle, G. (2004). The Analytic Hierarchy Process, Practical Strategy. Open Access Material. Pearson Education Limited. www.booksites.net

Elçi, A. (2010). Groundwater vulnerability mapping optimized with groundwater quality data: The Tahtalı Basin Example Dokuz Eylül University, Dept. of Environmental Engineering Izmir, TURKEY.

El-Naqa, A., Hammouri, N. and Kuisi, M. (2006). GIS-based evaluation of groundwater vulnerability in the Russeifa area, Jordan. Revista Mexicana de Ciencias Geológicas 23: 277-287

ESRI (2007). ArcGIS 9.2 Desktop help ArcGIS resource centre. http://resources.arcgis.com.

ESRI (2010) ArcGIS10 Desktop. ArcGIS resource centre. http://resources.arcgis.com.

Esser, B., Hudson, B., Moran, J., Beller, H., Carlsen, T., Dooher, B., Krauter, P., Mcnab, W., Madrid, V., Rice, D. and Verce, M. (2002). Nitrate contamination in California groundwater: An integrated approach to basin assessment and resource protection. Nitrate white paper V8. Lawrence Livermore National Laboratory, USA.

Evans, T. A. and Maidment, D. R. (1995). A spatial and statistical assessment of the vulnerability of Texas groundwater to nitrate contamination. Centre for Research in Water Resources The University of Texas at Austin.

Focazio, M. J., Reilly, T. E., Rupert, M G. and Helsel, D. R. (2002). Assessing ground-water vulnerability to contamination: Providing scientifically defensible information for decision makers. U.S. Geological Survey Circular 1224.

Foster, S. S. D. and Skinner, A. C. (1995). Groundwater quality: Remediation and protection. Proceedings of the Prague Conference. IAHS Publ. 225:471-482

Foster, S.S.D. and Hirata, R. (1988). Groundwater pollution risk assessment: A methodology using available data. WHO/PAHO-CEPIS Technical manual, Lima, Peru. 88 p

Freeze, R. A. and Cherry, J. A. (1979). Groundwater. Prentice Hall, USA 604 p

Garrett, P., Williams, J.S., Rosoll, T.F. and Tolman A.L. (1989). Are groundwater vulnerability classifications systems working? In: Proceedings of the FOCUS conference on Eastern Regional groundwater issues. National Groundwater Association, Columbus OH. PP 329-343

Ghana Statistical Service (2000) Population and housing census. Ghana Statistical Service, Accra.

Gogu, R. C., Hallet, V. and Dassargues, A. (2003) Comparison of aquifer vulnerability assessment techniques. Application to the Néblon River basin, Belgium. Environmental Geology. 44: 881–892.

Gougazeh, M. and Sharadqah S. (2009). Groundwater vulnerability to contamination in Jordan evaluated in two levels of analysis. Jordan Journal of Civil Engineering. 3(4):314-321

Gurdak, J. J. and Qi, S. L. (2006). Vulnerability of recently recharged ground water in the High Plains Aquifer to nitrate contamination. U.S. Geological Survey Scientific Investigations Report 2006–5050, 39 p.

Harter, T and Walker, L. G. (2001). Assessing vulnerability of groundwater. California Department of Health Services. www.dhs.ca.gov/ps/ddwem/dwsap/DWSAPindex.htm

Hasan, M.K., Burgess, W. and Dottridge J. (1999). The vulnerability of the Dupi Tila Aquifer of heavy metals using ordinal logistic regression. Proceedings of IUGG 99 Symposium HS5, Birmingham, July 1999. IAHS Publ. 259:91-98.

Hasiniaina, F., Zhou, J. and Guoyi, L. (2010). Regional assessment of groundwater vulnerability in Tamtsag basin, Mongolia using DRASTIC model.
Journal of American Science. 6(11):65-78.

Helsel, D.R. and Hirsch R.M. (1992). Statistical methods in water resources. New York: Elsevier.

Hotor, V.K. (2003). Assessment of water quality and the freshwater-salinewater interface in the Anloga area of the Keta basin, Ghana. MPhil thesis, University of Ghana, Accra.

Jasem, A. H. and Alraggad M. (2010). Assessing groundwater vulnerability in Azraq basin area by a modified DRASTIC index. Journal of Water Resource and Protection. 2:944-951.

Javadi S., Kavehkar N, Mousavizadeh M.H. and Mohammadi K., (2011). Modification of DRASTIC model to map groundwater vulnerability to pollution using nitrate measurements in agricultural areas. Journal of. Agr. Sci. Tech. 13:239-249.

Jorgensen, N. O. Banoeng-Yakubo, B. K. (2001) Environmental isotopes as a tool in groundwater investigations in the Keta Basin, Ghana. Hydrogeology Journal. 9:190-201

Juan, J., Bastida M., Arauzo, M. and Valladolid, M. (2009) Intrinsic and specific vulnerability of groundwater in central Spain: The risk of nitrate pollution. Hydrogeology Journal 18: 681–698.

Kachi ,S., Kherici, N. and Kachi, N. (2007) Vulnerability and pollution risks in the Alluvial Aquifer of Tebessa-Morsott. American Journal of Environmental Sciences 3(4):219-224

Kaur, R. and Rosin, K.G (2009). Ground water vulnerability assessment: Challenges and opportunities. Quarterly Journal of Central Ground Water Board. Ministry of Water Resources, Government of India. 24(4):82-89

Kesseh, G. O. (1985). The mineral and rock resources of Ghana. A.A. Balkema/Rotterdam/Boston.

Klug, J. L. (2009). Modeling the risk of groundwater contamination using DRASTIC and Geographic Information Systems in Houston County, Minnesota. Volume 11, Papers in Resource Analysis. 12 pp. Saint Mary's University of Minnesota University Central Services Press. Winona, MN.

Kortatsi, B.K. (1994). Groundwater utilization in Ghana. Future Groundwater Resources at Risk: Proceedings of the Helsinki Conference, June 1994, IAHS Publ. no. 222, 1994.

Kortatsi, B.K. and Agyekum, W.A. (1999). Environmental impact assessment of large scale groundwater abstraction in the Keta Strip of the Volta Region of Ghana. Water Research Institute. Final report, December 1999. 75 pp.

Kortatsi,B.K., Young, E. and Mensah-Bonsu, A. (2005). Potential impact of large scale abstraction on the quality of shallow groundwater for irrigation in the Keta Strip, Ghana. West African Journal of Applied Ecology. 8(1): 1-10.

Koterba, M.T., Wilde, F.D and Lapham, W.W. (1995). Groundwater data-collection protocols and procedures for the National Water-Quality Assessment Program: Collection and documentation of water-quality samples and related data. USGS Open-File Report 95–399.

Kouli, M., Lydakis-Simantiris, N. and Soupios, P. (2008). GIS-based aquifer modeling and planning using integrated geoenvironmental and chemical approaches. Department of Natural Resources and Environment Technological Educational Institute of Crete, Greece.

Lam, N. S. (1983). Spatial interpolation methods review. The American Cartographer. 10: 129-149.

Liggett, J., Gilchrist, A., Denny, S., R., Purdy, L., Munro, P., Lapcevic, V., Carmichael, S., Earle, S., Talwar, S. and Journeay, J.M. (2010). Technical summary of intrinsic vulnerability mapping methods in the Regional Districts of Nanaimo and Cowichan Valley. Geological Survey of Canada, open file 6168.

Liggett, J.E and Talwar, S. (2009). Groundwater vulnerability assessments and integrated water resource management. Streamline Watershed Management Bulletin 13(1): 18-29

Martínez-Bastida, J.J., Arauzo, M. and Valladolid, M. (2009). Intrinsic and specific vulnerability of groundwater in central Spain: The risk of nitrate pollution. Hydrogeology Journal. 18: 681–698

Massone, H., Londoño, M. Q. and Martínez, D. (2010). Enhanced groundwater vulnerability assessment in geological homogeneous areas: a case study from the Argentine Pampas. Hydrogeology Journal. 18: 371–379.

Matkan, A.A., Nassery, H.R. and Ostadhashemi, Z. (2008) Improvement in GIS-based DRASTIC model using statistical methods and Analytical hierarchy process (AHP). Asian Conference on Remote Sensing. Papers/PS202.29.

McDonald, M. G. and Harbaugh, A. (1988). A modular three-dimensional finite-difference groundwater flow model. Techniques of Water Resources Investigation. Book 6, Chapter Al. USGS.

Michael, A.M. and Khepar, S.D. (1997). Water Well and Pump Engineering. Tata McGraw-Hill, New Delhi

Ministry of Local Government and Rural Development (2006). Accra. www.ghanadistricts.com

Napolitano, P. and Fabbri A. G. (1996). Single-parameter sensitivity analysis for aquifer vulnerability assessment using DRASTIC and SINTACS. Proceedings of the Vienna conference on HydroGIS. IAHS Pub. No. 235, pp. 559–566.

National Research Council (1993). Ground-water vulnerability assessment-Predicting relative contamination potential under conditions of uncertainty.Washington, D.C., National Academy Press,

Nerquaye-Tetteh B. H. (1993). Water, sanitation, environment and development. Water resources appraisal in the Keta Basin. In: Proc. 19th WEDC Conference, Accra, Ghana: 102-108.

Nolan, B. T. (1998). Modelling approaches for assessing risk of non-point contamination of ground water: U.S. Geological Survey Open-File Report 98-531, 22 p

Nolan, B. T., and K. J. Hitt (2006). Vulnerability of shallow groundwater and drinking water wells to nitrate in the United States. Environmental Science Technology 40(24): 7834-7840.

Nolan, B. T., Hitt, K. J. and Ruddy, B. C., (2002). Probability of Nitrate contamination of recently recharged ground waters in the Conterminous United States. Environmental Science and Technology 36(10): 2138-2145.

Odong, J. (2007). Evaluation of empirical formulae for determination of hydraulic conductivity based on grain-size analysis. Journal of American Science 3(3): 54-60

Panagopoulos, G.P., Antonakos, A. K. and Lambrakis, N. J (2006). Optimization of the DRASTIC method for groundwater vulnerability assessment via the use of simple statistical methods and GIS. Hydrogeology Journal 14: 894–911.

Panno, S.V., Kelly, W.R., Martinsek, A.T. and Hackley K.C. (2006). Estimating background and threshold nitrate concentrations using probability graphs. Ground water 44(5): 697–709).

Piscopo, G. (2001). Lachlan catchment groundwater vulnerability map explanatory notes, Department of Land and Water Conservation, Sydney, New South Wales.

Pollock, D. W. (1994). Users Guide for MODPATH, version 3: A particle tracking post-processing package for MODFLOW. USGS Open-file Report 94-464.

Qamhieh, N.S.A.R. (2006). Assessment of groundwater vulnerability to contamination in the West Bank, Palestine MSc. Thesis, An- Najah National University, Nablus, Palestine.

Rahman, A. (2008). A GIS based DRASTIC model for assessing groundwater vulnerability in shallow aquifer in Aligarh, India. Applied Geography 28: 32–53.

Ranade, P., Irmak, A. and Maidment, D.R. (2008). Geostatistical analyst. University of Texas at Austin. http://www.ce.utexas.edu

Ranjan, S. P. (2006). Assessment of groundwater vulnerability in Walawe basin, Sri Lanka. IAEG 2006 Paper number 54.

Rosen, L. (1994). A study of the DRASTIC methodology with emphasis on Swedish conditions. Groundwater 32(2): 278–285.

Rupert, M., Dace, T., Maupin, M. and Wichesrki, B. (1991). Groundwater vulnerability assessment, Snake River plain, Idaho. Idaho department of health and welfare, Division of Environmental quality.

Rupert, M.G. (1999). Improvements to the DRASTIC Ground-Water Vulnerability Mapping Method. National Water-Quality Assessment program - NAWQA, USGS Fact Sheet FS–066–99.

Rupert, M.G. (2001). Calibration of the DRASTIC Groundwater Vulnerability Mapping Method. Groundwater 39(4): 625-630.

Saaty, T.L. (2008). Decision making with the analytic hierarchy process, Int. J. Services

Saidi, S., Bouri, S. and Dhia, H., (2009). Groundwater vulnerability and risk mapping of the Hajeb-jelma aquifer (Central Tunisia) using a GIS-based DRASTIC model. Environ. Earth Sci. 59:1579–1588.

Samake, M., Tang, Z., Hlaing, W., M'Bue, I. and Kasereka, K. (2010). Assessment of groundwater pollution potential of the Datong Basin, Northern China. Journal of Sustainable Development 3(2):140-152.

Samake, M., Tang, Z., Hlaing, W., M'Bue, I., Kasereka, K. and Balogun, W.O. (2011). Groundwater vulnerability assessment in shallow aquifer in Linfen Basin, Shanxi Province, China using DRASTIC model. Journal of Sustainable Development 4(1): 53-71.

Schleyer, R. (1994). Quantification of groundwater vulnerability using statistical methods. Future Groundwater Resources at Risk. Proceedings of the Helsinki Conference, June 1994). IAHS Publ. no. 222,

Secunda, S., Collin, M.L. and Melloul, A.J. (1998). Groundwater vulnerability assessment using a composite model combining DRASTIC with extensive agricultural land use in Israel's Sharon Region. Journal of Environmental Management, 54: 39–57.

Statistical Services, (2000). Ghana Population Census Reports, 1970, 1984, 2000, Accra.

Stigter T.Y., Ribeiro, L., Carvalho, A. M. M. (2005) Evaluation of an intrinsic and a specific vulnerability assessment method in comparison with groundwater salinisation and nitrate contamination levels in two agricultural regions in the south of Portugal. Hydrogeol J. 14:79–99.

Sunil, P., Kiran, r., Kumar, R. S., Stalin, K., Archana, P., Sridevi, L., and Radha, A.S., (2008) GIS techniques for groundwater contamination risk mapping: Map India 2008 Conference. College of Engineering, Guindy, Anna University, Chennai - 25

Suresh, R.H., Rao, P.C., Siegel, D.I., Gale, W., Teselle, G.W., Teso, R.R. and Yates, S.R. (1993). Ground water vulnerability assessment- contamination potential under conditions of uncertainty. Committee on techniques for assessing ground water vulnerability. Water Science and Technology Board, Commission on Geosciences, Environment and Resources, National Research Council. National Academy Press., Washington, D.C. 1993.

Sutton, T., Dassau, O. and Sutton, M. (2009) A gentle introduction to GIS. Chief Directorate: Spatial Planning and Information, Department of Land Affairs, Eastern Cape South Africa. Copyright (c) 2009

Technical Cooperation Project (2003). Management, protection and sustainable use of groundwater and soil resources in the Arab Region. Guideline for groundwater vulnerability mapping and risk assessment for susceptibility of groundwater resources to contamination. Technical cooperation project-no.: 2004.2032.3 phase iii.

Tesoriero, A.J., and Voss, F.D. (1997). Predicting the probability of elevated nitrate concentrations in the Puget Sound Basin: Implications for aquifer susceptibility and vulnerability. Groundwater 35(6):1029-1039.

Tesoriero, A.J., Inkpen, E.L. and Voss, F.D. (1998). Assessing groundwater vulnerability using logistic regression. In Proceedings for the Source Water Assessment and Protection '98 Conference. Fountain Valley, California: National Water Research Institute.

Twarakavi, N. K. C. and Kaluarachchi, J.J. (2005). Aquifer vulnerability assessment to heavy metals using ordinal logistic regression. Groundwater 43(2): 200–214.

US Environmental Protection Agency, (1996). Environmental Indicators of Water Quality in the United States. Washington, D.C., U.S. Environmental Protection Agency, Office of Water, EPA 841-R-96-002, 25.

Voudouris, K., Nazakis, N., Polemio, M. and Karaklas, K. (2010). Assessment of intrinsic vulnerability using DRASTIC model and GIS in Kiti Aquifer-Cyprus. European Water Publications 30:13-24.

Vrba, J. and Zaporozec, A. (eds.). (1994). Guidebook on Mapping Groundwater Vulnerability. IAH International Contribution for Hydrogegology. 16:94-131.

Weight, W.D. (2008) Hydrogeology field manual, second edition. McGraw-Hill.

White, F.M. (2008) Fluid mechanics, sixth edition. McGraw-Hill International Edition.

Zaporozec, A (ed) (2002). Groundwater contamination inventory: A Methodological Guide. IHPVI Series on Groundwater No 2. UNESCO, Paris.

APPENDIX 1 SOME DEFINITIONS OF VULNERABILITY AS PROVIDED BY CARBONELLET AL. (1993)

Foster (1987)

- **Aquifer Pollution Vulnerability** - "the intrinsic characteristics which determine the sensitivity of various parts of an aquifer to being adversely affected by an imposed contaminant load." U.S. General Accounting Office (1991)
- **Hydrogeologic Vulnerability** - "a function of geologic factors such as soil texture and depth to ground water."
- **Total Vulnerability** - "a function of these hydrogeologic factors, as well as the pesticide use factors that influence the site's susceptibility."

- **Aquifer Vulnerability** - "The geology of the physical system determines vulnerability."

- **Aquifer Sensitivity** - "Aquifer sensitivity is related to the potential for contamination. That is, aquifers that have a high degree of vulnerability and are in areas of high population density, are considered to be the most sensitive …"U.S. Environmental Protection Agency (1993)
- **Aquifer Sensitivity** - "The relative ease with which a contaminant applied on or near the land surface can migrate to the aquifer of interest. Aquifer sensitivity is a function of the intrinsic characteristics of the geologic materials of interest, any overlying saturated materials, and the overlying unsaturated zone. Sensitivity is not dependent on agronomic practices or contaminant characteristics."

APPENDIX 2 DRASTIC PARAMETER RATINGS, WEIGHTS AND RANGES (Aller et al., 1987)

Depth to Water (D)		
Range (m)	Rating	Index
≤ 1.5	10	50
1.6 – 4.6	9	45
4.6 – 9.1	7	35
9.1 – 15.2	5	25
15.2 – 22.5	3	15
22.5 – 30	2	10
≥ 30	1	5
Weight:5		

Soil media (S)						**Hydraulic conductivity (C)**		
Media type	Rating	Index	**Influence of the vadose zone (I)**			Range (m/day)	Rating	Index
Gravel	10	20	Media type	Rating	Index	0.005 - 0.5	1	3
Sand	9	18	Clay and Silt	3	15	0.5 - 1.5	2	6
Sandy loam	6	12	Sandy/ Clay	4	20	1.5 - 3.5	4	12
Loam	5	10	Clay Sand	6	30	3.5 - 5.0	7	21
Silty-loam	4	8	Sand and Gravel	8	40	5.0 - 10.0	8	24
Clay-loam	3	6				>10.0	10	30
Weight:2			**Weight:5**			**Weight:3**		

Topography (T)		
Range (% slope)	Rating	Index
0-2	10	10
2-4.0	9	9
4-6.0	8	8
6-8.0	7	7
8-10.0	6	6
10-12.0	5	5
12-14.0	4	4
14-16.0	3	3
16-18.0	2	2
>18.0	1	1
Weight:1		

APPENDIX 3: MEAN STATIC WATER LEVELS OF ALL SAMPLED WELLS

ID	Lat.	Long.	**Mean SWL (m)**	**Min(m)**	**Max(m)**
WE1	0.96481	5.83900	**1.16**	**0.39**	**1.72**
WE2	0.96574	5.84197	**0.88**	**0.6**	**1.42**
WE3	0.96357	5.84132	**0.99**	**0.24**	**1.48**
WE4	0.96283	5.83369	**0.85**	**0.42**	**1.34**
WE5	0.95987	5.83760	**1.22**	**0.34**	**3**
WE6	0.95553	5.83487	**2.73**	**1.96**	**3.37**
WE7	0.95247	5.83092	**2.57**	**1.09**	**3.52**
WE8	0.94919	5.82829	**0.96**	**0.42**	**1.47**
WE9	0.94650	5.82436	**0.71**	**0.11**	**1.16**
WE10	0.94340	5.82257	**0.35**	**0.05**	**0.53**
WE11	0.94242	5.81910	**0.56**	**0.22**	**0.81**
WE12	0.93932	5.81582	**0.45**	**0.25**	**0.8**
WE13	0.93533	5.81403	**0.83**	**0.05**	**3.02**
WE14	0.96717	5.83982	**2.34**	**1.2**	**3.18**
WE15	0.96690	5.83766	**1.04**	**0.54**	**1.5**
WE16	0.96497	5.83582	**0.99**	**0.59**	**1.48**
WE17	0.96222	5.83617	**1.04**	**0.55**	**1.52**
WE18	0.96018	5.83596	**2.46**	**2.34**	**2.56**
WE19	0.95971	5.83380	**0.75**	**0.37**	**1.15**
WE20	0.95790	5.83162	**0.61**	**0.08**	**1.24**
WE21	0.95722	5.82952	**0.71**	**0.37**	**1.02**
WE22	0.95433	5.83305	**3.48**	**2.91**	**3.96**
WE23	0.95188	5.82861	**0.67**	**0.41**	**0.99**
WE24	0.94941	5.82565	**3.48**	**2.9**	**4.03**
WE25	0.94711	5.82123	**2.76**	**2.07**	**3.47**

WE26	0.94504	5.81941	**2.37**	**1.56**	**3.09**
WE27	0.94259	5.87132	**2.11**	**1.38**	**2.49**
WE28	0.94153	5.81312	**0.90**	**0.6**	**1.29**
WE29	0.93729	5.81235	**2.19**	**1.44**	**2.71**
TG 1	0.97843	5.87552	**1.30**	**0.79**	**2.35**
TG 2	0.98145	5.87165	**1.83**	**1.38**	**2.66**
TG 3	0.97988	5.87214	**2.41**	**2**	**3.22**
TG 6	0.98638	5.86503	**2.03**	**1.92**	**2.34**
TG 7	0.98290	5.86106	**2.24**	**1.59**	**3.24**
TG 8	0.97512	5.85751	**2.16**	**1.5**	**3.28**
TG 10	0.98478	5.85414	**1.77**	**1.16**	**2.42**
TG 11	0.97231	5.85297	**2.07**	**1.52**	**2.95**
TG 12	0.97631	5.84831	**2.23**	**1.41**	**3.21**
TG **13**	0.98190	5.84655	**1.80**	**1.39**	**2.21**
TG **16**	0.97368	5.84093	**1.96**	**1.26**	**2.83**
TG **17**	0.96909	5.84394	**2.03**	**0.65**	**3.43**
TG **18**	0.96878	5.84512	**0.73**	**0.57**	**0.88**
AL1	0.93382	5.81227	**0.46**	**0.15**	**0.78**
AL2	0.93162	5.81181	**0.51**	**0.21**	**0.82**
AL3	0.93050	5.80967	**0.65**	**0.07**	**1.09**
AL4	0.92804	5.80969	**0.62**	**0.09**	**1**
AL5	0.92657	5.80807	**0.64**	**0.13**	**1**
AL6	0.92500	5.80588	**0.69**	**0.29**	**1.12**
AL7	0.92315	5.80662	**2.07**	**0.69**	**5.18**
AL8	0.92201	5.80435	**1.14**	**0.21**	**5.2**
AL9	0.92067	5.80879	**1.14**	**0.23**	**5.32**
AL10	0.91822	5.80261	**0.38**	**0.23**	**0.46**
AL11	0.91622	5.80243	**1.49**	**0.42**	**5.25**
AL12	0.91454	5.80089	**1.08**	**0.1**	**5.3**
AL13	0.91278	5.79937	**1.33**	**0.4**	**5.26**
AL14	0.91083	5.80032	**1.07**	**0.03**	**5.26**
AL15	0.93551	5.81015	**2.94**	**1.92**	**5.49**
AL16	0.93305	5.80868	**2.96**	**1.31**	**5.51**
AL17	0.92962	5.80765	**2.34**	**0.61**	**5.39**
AL18	0.92799	5.80507	**1.00**	**0.61**	**1.4**
AL19	0.92569	5.80355	**1.10**	**0.7**	**1.49**
AL20	0.92315	5.80624	**1.00**	**0.4**	**1.55**
AL21	0.92059	5.80134	**1.91**	**1.15**	**3.25**
AL22	0.91800	5.79974	**2.18**	**1.16**	**3.17**
AL23	0.91525	5.79883	**3.72**	**3.51**	**3.96**
AL24	0.91219	5.79820	**2.42**	**1.42**	**3.48**
kk1	0.98955	5.90896	**2.76**	**1.68**	**3.33**
kk4	0.98738	5.90874	**1.63**	**0.48**	**2.7**
kk5	0.98883	5.90831	**2.31**	**1.33**	**2.86**

kk7	0.99034	5.91076	**1.85**	**1.18**	**2.8**
kk9	0.98957	5.91155	**0.97**	**0.42**	**1.47**
kk11	0.99010	5.90538	**1.89**	**0.87**	**2.41**
kk14	0.99141	5.90491	**1.06**	**0.41**	**1.43**
kk17	0.98874	5.90578	**2.10**	**1.14**	**2.8**
kk19	0.98680	5.90646	**1.54**	**0.39**	**2.14**
kk25	0.98813	5.90332	**2.38**	**1.68**	**2.82**
kk27	0.98593	5.90325	**0.76**	**0.29**	**1.12**
kk29	0.98765	5.90014	**2.34**	**1.7**	**2.75**
kk30	0.98505	5.89972	**0.56**	**0.08**	**0.9**
kk33	0.99105	5.91900	**1.65**	**0.81**	**2.24**
kk34	0.99216	5.90314	**0.47**	**0.47**	**0.47**
kk35	0.99363	5.89947	**0.97**	**0.97**	**0.97**
kk37	0.99069	5.89518	**1.87**	**1.33**	**2.33**
kk38	0.98565	5.89550	**2.08**	**1.11**	**2.78**
ket 1	0.99122	5.92131	**1.01**	**0.56**	**1.55**
ket 4	0.99211	5.92095	**2.27**	**1.9**	**2.62**
ket 5	0.99267	5.92149	**3.16**	**2.7**	**3.49**
ket 6	0.99181	5.92022	**0.64**	**0.28**	**0.99**
ket 8	0.99031	5.92045	**1.02**	**0.35**	**1.51**
ket 10	0.99021	5.92148	**0.80**	**0.5**	**1.09**
ket 12	0.99164	5.91902	**1.53**	**0.93**	**2.08**
ket 14	0.99126	5.91549	**1.73**	**1**	**2.47**
ket 16	0.99125	5.91640	**1.70**	**1.25**	**2.41**
ket 18	0.98872	5.91489	**1.49**	**0.47**	**2.45**
ket 20	0.99054	5.91314	**1.18**	**0.52**	**1.72**
DN 2	0.98210	5.89207	**2.17**	**1.25**	**2.87**
DN 4	0.98279	5.88746	**1.72**	**0.81**	**2.42**
DN 6	0.97860	5.89176	**1.89**	**0.92**	**2.68**
DN 9	0.98195	5.88294	**1.67**	**0.96**	**2.3**
DN 10	0.98744	5.89033	**1.62**	**1.15**	**2.08**
DN 11	0.99076	5.88863	**1.04**	**0.53**	**1.5**
DN 12	0.98835	5.88542	**1.57**	**0.73**	**2.22**
DN 14	0.99062	5.88063	**1.50**	**0.76**	**2.09**
DN 16	0.98587	5.87835	**2.15**	**1.37**	**2.79**

DN 2	0.98210	5.89207	**1.88**	**1.88**	**1.88**
DN 9	0.98195	5.88294	**2.25**	**2.25**	**2.25**
DN 10	0.98744	5.89033	**1.89**	**1.89**	**1.89**
DN 12	0.98835	5.88542	**2.34**	**2.34**	**2.34**

APPENDIX 4:

MODIFIED DRASTIC PARAMETER RATINGS, WEIGHTS AND RANGES IN RESEARCH AREA-(After Author 2010)

Depth to Water (D)			**Net Recharge (R)**			**Aquifer Media (A)**		
Range (m)	Rating	Index	Range (m)	Rating	Index	Media type	Rating	Index
0-1.5	10	50	0.01-0.1	1	4	Fine Sand	4	12
1.5-2.5	9	45	0.1-0.5	3	12	Medium Sand	6	18
2.5-3.0	7	35	0.5-1.5	6	24	Coarse Sand	8	24
≥ 3.0	5	25	1.5+	8	32	Gravel and Sand	9	27
						Gravel	10	30
Weight:5			**Weight:4**			**Weight:3**		

Soil media (S)			**Influence of the Vadose zone (I)**			**Hydraulic conductivity (C)**		
Media type	Rating	Index	Media type	Rating	Index	Range (m/day)	Rating	Index
Gravel	10	20	Clay and Silt	3	15	0-50	6	18
Sand	9	18	Sandy/ Clay	4	20	50-85	7	21
Sandy loam	6	12	Clay Sand	6	30	85-100	8	24
Loam	5	10	Sand and Gravel	8	40	100-150	9	27
Silty-loam	4	8						
Clay-loam	3	6						
Weight:2			**Weight:5**			**Weight:3**		

Topography (T)		
Range	Rating	Index

0-0.2	10	10
0.2-0.33	9	9
0.33-0.42	8	8
0.42-0.53	7	7
0.53-0.66	6	6
0.66-0.75	5	5
0.75-0.79	4	4
0.79-0.93	3	3
Weight:1		

APPENDIX 5:

RANGES OF HYDRAULIC CONDUCTIVITY VALUES FOR VARIOUS EARTH MATERIALS. [SOURCE: DOMENICO AND SCHWARTZ (1990)]

Material	Hydraulic conductivity (cm/**sec)**
Clay	1x10-11-4.7x10-7
Silt, loess	1x10-7-2x10-3
Fine sand	2x10-5-2x10-2
Medium sand	9x10-5-5x10-2
Coarse sand	9x10-5-6x10-1
Gravel	$3x10^{-2}$-3.0

APPENDIX 6:

RANGES OF VALUES OF SPECIFIC YIELD (S_Y) FOR SOME AQUIFER MEDIA. [SOURCE ANDERSON AND WOESSNER (1992)]

Material	No. of analysis	Range (S_y)	Arithmetic Means
Sandstone (fine)	47	0.02-0.40	0.21
Sandstone (medium)	10	0.12-0.41	0.27
Siltstone	13	0.01-0.33	0.12
Sand (fine)	287	0.01-0.46	0.33
Sand (medium)	297	0.16-0.46	0.32
Sand (coarse)	143	0.18-0.43	0.3
Gravel (fine)	33	0.13-0.40	0.28

Gravel (medium)	13	0.17-0.44	0.24
Gravel (coarse)	9	0.13-0.25	0.21
Silt	299	0.01-0.39	0.2
Clay	27	0.01-0.18	0.06

APPENDIX 7 SOIL AND AQUIFER MEDIA PARTICLE SIZE DISTRIBUTION CURVES

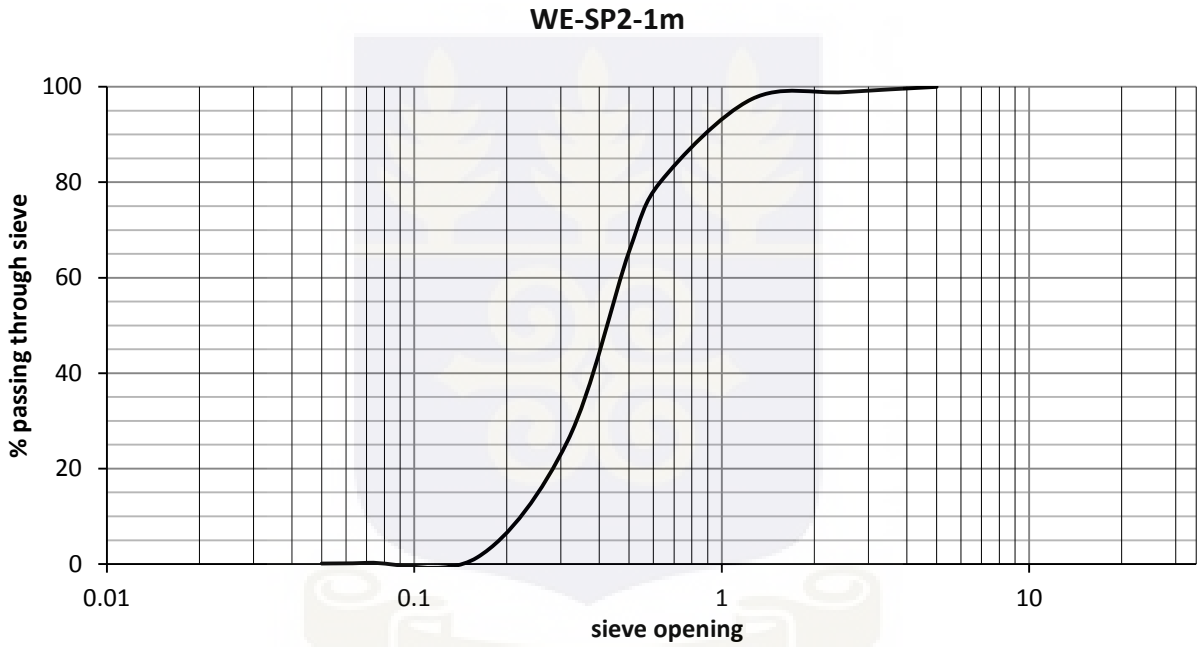

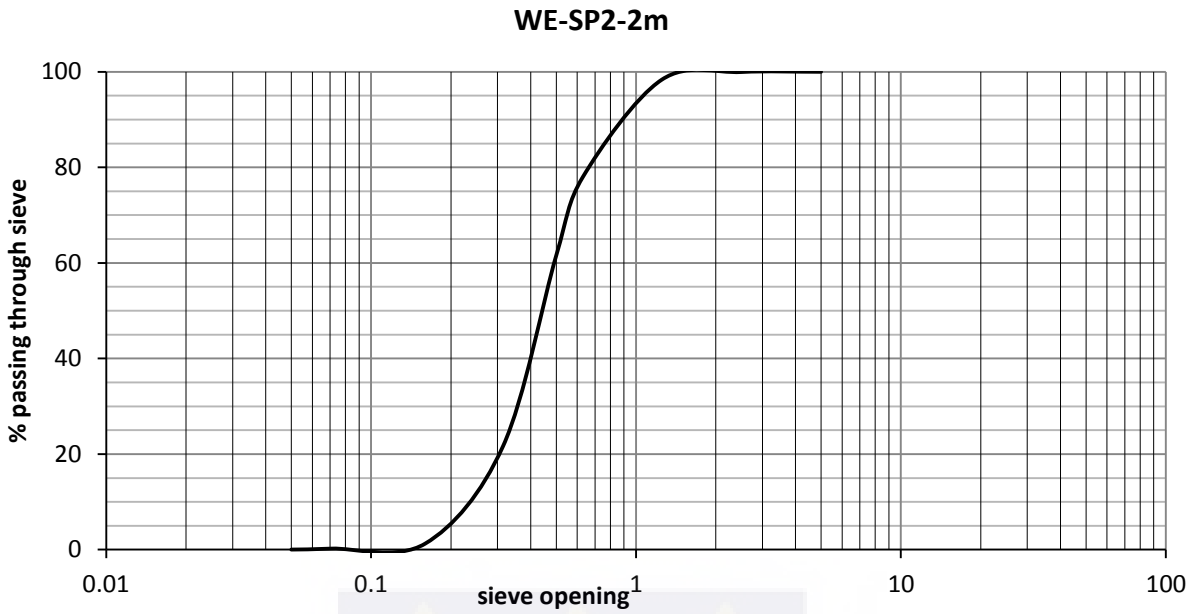

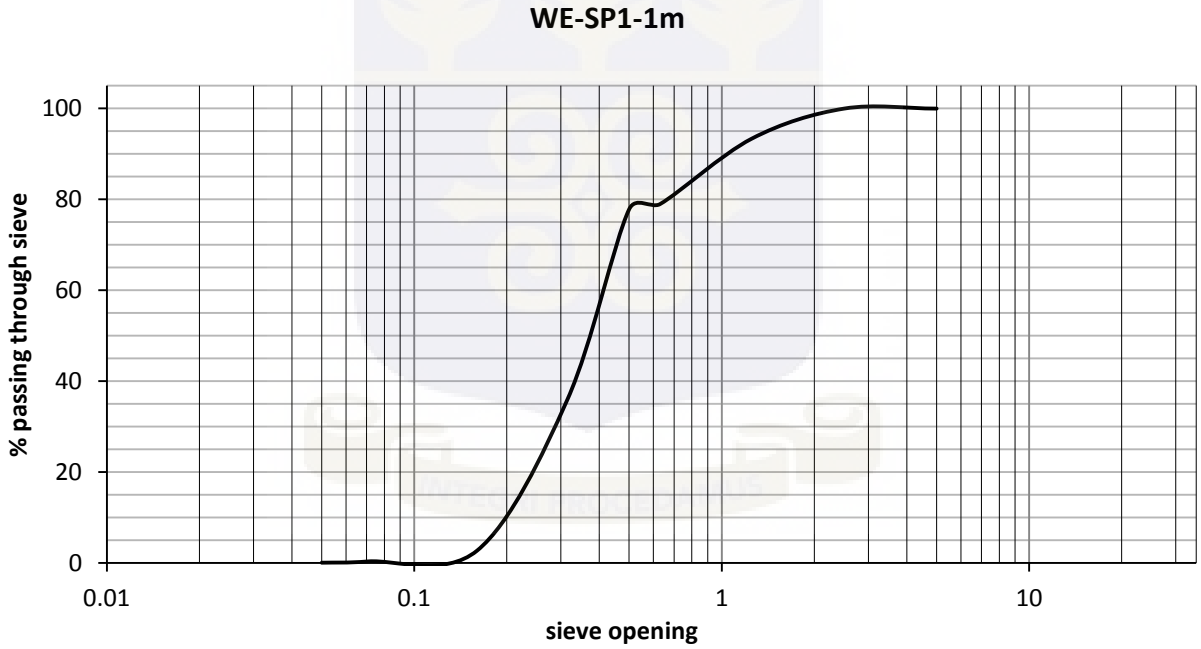

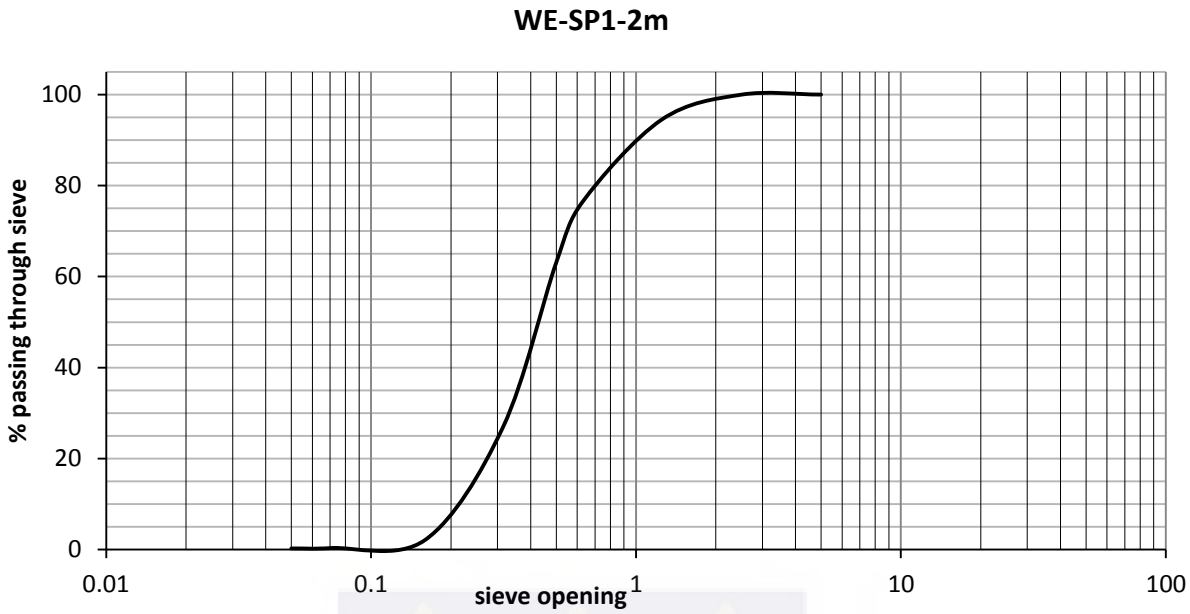

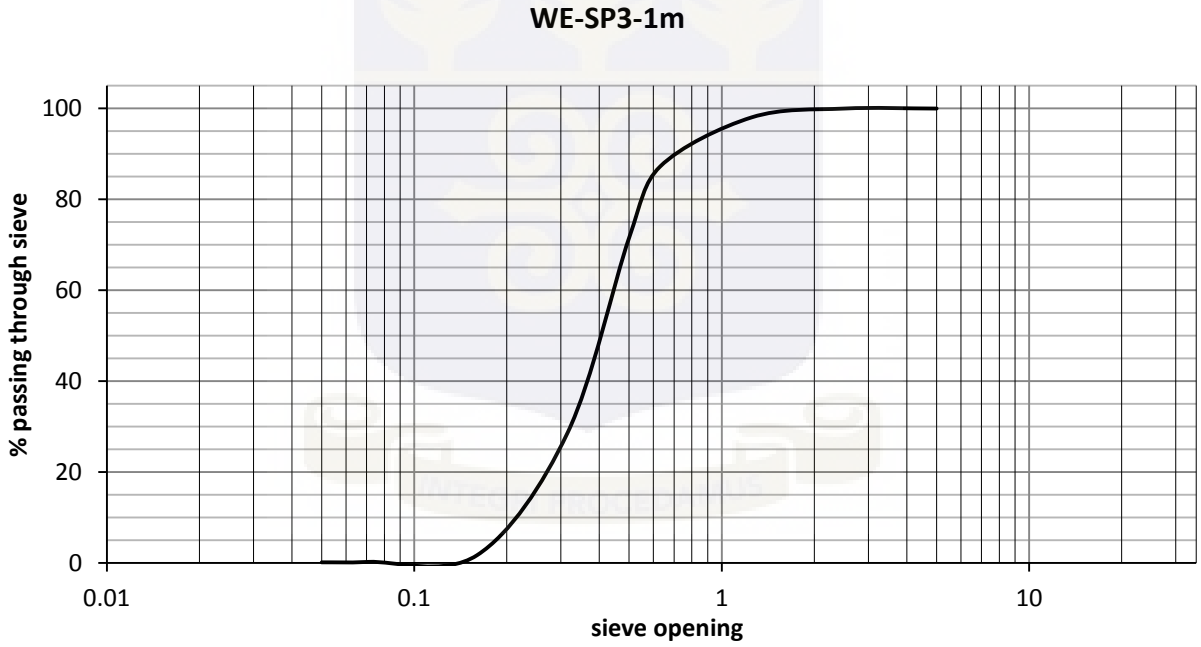

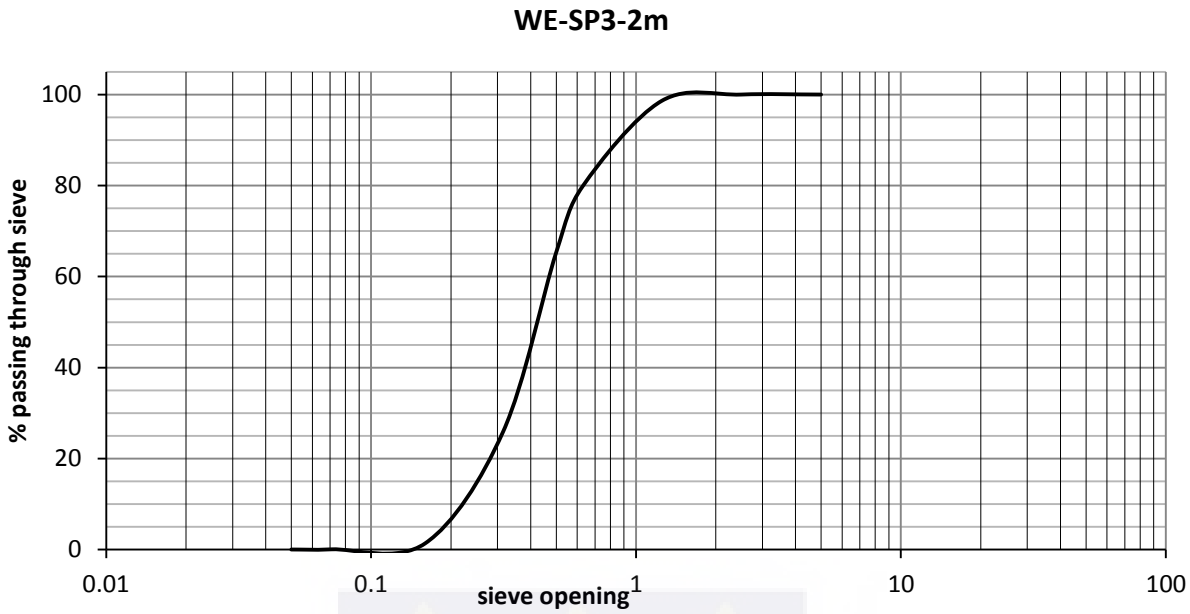

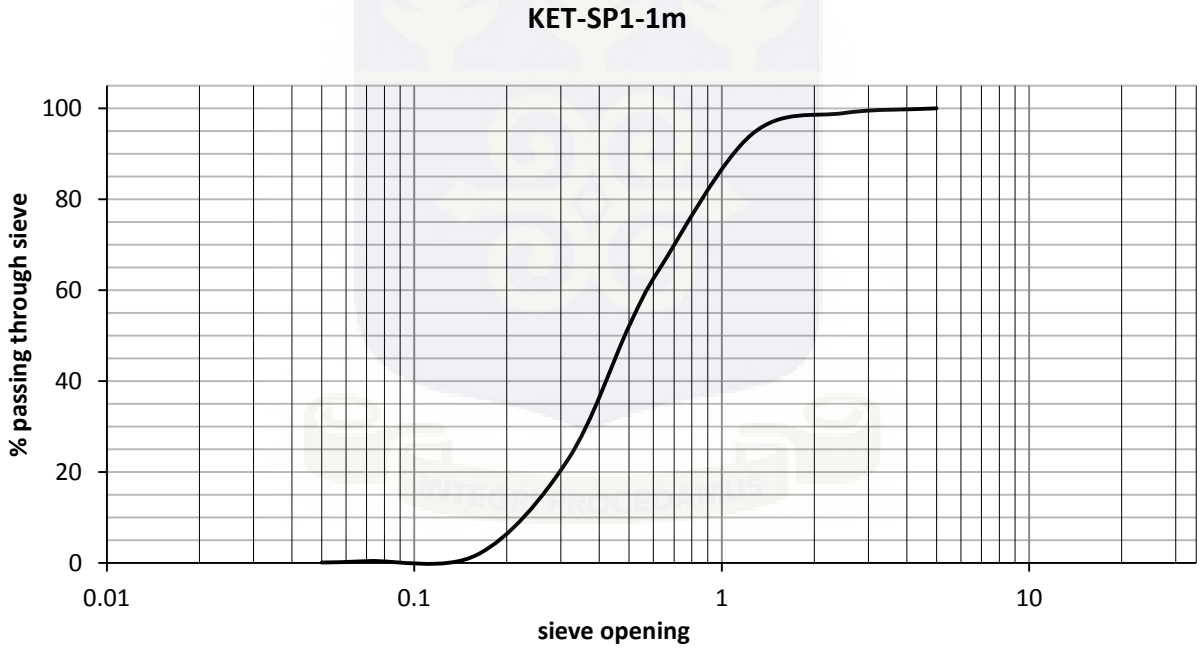

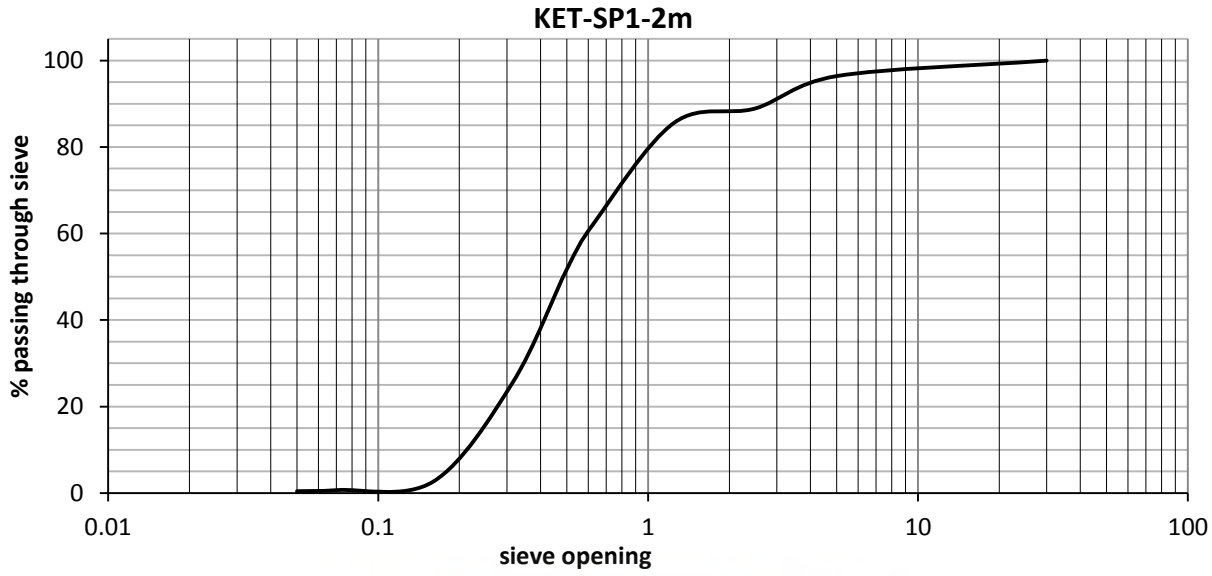

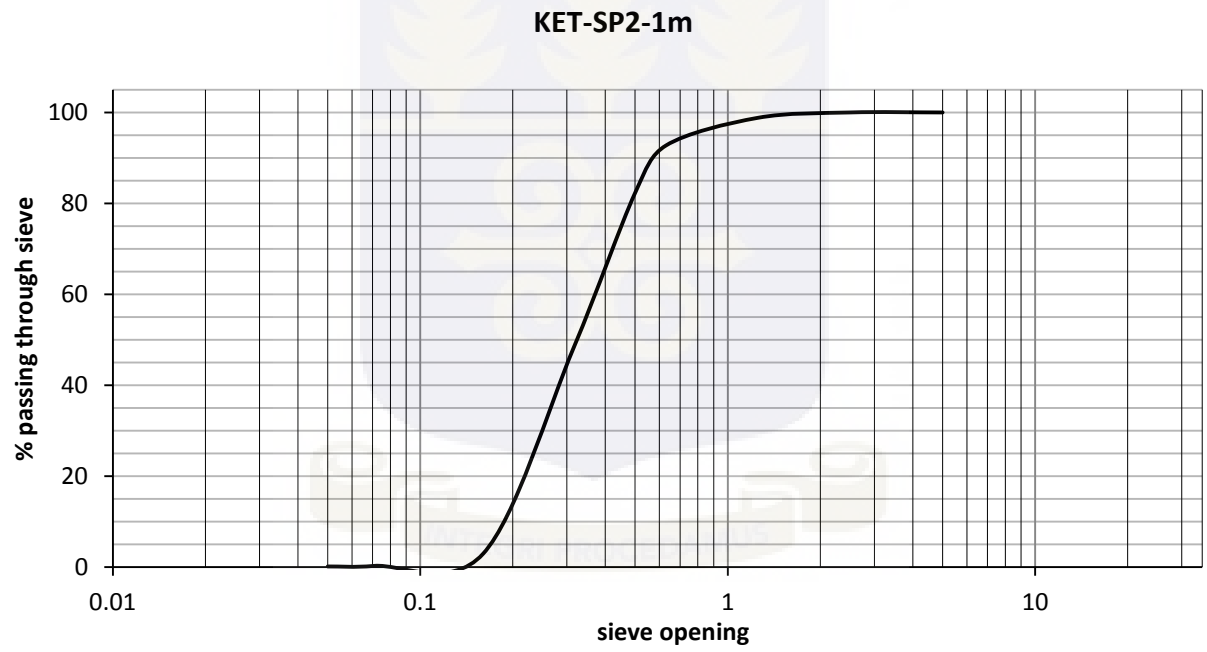

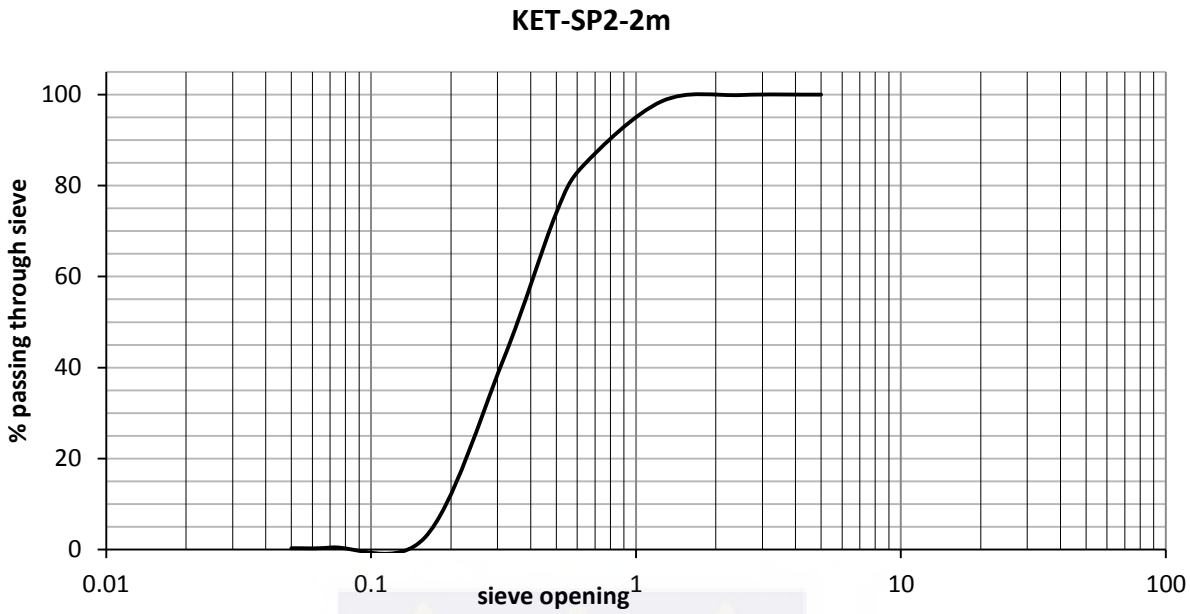

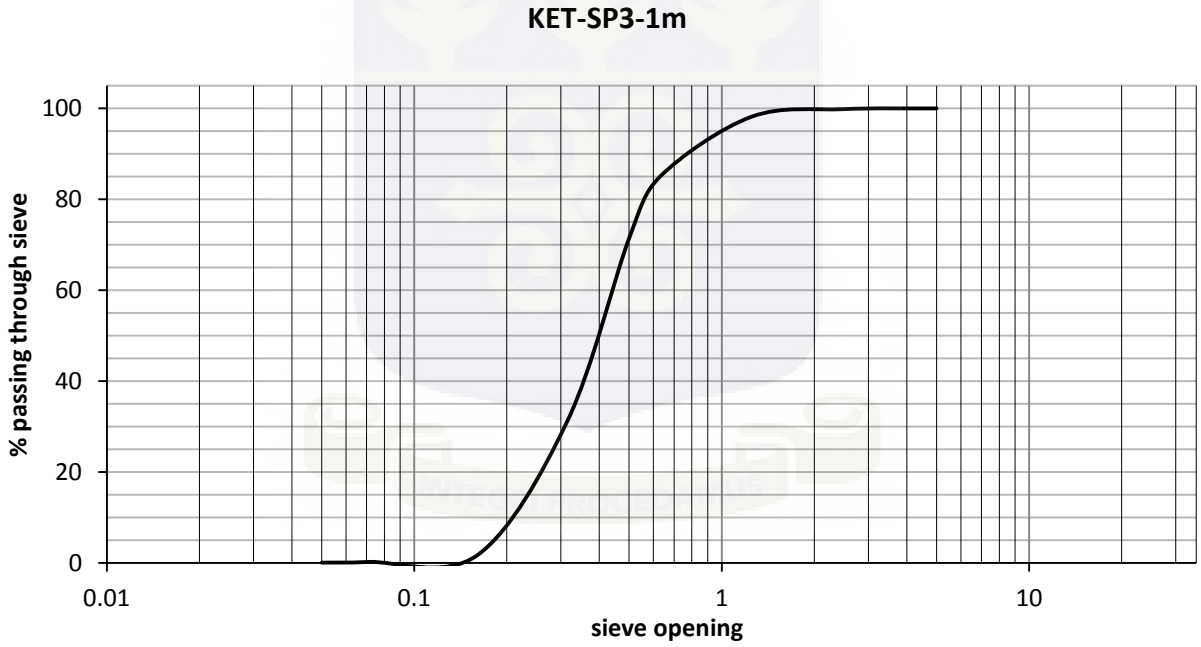

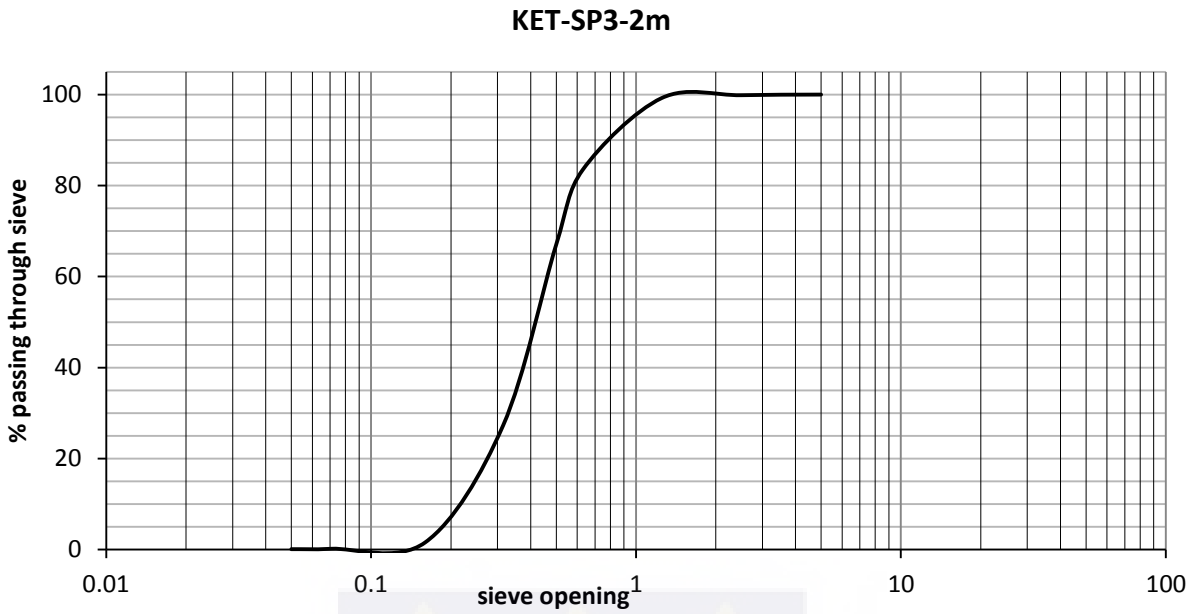

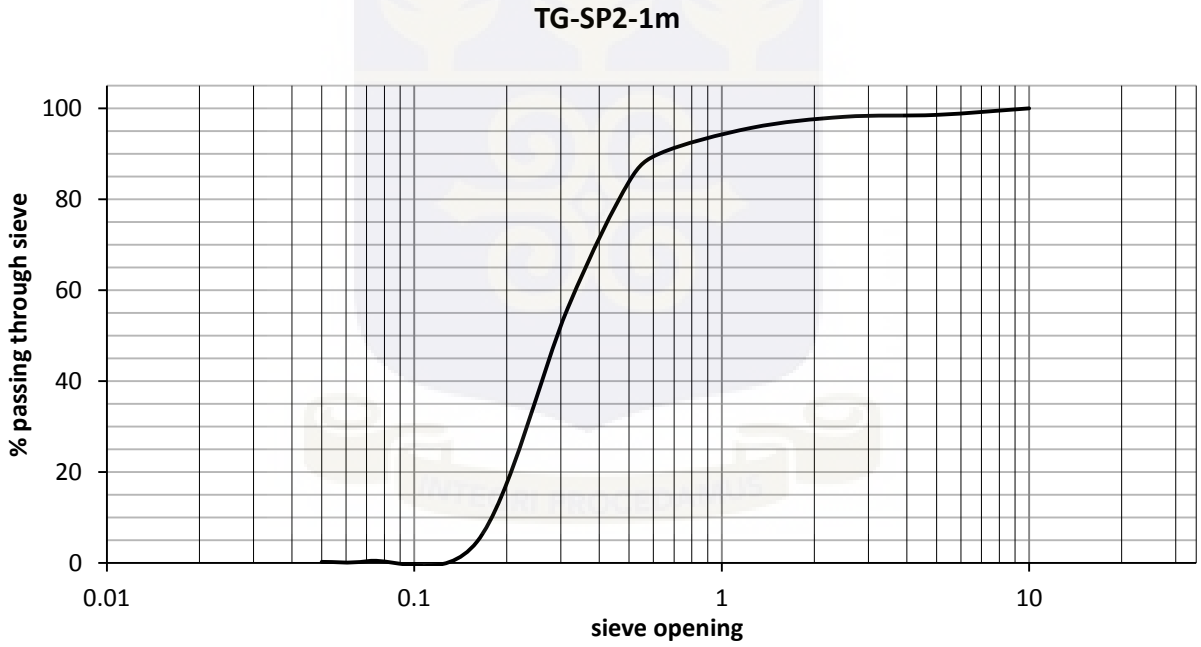

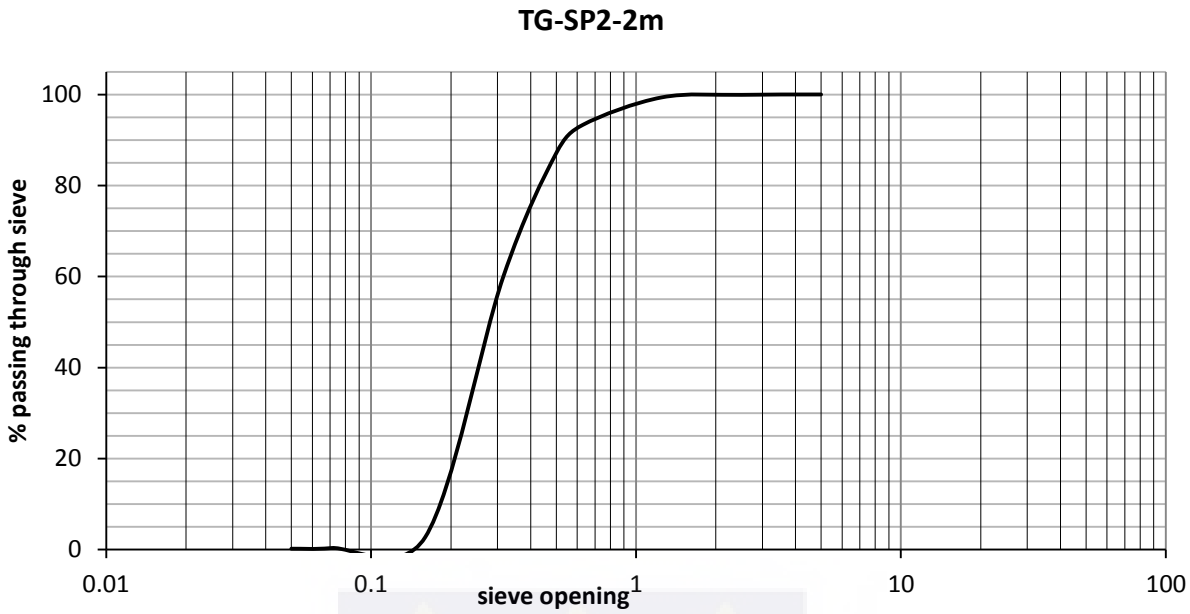

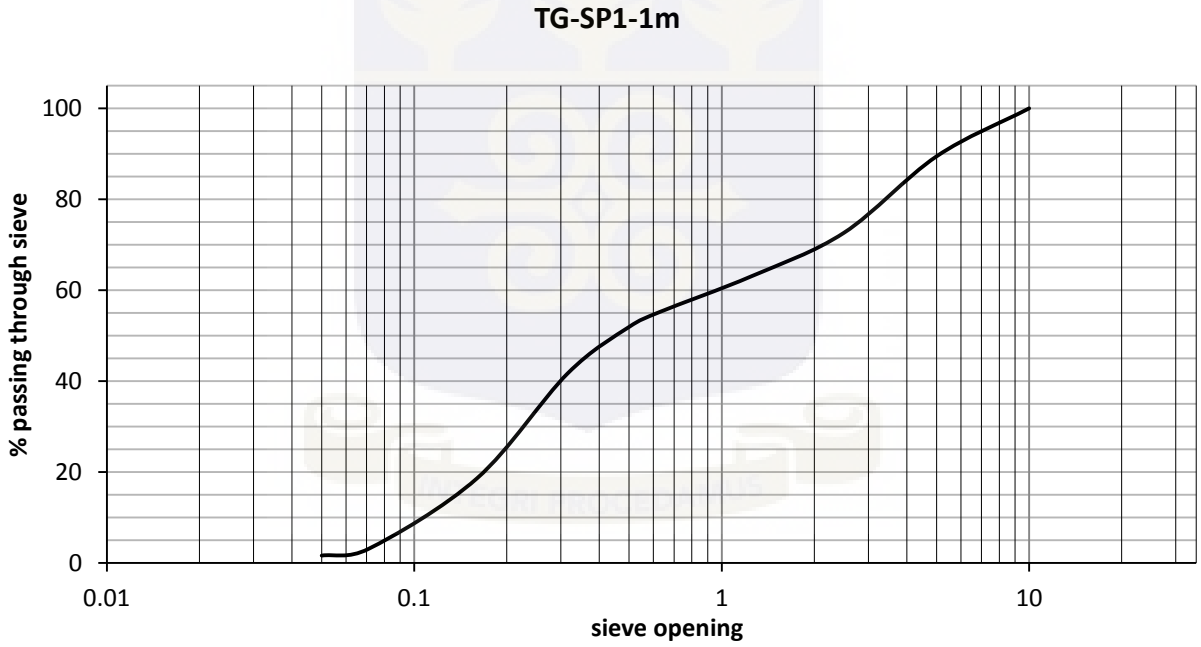

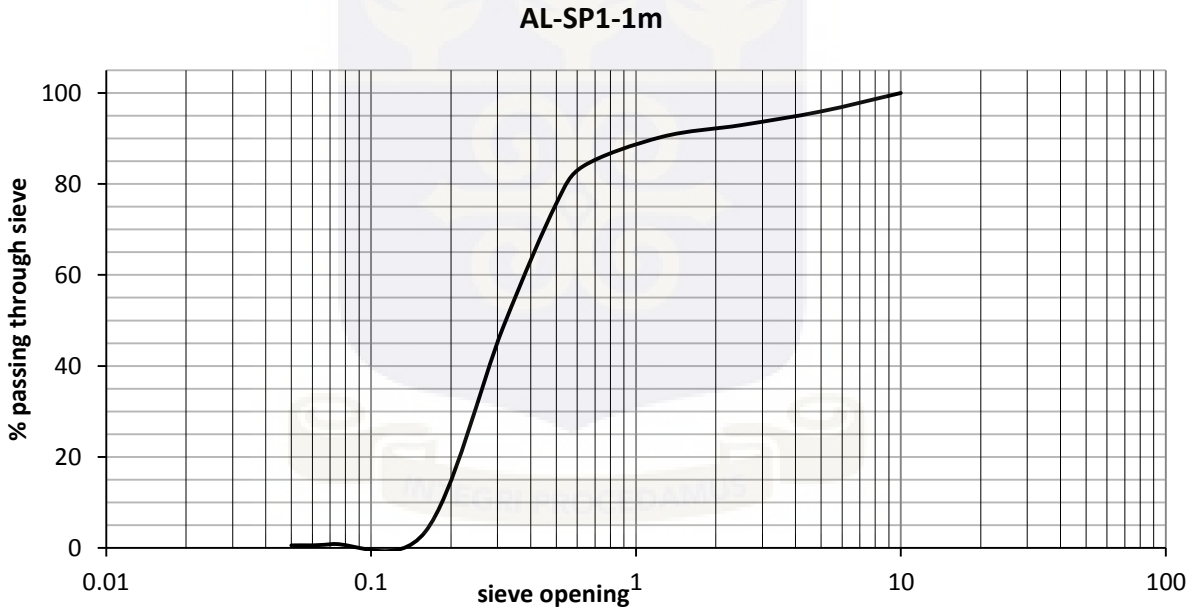

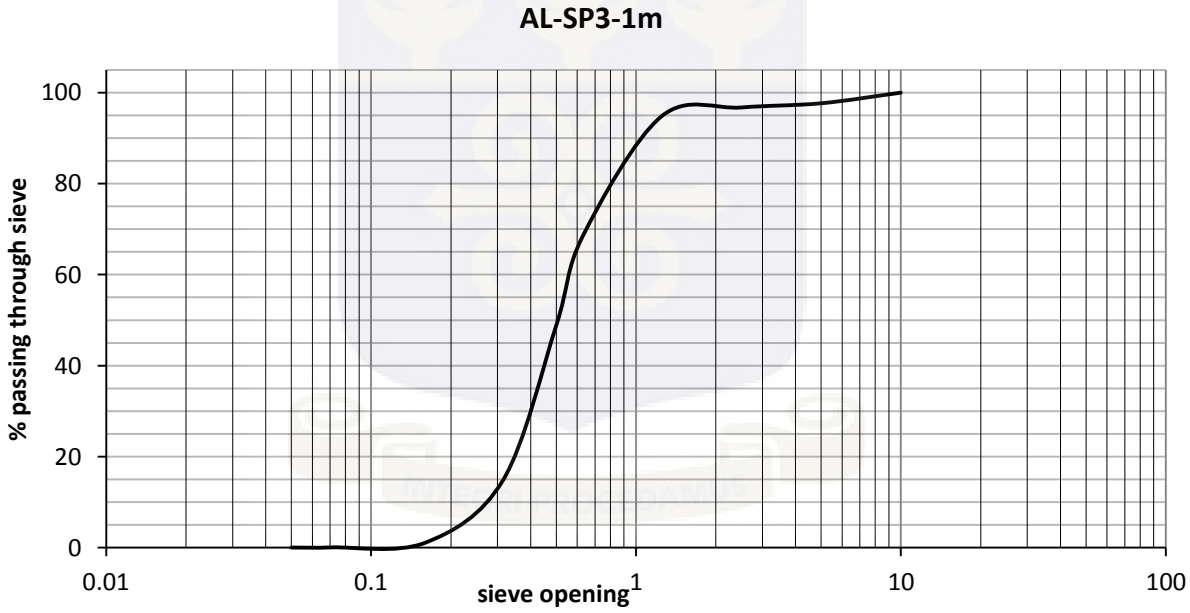

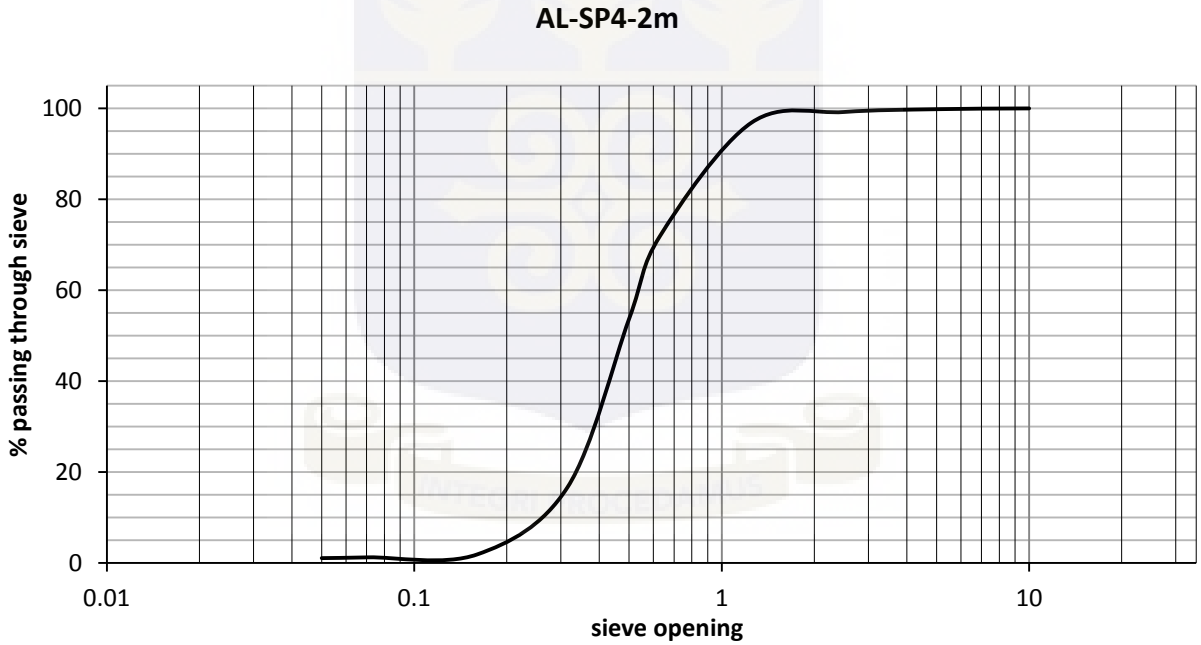

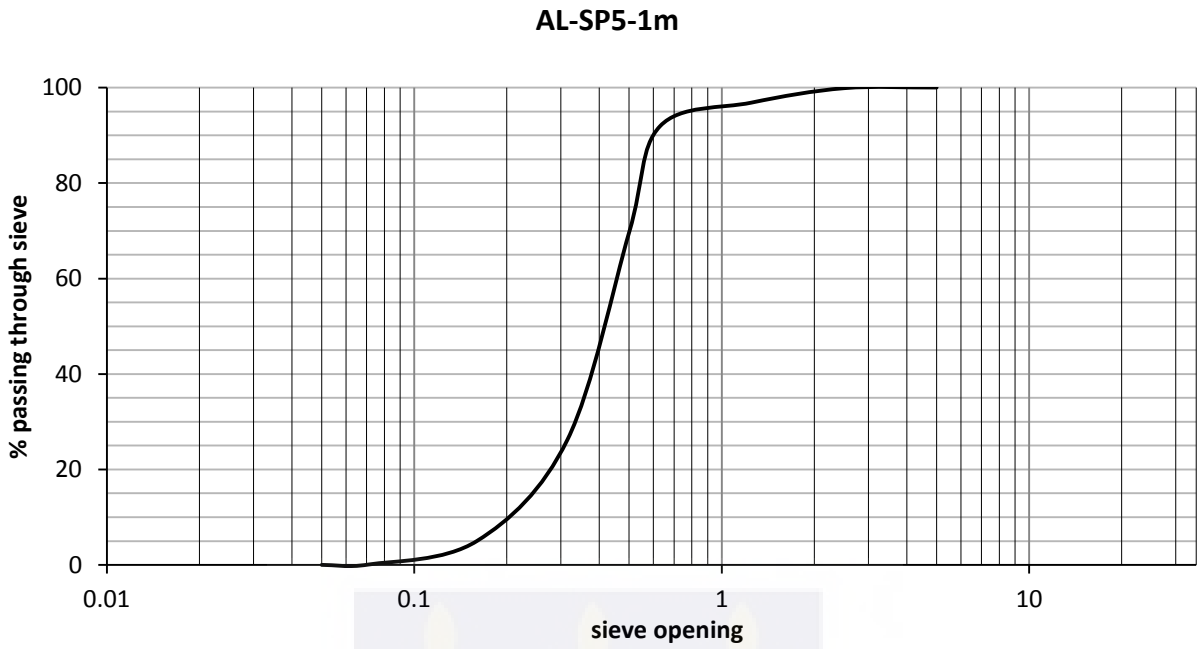

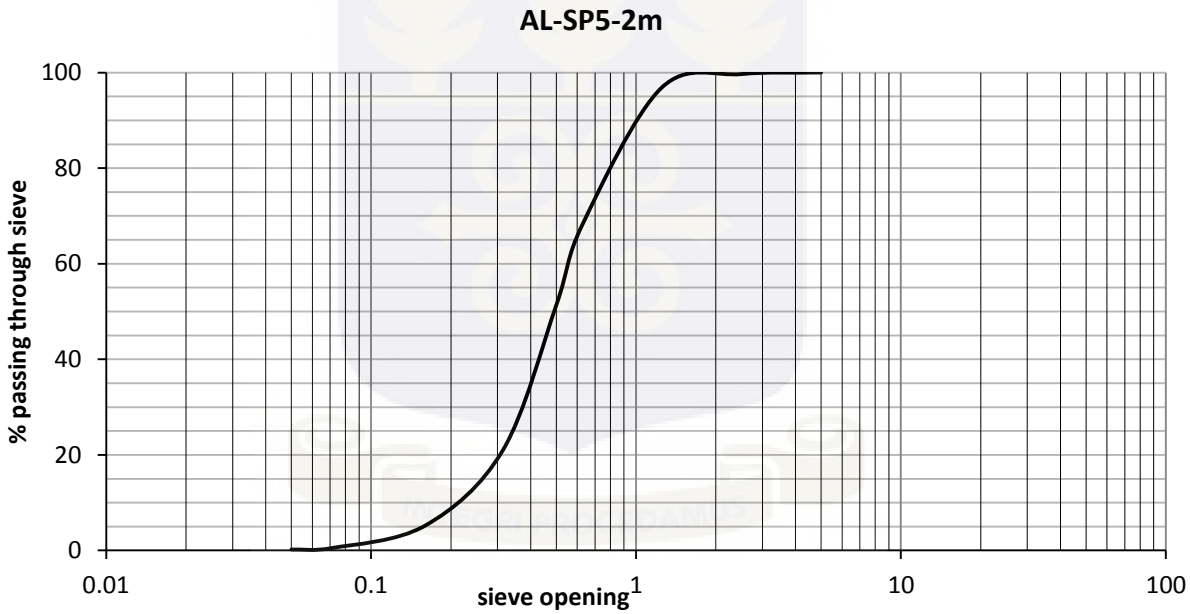

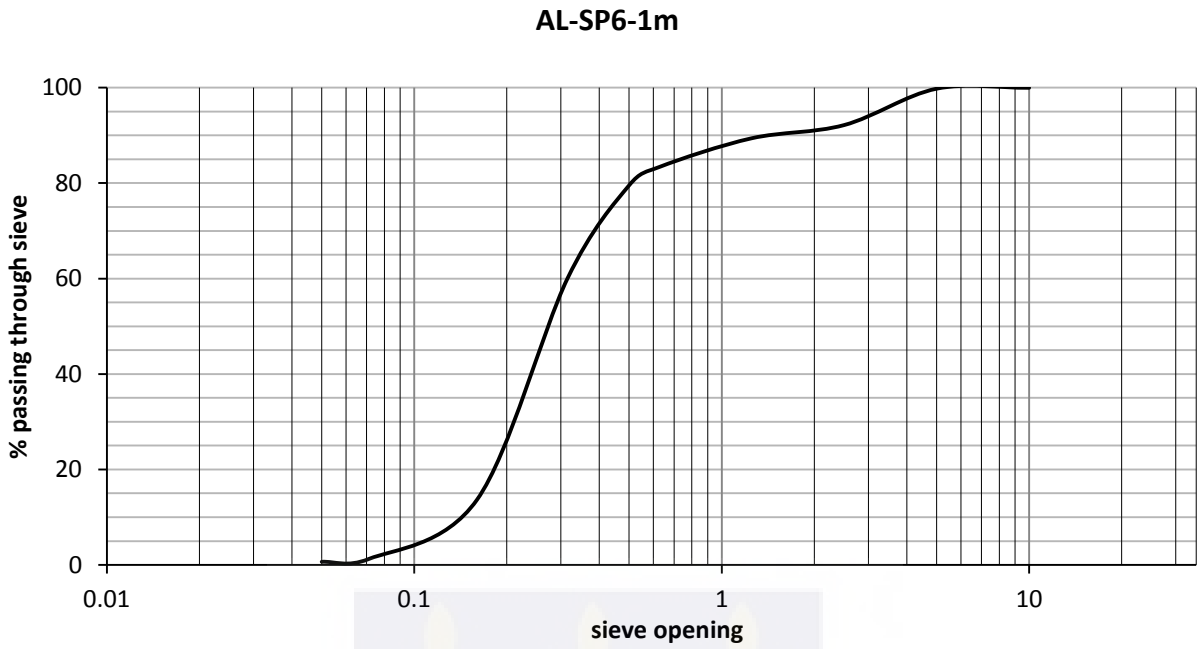

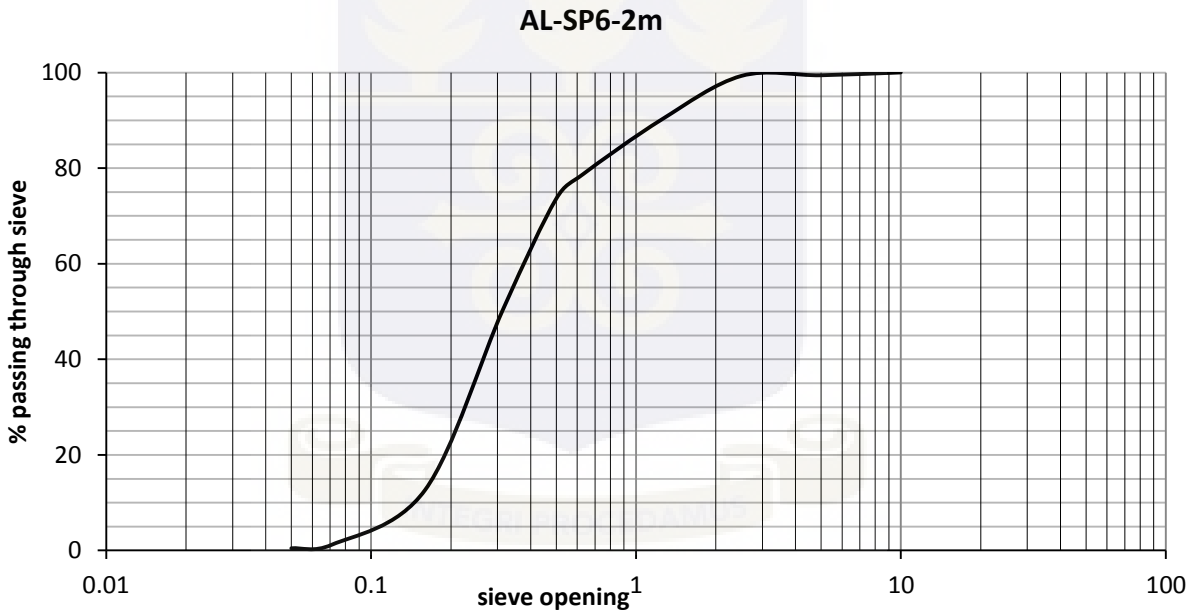

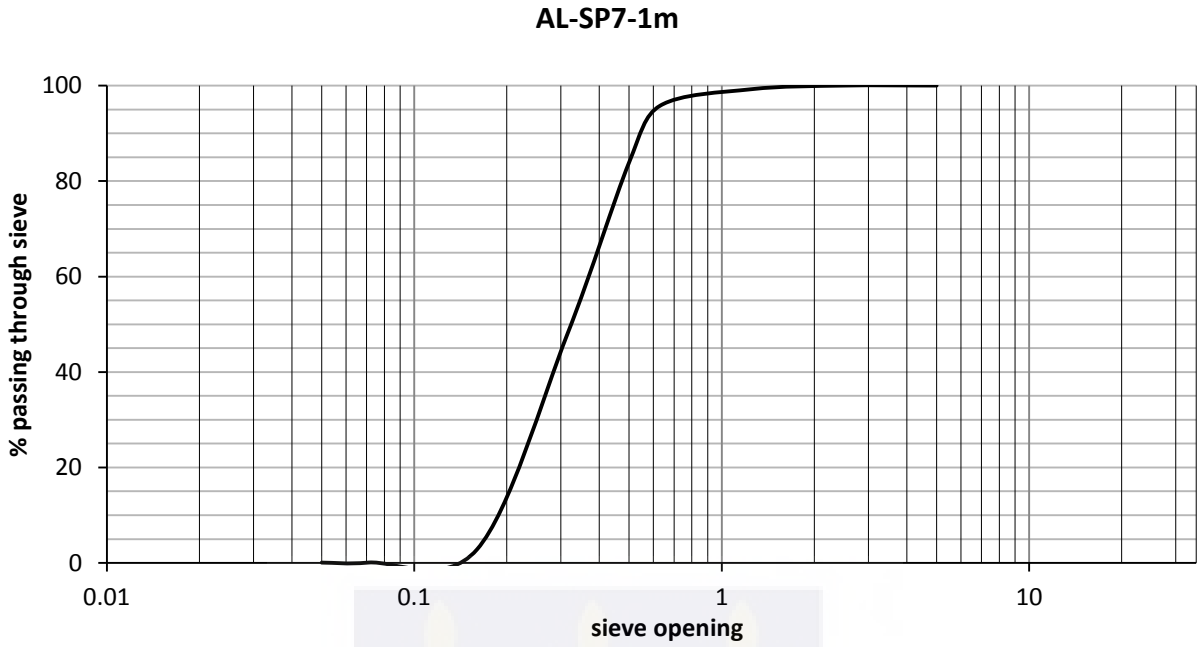

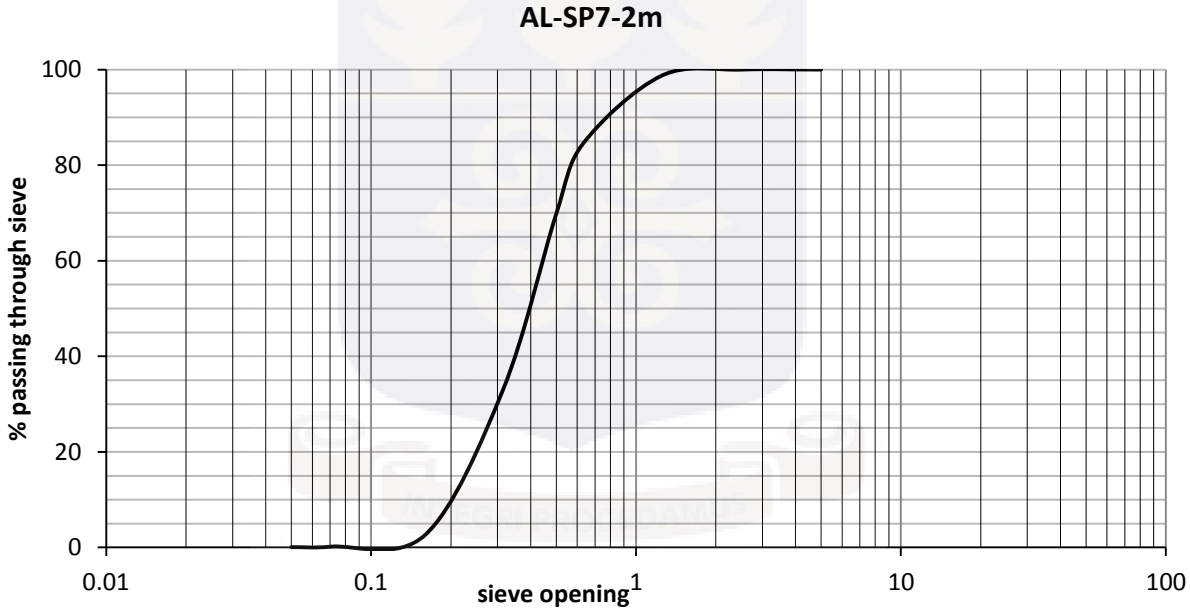

APPENDIX 8 PARTICLE SIZE DISTRIBUTION TABLE

Soil analysis: Particle Size Distribution Table

Station/Sample No.	*Clay Fraction %*	*Silt Fraction %*	*Fine Sand %*	*Medium Sand %*	*Coarse Sand %*	*Gravel Fraction %*	*Carbon %*
AL-SP1-1m	0.58	0.27	47.60	35.39	9.09	7.05	-
AL-SP2-1m	0.97	0.59	46.83	30.77	8.51	12.33	0.95
AL-SP3-1m	0.06	0.04	14.76	53.63	28.27	3.25	-
AL-SP4-1m	1.05	0.17	15.40	55.30	27.29	0.79	-
AL-SP4-2m	0.26	0.16	18.00	55.42	24.30	1.86	-
AL-SP5-1m	0.00	0.07	26.16	65.67	7.96	0.14	-
AL-SP5-2m	0.22	0.30	20.51	47.32	31.31	0.34	-
AL-SP6-1m	0.65	0.57	58.81	23.42	8.73	7.82	0.91
AL-SP6-2m	0.45	0.75	49.25	28.24	20.60	0.73	-
AL-SP7-1m	0.06	0.01	47.90	47.79	4.23	0.00	-
AL-SP7-2m	0.07	0.11	32.82	51.43	15.43	15.57	1.10
WE-SP1-1m	0.09	0.29	35.64	42.97	21.01	0.00	-
WE-SP1-2m	0.27	0.09	26.57	49.56	23.50	0.02	-
WE-SP2-1m	0.08	0.15	25.49	54.25	18.93	1.10	9.63
WE-SP2-2m	0.20	0.03	21.40	56.33	21.99	0.05	5.43
WE-SP3-1m	0.13	0.09	28.36	58.63	12.78	0.00	16.24
WE-SP3-2m	0.02	0.04	25.81	54.01	20.12	0.00	-
TG-SP1-1m	1.65	1.47	38.55	13.57	17.40	27.35	-
TG-SP1-2m	0.44	0.50	25.44	18.37	11.26	43.99	-
TG-SP2-1m	0.27	0.18	55.46	34.18	8.05	1.86	-
TG-SP2-2m	0.19	0.15	59.44	33.53	6.60	0.08	-
KET-SP1-1m	0.07	0.32	22.16	42.30	34.12	1.03	-
KET-SP1-2m	0.40	0.28	24.87	36.86	26.54	11.05	-
KET-SP2-1m	0.12	0.12	47.90	44.6	7.26	0	0.48
KET-SP2-2m	0.30	0.17	41.10	42.71	15.61	0.09	1.41
KET-SP3-Im	0.10	0.14	31.03	53.72	14.84	0.16	0.64
KET-SP3-2m	0.13	0.09	27.04	56.23	16.38	0.13	0.45

Appendix 9 Parameter Interpolation Data

Depth to water interpolation data			
ID	N	E	Depth
AL15	0.93551	5.81015	2.366
AL2	0.93162	5.81181	2.135
AL4	0.92804	5.80969	2.005
AL19	0.92569	5.80355	3.281
AL8	0.92201	5.80435	1.982
AL12	0.91454	5.80089	1.964
WE13	0.93533	5.81403	1.698
WE28	0.94153	5.81312	3.045
WE8	0.94919	5.82829	1.963
WE21	0.95722	5.82952	2.729
WE16	0.96497	5.83582	2.463
TG16	0.97368	5.84093	1.913
TG13	0.93533	5.81403	1.945
TG11	0.91622	5.80243	0.477
TG6	0.98638	5.86503	1.635
TG1	0.97843	5.87552	1.809
DN10	0.98744	5.89033	2.392
KK35	0.99363	5.89947	2.3
KK25	0.98813	5.90332	2.398
KK9	0.98957	5.91155	3.003
KET5	0.99267	5.92149	1.039

Recharge interpolation data			
ID	N	E	Recharge
WE11	0.94242	5.8191	0.1888
WE17	0.96222	5.83617	0.3104
WE23	0.95188	5.82861	0.1624
TG 2	0.98145	5.87165	0.4224
TG 18	0.96878	5.84512	0.0651
AL1	0.93382	5.81227	0.1764
AL11	0.91622	5.80243	1.5456
AL12	0.91454	5.80089	1.456
AL14	0.91083	5.80032	1.4644
AL16	0.93305	5.80868	1.386
AL23	0.91525	5.79883	0.1485
AL24	0.91219	5.7982	0.5768
kk29	0.98765	5.90014	0.336
kk30	0.98505	5.89972	0.2296
kk38	0.98565	5.8955	0.5344
ket 5	0.99267	5.92149	0.2528

Aquifer media interpolation data			
ID	N	E	Rating
AL-SP1	0.91163	5.79957	9
AL-SP2	0.91069	5.80074	9
AL-SP3	0.91423	5.7974	9
AL-SP4	0.91541	5.78957	4
AL-SP5	0.91574	5.7867	6
AL-SP6	0.93259	5.81272	4
AL-SP7	0.93375	5.81004	9
WE-SP1	0.9424	5.8121	6
WE-SP2	0.95076	5.81351	9
WE-SP3	0.96136	5.82342	6
TG-SP1	0.96689	5.84443	10
TG-SP2	0.98104	5.84579	4
KET-SP1	0.98415	5.8265	9
KET-SP2	0.98466	5.89668	6
KET-SP3	0.99271	5.92148	6

Soil Media interpolation data			
ID	N	E	Rating
AL-SP3-1m	0.91423	5.7974	10
AL-SP4-1m	0.91541	5.78957	3
AL-SP5-1m	0.91574	5.7867	9
AL-SP6-1m	0.93259	5.81272	10
AL-SP7-1m	0.93375	5.81004	9
KET-SP1-1m	0.98415	5.8265	9
KET-SP2-1m	0.98466	5.89668	9
KET-SP3-Im	0.99271	5.92148	9
TG-SP1-1m	0.96689	5.84443	4
TG-SP2-1m	0.98104	5.84579	10
WE-SP1-1m	0.9424	5.8121	9
WE-SP2-1m	0.95076	5.81351	9
WE-SP3-1m	0.96136	5.82342	9

Topography(% slope) interpolation data			
Well ID	Longitude	Latitude	Elevation
AL15	0.93551	5.81015	5.306
AL2	0.93162	5.81181	2.645
AL4	0.92804	5.80969	2.625
AL19	0.92569	5.80355	4.381
AL8	0.92201	5.80435	3.122
AL12	0.91454	5.80089	3.044
WE13	0.93533	5.81403	2.528
WE28	0.94153	5.81312	3.945
WE8	0.94919	5.82829	2.923
WE21	0.95722	5.82952	3.439
WE16	0.96497	5.83582	3.453
TG16	0.97368	5.84093	3.873
TG13	0.93533	5.81403	3.745
TG11	0.91622	5.80243	2.547
TG6	0.98638	5.86503	3.665
TG1	0.97843	5.87552	3.109
DN10	0.98744	5.89033	4.012
KK35	0.99363	5.89947	3.27
KK25	0.98813	5.90332	4.778
KK9	0.98957	5.91155	3.973
KET5	0.99267	5.92149	4.199

Hydraulic conductivity interpolation data				
Sample	Latitude	Longitude	Aquifer media Class.	Hydraulic Conductivity
ID	E	N		(m/d)
AL-SP1	5.79957	0.91163	Slightly Gravely Sand	60.94369
AL-SP2	5.80074	0.91069	Slightly Gravely Sand	51.85657
AL-SP3	5.7974	0.91423	Slightly Gravely Sand	150.3586
AL-SP4	5.78957	0.91541	Slightly Silty Sand	31.61113
AL-SP5	5.7867	0.91574	medium Sand	43.61401
AL-SP6	5.81272	0.93259	Fine Sand	9.991413
AL-SP7	5.81004	0.93375	Gravely Sand	63.43507
WE-SP1	5.8121	0.9424	Medium Sand	46.92183
WE-SP2	5.81351	0.95076	Gravely Sand	96.57997
WE-SP3	5.82342	0.96136	medium Sandy	47.31507
TG-SP1	5.84443	0.96689	Fine sand	67.636
TG-SP2	5.84579	0.98104	Fine Sandy	11.17795
KET-SP1	5.8265	0.98415	Gravely Sand	53.90947
KET-SP2	5.89668	0.98466	Medium Sandy	44.75587
KET-SP3	5.92148	0.99271	Medium Sand	46.92183